ASD-TR-77-6 Vol. I

AN EXTENDED PREDICTION MODEL FOR AIRPLANE BRAKING DISTANCE AND A SPECIFICATION FOR A TOTAL BRAKING PREDICTION SYSTEM

Volume I

M. K. Wahi, S. M. Warren, H. H. Straub
Boeing Commercial Airplane Company
P. O. Box 3707, Seattle, Washington 98124

March 1977

Technical Report ASD-TR-77-6, Volume I
Combat Traction II, Phase II (Extended)
Final Report Tasks II and III
August 1975 - December 1976

AERONAUTICAL SYSTEMS DIVISION
AIR FORCE SYSTEMS COMMAND
Wright-Patterson Air Force Base, Ohio 45433

NOTICE

When Government drawings, specifications, or other data are used for any purpose other than in connection with a definitely related Government procurement operation, the United States Government thereby incurs nc responsibility nor any obligation whatsoever: and the fact that the Government may have formulated, furnished, or in any way supplied the said drawings, specifications, or other data, is not to be regarded by implication or otherwise as in any manner licensing the holder or any other person or corporation, or conveying any rights or permission to manufacture, use, or sell any patented invention that may in any way be related thereto.

This report has been prepared by the Boeing Commercial Aircraft Company, Renton, Washington, under USAF Contract F33657-74-C-0129 for the Deputy for Engineering, Aeronautical Systems Division, Wright-Patterson AFB, Ohio.

This report has been reviewed and cleared for open publication and/or public release by the appropriate Office of Public Information (OI) in accordance with AFR 190-13 and DOD 5230.0. There is no objection to unlimited distribution to the public at large or by the Defense Documentation Center (DDC) to the National Technical Information Service (NTIS).

This report has been reviewed and approved for publication.

David B Tremblay

DAVID B. TREMBLAY
Technical Expert

FOR THE COMMANDER

John F. Andrews

JOHN F. ANDREWS, Lt Col, USAF
Chief, Flight Equipment Division
Directorate of Flight Systems Engineering
Deputy for Engineering

Copies of this report should not be returned unless return is required by security considerations, contractual obligations, or notice on a specific document.

SECURITY CLASSIFICATION OF THIS PAGE (When Data Entered)

REPORT DOCUMENTATION PAGE

READ INSTRUCTIONS BEFORE COMPLETING FORM

1. REPORT NUMBER: ASD TR-77-6-Vol [redacted] - 1

2. GOVT ACCESSION NO.

3. RECIPIENT'S CATALOG NUMBER: Rept.

4. TITLE (and Subtitle): An Extended Prediction Model for Airplane Braking Distance and a Specification for a Total Braking Prediction System. Volume I

5. TYPE OF REPORT & PERIOD COVERED: Final Aug [redacted]75 - Dec [redacted]76

6. PERFORMING ORG. REPORT NUMBER

7. AUTHOR(s): M. K. Wahi, S. M. Warren [redacted] H. H. Straub

8. CONTRACT OR GRANT NUMBER(s): F33657-74-C-0129 (Extended)

9. PERFORMING ORGANIZATION NAME AND ADDRESS: The Boeing Commercial Airplane Company, Renton, Washington

5/C 402 120

10. PROGRAM ELEMENT, PROJECT, TASK AREA & WORK UNIT NUMBERS: 021A9363

11. CONTROLLING OFFICE NAME AND ADDRESS: Aeronautical Systems Division (AEAA), Air Force Systems Command, Wright-Patterson AFB, OH 45433

12. REPORT DATE: Mar [redacted] 1977

13. NUMBER OF PAGES: 119

120p.

14. MONITORING AGENCY NAME & ADDRESS (if different from Controlling Office)

15. SECURITY CLASS. (of this report): Unclassified

15a. DECLASSIFICATION/DOWNGRADING SCHEDULE

16. DISTRIBUTION STATEMENT (of this Report)

Approved for public release; distribution unlimited.

17. DISTRIBUTION STATEMENT (of the abstract entered in Block 20, if different from Report)

18. SUPPLEMENTARY NOTES

19. KEY WORDS (Continue on reverse side if necessary and identify by block number)

Combat Traction
Antiskid
Simulator
Total Braking Prediction System
Verification Test Program

20. ABSTRACT (Continue on reverse side if necessary and identify by block number)

A sensitivity analysis of airplane braking distance was conducted on a hardware-analog brake control simulator for the USAF B-52, KC-135 and F-111 airplanes. Using dimensional analysis a braking distance prediction equation was developed for each airplane. The results of this study were combined/compared with the braking prediction equations developed, for five other airplanes, Boeing 727, 737 and 747 and USAF C-141 and F-4, [illegible] a similar previously contracted effort. The resulting braking prediction subsystem (BPSS) model (equations) are shown to be compatible and valid. The BPSS has been integrated with a ground Friction Prediction Subsystem (FPSS) and a specification criteria is developed for this Total Braking Prediction System (TBPS). A test program is also outlined to verify the effectiveness and reliability of the TBPS.

DD FORM 1 JAN 73 1473 EDITION OF 1 NOV 65 IS OBSOLETE

SECURITY CLASSIFICATION OF THIS PAGE (When Data Entered)

402 120

PREFACE

This report was prepared by M. K. Wahi, S. M. Warren, and H. H. Straub of the Boeing Commercial Airplane Company under a USAF Contract F33657-74-C-0129 (extended). The program was divided into three tasks. Task I involved the formulation of a tire correlation model, a test outline to validate the model, establishment of a friction prediction subsystem specification criteria and evaluation of existing ground vehicles. The work completed under Task I of this contract was performed from May 1975 to December 1975 and all aspects of that work are described in a separate report ASD-TR-77-7.

Task II involved a sensitivity analysis of airplane braking distance by using the Boeing Brake Control Simulator for the USAF B-52, KC-135 and F-111 airplanes to validate the general prediction model developed in the previously contracted effort. Task III objectives were to establish compatibility between Task II and Task I subsystems and to recommend a test program to verify the effectiveness and reliability of the Total Braking Prediction System (TBPS). The present volume describes all essential aspects of the work performed in completing Tasks II and III of this contract. Volume II describes the hardware and antiskid systems used on the brake control simulator as well as the test conditions and parameters used in developing data required for the dimensional analysis. The work described herein was performed from August 1975 to December 1976.

The authors are indebted to Messers N. S. Attri, and A. J. P. Lloyd for their guidance and technical contribution as respective program managers at various stages of the contract.

The authors are also indebted to Messers W. B. Tracy ASD/ENFEM, D. B. Tremblay ASD/ENFE, Lt. Col. R. Kennah, ASD/AEAA and Maj. R. Cauley, AFCEC/EMR of the USAF for their program support

TABLE OF CONTENTS

TABLE OF CONTENTS (Continued)

TABLE OF CONTENTS (Concluded)

LIST OF ILLUSTRATIONS

LIST OF TABLES

LIST OF ABBREVIATIONS AND SYMBOLS

AC	alternating current
C_D	coefficient of drag
CG	center of gravity
C_L	coefficient of lift
DC	direct current
F_e	engine idle thrust
F_{eo}	engine idle thrust at zero velocity
g	acceleration caused by gravity
KE	change in idle thrust with velocity
P_B	brake pressure
PRI	parameter rating index
s, X_A	braking distance
T_B	brake torque
TA	time to brake application
v, VI	brake application speed
V_w	headwind or tailwind velocity
W	airplane landing weight
X_P	perfect braking distance
μ, mu	peak available friction coefficient
η_s	braking distance efficiency
π	pi term
ρ	air density
σ	slip, percentage of slip
ω	wheel velocity

SUMMARY

An airplane braking sensitivity study has been extended to the F-111A, KC-135 and B-52H airplanes with an analog-hardware brake control simulation. As indicated in earlier studies, the peak available ground friction (μ), drag device effectiveness (C_L/C_D), brake application speed (V), air density (ρ), and engine idle thrust (Fe) are the resulting parameters which have the most significance on braking distance. The braking distance prediction equations involving these parameters have been developed for each of the above three airplanes, and are compatible with those developed for other aircraft. Recommendations for the operational application of the Total Braking Prediction System are described and involve the use of a suitable ground friction vehicle (Friction Prediction Subsystem), a proven tire correlation model, and the prediction equations. The feasibility of the Total Braking Prediction System must be verified with a recommended test program.

SECTION I
INTRODUCTION

This report presents in two volumes the results of Task II and III of Combat Traction II, Phase II, Extended. Results of Task I of this program are presented in a separate report "Tire Runway Interface Friction Prediction System" ASD-TR-77-7. The Task, summarized diagrammatically in Figure 1, describes a tire correlation model concept, recommends a test program for validation of the correlation model, and presents a specification for a ground friction measuring vehicle.

Task II consists of an airplane braking sensitivity study similar to that of References 1 and 2 as applied to the F-111A, KC-135 and B-52H. Results of the sensitivity analysis (Task IIa, Figure 2) combined with those of the earlier sensitivity study (Reference 1) were used to form a composite group of significant factors affecting braking performance. This list of factors was used to form an expanded Braking Performance Prediction Model (Task IIb). Using this expanded model individual prediction equations for each aircraft under consideration have been developed (Task IIc).

Results of the tire-runway friction study (Task I) and the airplane braking study (Task II) were combined in Task III to form a Total Airplane Braking Prediction System. In addition a test program is recommended to verify the total airplane braking prediction system concept.

PRECEDING PAGE BLANK-NOT FILMED

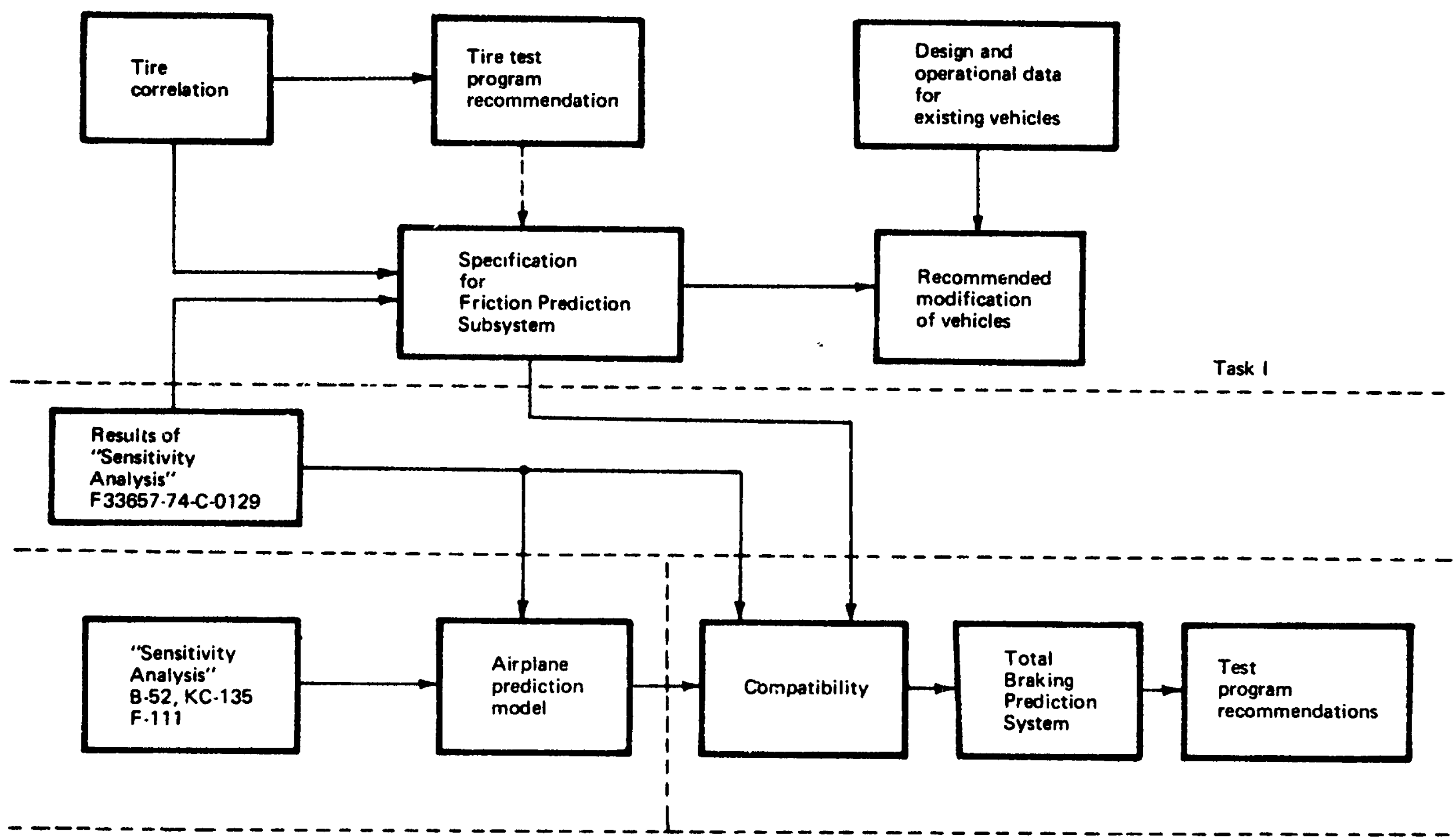

Figure 1.—Overall Program Plan

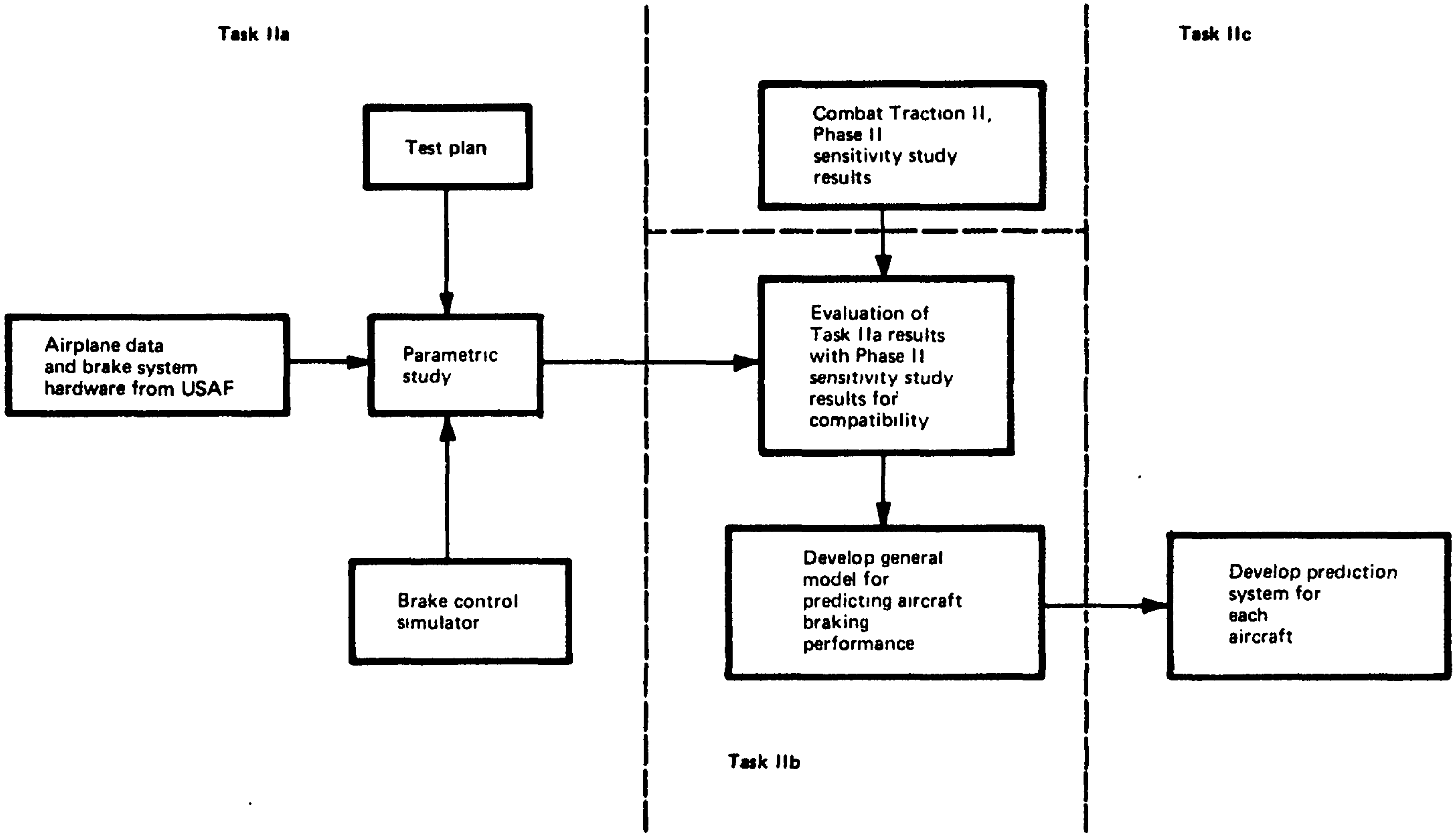

Figure 2.—Sensitivity Analysis and Prediction Models

SECTION II
TASK II SENSITIVITY STUDY

The objective of this sensitivity study was to determine the parameters that influence the braking distance of the F-111A, KC-135 and B-52H. Only those parameters which vary during the normal operation of the airplane were considered. Parameter variations involving modification of the brake system or dependent upon pilot input were not considered.

The data used in the brake control simulator for the three aircraft were supplied primarily by the USAF. A list of documents used during data acquisition may be found in the reference list (References 3 thru 23). The data in many cases were reduced to the form required for use in the simulator.

As a starting point, a baseline airplane was defined for each aircraft. The baseline airplane represents an aircraft in a three-point taxi attitude and of typical (mid-range) landing weight, approach speed, center-of-gravity location, landing flap setting, and engine thrust. The actual parameters required for the airplane simulator are defined in Table 1. Table 2 lists the baseline values used for each airplane. In some cases insufficient data was available to define an airplane parameter, in these cases a value was assumed based on experience and engineering judgment. Table 3 lists the parameters (for each aircraft) for which an assumption was necessary. As pointed out in the table, brake parameters and strut damping values were most often undefined.

During the sensitivity study each parameter was changed and the new value of braking distance was evaluated on the simulator. Some of the variables were not independent, and those groups of interrelated parameters were varied appropriately together. An example of this is stall speed and gross weight. During previous work the range over which a parameter was varied represented a normal operating range, however for this study parameters were varied to their maximum (minimum) allowable operating values.

Table 1.—Definition of Simulator Parameters

PARAMETER	DEFINITION	UNIT
AIRPLANE PARAMETERS		
AW	Effective wing area	ft^2
CD	Drag coefficient	
CDD	Drag coefficient without spoilers	
CL	Lift coefficient	
CLD	Lift coefficient without spoilers	
FEO	Engine idle Thrust at zero velocity	lbf
HB	Height of CG above ground	ft
IYY	Mass moment of inertia, pitch	$ft\text{-}lb\text{-}sec^2$
KE	Change of idle thrust with velocity	lbf-sec/ft
LA	Nose gear to CG distance	ft
LB	Main gear to CG distance	ft
NB	Number of brakes per main strut	
NBA	Number of main gear brakes per airplane	
NBN	Number of nose gear wheels	
NS	Number of main gear struts per airplane	
RHO	Air density	$lbf\text{-}sec^2/ft^4$
VI	Initial airplane velocity	ft/sec
VSTOP	Final airplane velocity	ft/sec
WA	Weight of airplane	lbf
BRAKE PARAMETERS		
KP	Torque peaking gain	
MB	Mass of brake heat sink	lbm
OMGP	Wheel velocity at start of torque peaking	rad/sec
PC	Retractor spring pressure	psi
TBG	Torque gain	ft-lbf/psi
THBB	Temperature at initiation of fade	^oF
WN	Natural frequency of torque response	Hz
ZETA	Damping ratio of torque response	
TIRE PARAMETERS		
D	Tire diameter	in.
DO	Tire deflection	in.
IW	Mass moment of inertia of tire, wheel and brake	$ft\text{-}lbf\text{-}sec^2$

Table 1.—Definition of Simulator Parameters (Concluded)

PARAMETER	DEFINITION	UNIT
	TIRE PARAMETERS (Continued)	
PI	Tire operating inflation pressure	psi
PR	Tire rated inflation pressure	psi
RR	Tire rolling radius	ft
RT	Tire torque radius	ft
	STRUT PARAMETERS	
CO	Main gear vertical damping coefficient	lbf-sec/ft
CON	Nose gear vertical damping coefficient	lbf-sec/ft
CS	Main gear fore-aft damping coefficient	lbf-sec/ft
CT	Torsional Damping between strut and brake	lbf-ft-sec
IS	Mass moment of inertial of main gear strut	ft-lbf-sec^2
KO	Main gear vertical stiffness	lbf/ft
KON	Nose Gear vertical stiffness	lbf/ft
KS	Main gear fore-aft stiffness	lbf/ft
L	Effective strut length	ft
MS	Effective mass of strut	lbf-sec^2/ft

Table 2.—Baseline Values Used in Airplane Simulation

PARAMETER	DEFINITION	UNIT	AIRPLANE MODEL		
			B-52	KC-135	F-111
AIRPLANE PARAMETERS					
AW	Effective wing area	ft^2	4000	2435	525
CD	Drag coefficient		321	.202	217
CDO	Drag coefficient without spoilers		.257	.131	.144
CL	Lift coefficient		.305	.310	28
CLO	Lift coefficient without spoilers		1.000	.860	1.05
FEU	Engine idle thrust at zero velocity		4800	2400	904
HB	Height of CG above ground	ft	13.49	8.633	6.86
IYY	Mass moment of inertia, pitch	ft-lb-sec^2	5.589×10^6	3.761×10^6	2.08×10^5
KE	Change of idle thrust with velocity	lbf-sec/ft	-10.65	-5.325	-1.258
LA	Nose gear to CG distance	ft	26.39	42.5	21.62
LB	Main gear to CG distance	ft	21.36	3.15	2.77
NB	Number of brakes per main strut		2	4	1
NBA	Number of main gear brakes per airplane		4	8	2
NBN	Number of nose gear wheels		2	2	2
NS	Number of main gear struts per airplane		4	2	2
RHO	Air density	lbf-sec^2/ft^4	.00238	.00238	.00239
VI	Initial airplane velocity	ft/sec	152	209	219.8
VSTOP	Final airplane velocity	ft/sec	24	24	24
WA	Weight of airplane	lbf	290000	185000	57000
BRAKE PARAMETERS					
KP	Torque peaking gain		1.25	1.25	1.25
MB	Mass of brake heat sink	lbm	167.	155.6	138.
OMGP	Wheel velocity at start of torque peaking	rad/sec	25.0	25.0	17.56
PC	Retractor spring pressure	psi	65.	50	150
TBG	Torque gain	ft-lbf/psi	19.7	24.0	18.0
THBB	Temperature at initiation of fade	^oF	600	500.0	700.
WN	Natural frequency of torque response	Hz	40.0	40.0	40
ZETA	Damping ratio of torque response		.707	.707	.707
TIRE PARAMETERS					
D	Tire diameter	in.	55.60	48.25	46.5
DD	Tire deflection	in.	2.55	2.11	3.02
IW	Mass moment of inertia of tire, wheel, and brake	ft-lbf-sec^2	46.23	18.92	13.2
PI	Tire operating inflation pressure	psi	200.0	140.0	155.
PR	Tire rated inflation pressure	psi	290.0	150.0	178.
RR	Tire rolling radius	ft	2.25	1.952	1.85
RT	Tire torque radius	ft	2.10	1.835	1.68
STRUT PARAMETERS					
CO	Main gear vertical damping coefficient	lbf-sec/ft	13490.0	16400	4440
CON	Nose gear vertical damping coefficient	lbf-sec/ft	13663.0	14000	2670
CS	Main gear fore-aft damping coefficient	lbf-sec/ft	1082.	911	549
CT	Torsional Damping between strut and brake	lbf-sec-ft	546.	449	101
IS	Mass moment of inertia of main gear strut	ft-lbf-sec^2	5.15	1.81	1.24
KO	Main gear vertical stiffness	lbf/ft	81900	136000	29300
KON	Nose gear vertical stiffness	lbf/ft	81900	52000	16900
KS	Main gear fore-aft stiffness	lbf/ft	470400	508200	376000
L	Effective strut length	ft	4.525	6.04	1.91
MS	Effective mass of strut	lbf-sec^2/ft	62.17	40.9	19.97

Table 3.—Assumed Airplane Parameters

B-52	KC-135	F-111A
AIRPLANE PARAMETERS		
CL CD		
BRAKE PARAMETERS		
KP OMGP THBB WN ZETA	KP OMGP THBB WN ZETA	KP OMGP THBB WN ZETA
STRUT PARAMETERS		
CO CON CS CT	CO CON CS CT	CO CON CS CT

SECTION III
SENSITIVITY STUDY TEST CONDITIONS

The sensitivity study involved changing a parameter or group of parameters to analyze the resulting influence on braking distance. The test conditions, as listed in Table 4, were performed on the analog-hardware simulator to determine braking distance. Table 5 lists the parameters changed and the numerical value of the parameters associated with each test condition for the three aircraft.

Nine sensitivity tests were formulated to analyze the sensitivity of the various aircraft systems to a parameter change. The tests were performed selectively at each test condition. The nine sensitivity tests have been divided into three major categories. The categories and the tests associated with each are as follows:

- Stability studies.

  Test 1 – strut stability

- Performance studies:

  Test 2 – touchdown dynamics

  Test 3 – stabilized landing

  Test 4 – mu steps

  Test 5 – wet runway

- Hydraulic system studies:

  Test 6 – frequency response

  Test 7 – step response

  Test 8 – antiskid valve characteristics

  Test 9 – brake pressure – volume characteristics

A detailed description of the test procedure and sequence can be found in Volume II. The three major categories of sensitivity tests are briefly described below to point out their general significance.

1. STABILITY STUDIES

System stability is directly related to stopping performance. Severe instability can result in the loss of braking and can cause serious safety hazards. The study's purpose was to evaluate the ability of a brake control system to contribute to the fore-aft stability of the gear.

Table 4.—Test Conditions

Baseline Study

Nominal values of all parameters

Parametric Studies

Airplane

1. Weight

   a. Maximum, with VI effect
   b. High intermediate with VI
   c. Low intermediate with VI
   d. Minimum with VI
   e. Maximum without VI effect
   f. High intermediate without VI
   g. Low intermediate without VI
   h. Minimum without VI

2. Center of Gravity

   a. Forward
   b. Aft

3. Brake Application Speed

   a. + 5 knots
   b. + 10 knots
   c. + 20 knots
   d. + 30 knots
   e. - 5 knots
   f. - 10 knots

4. Aerodynamics

   a. No spoilers
   b. 80% effective spoilers
   c. 60% effective spoilers
   d. 40% effective spoilers
   e. 20% effective spoilers
   f. 120% engine idle thrust
   g. 110% engine idle thrust
   h. 90% engine idle thrust
   i. 80% engine idle thrust

5. Pilot Technique

   a. 75% of full metered pressure
   b. 50% of full metered pressure

Table 4.—Test Conditions (Concluded)

Parametric Studies (Continued)

Runway and Environmental System

1. Wind

   a. 5 knots
   b. 10 knots
   c. 15 knots
   d. 20 knots
   e. -5 knots
   f. -10 knots

2. Air Density

   a. Hot day ($83^{o}F/28^{o}C$), high altitude (5000 ft)
   b. Cold day ($-60^{o}F/-51^{o}C$), sea level

Landing Gear Systems

1. Mu-Slip Curves

   a. Flat μ-σ peak
   b. Low tire heating
   c. Tire inflation pressure 80% of nominal
   d. Tire inflation pressure 120% of nominal

Table 5.—Parameter Values

Test Condition and Parameter Changed	Airplane Model		
	B-52	KC-135	F-111
Airplane Parameters			
1a Maximum Landing Weight with VI			
WA	*	300000	80000
VI		267.3	261.5
IYY x 10^{-6}		4.927	.225
1b High Landing Weight with VI	*		
WA		242500	68500
VI		240.8	241.5
IYY x 10^{-6}		4.344	.217
1c Low Landing Weight with VI	*		
WA		142500	52900
VI		183.3	211.0
IYY x 10^{-6}		3.330	.205
1d Minimum Landing Weight with VI	*		
WA		125000	48800
VI		171.1	202.3
IYY x 10^{-6}		3.153	.202
1e Maximum Landing Weight without VI			
WA	450000	300000	80000
IYY x 10^{-6}	8.16	4.927	.225
1f High Landing Weight without VI			
WA	370000	242500	68500
IYY x 10^{-6}	6.87	4.344	.217
1g Low Landing Weight without VI			
WA	245000	142500	52900
IYY x 10^{-6}	4.87	3.330	.205
1h Minimum Landing Weight without VI			
WA	20000	125000	48800
IYY x 10^{-6}	4.14	3.153	.202
2a Forward Center of Gravity			
% MAC	17	18	23
LA	24.33	40.89	19.41
LB	25.42	4.77	4.98
IYY x 10^{-6}	4.505	3.114	.2035

* TEST NOT COMPATIBLE WITH STANDARD B-52 OPERATION

Table 5.—Parameter Values (Continued)

Test Condition and Parameter Changed	Airplane Model		
	B-52	KC-135	F-111
Airplane Parameters			
2b Aft Center of Gravity			
% MAC	35	35	60
LA	28.46	44.32	22.76
LB	21.29	1.35	1.64
IYY x 10^{-6}	7.515	4.635	.221
3a Brake Application Speed + 5 Knots			
VI	160.4	217.4	228.2
3b Brake Application Speed + 10 Knots			
VI	168.9	225.9	236.7
3c Brake Application Speed + 20 Knots			
VI	185.8	242.8	253.6
3d Brake Application Speed + 30 Knots			
VI	202.7	259.7	270.5
3e Brake Application Speed - 5 Knots			
VI	143.6	200.6	211.4
3f Brake Application Speed - 10 Knots			
VI	135.2	192.1	202.9
4a No Spoilers			
CL	1.0	.860	1.05
CD	.257	.131	.144
4b 80% Effective Spoilers			
CL	.444	.420	.434
CD	.3082	.1878	.2184
4c 60% Effective Spoilers			
CL	.583	.530	.588
CD	.2954	.1736	.1998
4d 40% Effective Spoilers			
CL	.722	.640	.742
CD	.2826	.1594	.1812

Table 5.—Parameter Values (Continued)

Test Condition and Parameter Changed	Airplane Model		
	B-52	KC-135	F-111
Airplane Parameters			
4e 20% Effective Spoilers			
CL	.861	.750	.896
CD	.2698	.1452	.1626
4f 120% Engine Idle Thrust			
FEO	5760	2880	1085
KE	-8.52	-4.26	-1.006
4g 110% Engine Idle Thrust			
FEO	5280	2640	994
KE	-9.59	-4.793	-1.132
4h 90% Engine Idle Thrust			
FEO	4320	2160	814
KE	-11.72	-5.858	-1.384
4i 80% Engine Idle Thrust			
FEO	3840	1920	723
KE	-12.78	-6.39	-1.51
5a 75% of Full Metered Pressure	-	-	-
5b 50% of Full Metered Pressure	-	-	-
Runway and Environmental System			
1a 5 Knots Wind			
VW	8.4	8.4	8.4
1b 10 Knot Wind			
VW	16.8	16.8	16.8
1c 15 Knot Wind			
VW	25.2	25.2	25.2
1d 20 Knot Wind			
VW	33.7	33.7	33.7

Table 5.—Parameter Values (Concluded)

Test Condition and Parameter Changed	Airplane Model		
	B-52	KC-135	F-111
Runway and Environmental System			
1e - 5 Knot Wind VW	- 8.4	- 8.4	- 8.4
1f - 10 Knot Wind VW	- 16.8	- 16.8	- 16.8
2a Hot Day RHO	.00189	.00189	.00189
2b Cold Day RHO	.00309	.00309	.00309
Landing Gear Systems			
1a Flat μ-σ Peak	Change Mu-Slip Curve		
1b Low Tire Heating	Change Mu-Slip Curve		
1c Tire Inflation Pressure 120% of Nominal	Change Mu-Slip Curve		
1d Tire Inflation Pressure 80% of Nominal	Change Mu-Slip Curve		

2. PERFORMANCE STUDIES

The performance studies provide a measure of the performance capability of the brake system. The tests performed fall into two categories. The first defines the operation of the airplane under stable landing conditions. The second evaluates the ability of the brake system to adapt to the typical dynamic operating conditions encountered during an actual landing.

3. HYDRAULIC SYSTEM STUDIES

The hydraulic system studies measure the response of the antiskid valve, control box, and the actual brake hydraulic system. Specific tests were designed to define both the overall and component performance of the system. The results provide an insight into aircraft braking system performance and can be used to further improve some of the systems.

The test conditions as listed in Table 4 were changed from previous work (Reference 1) to provide a more comprehensive and significant test program. Parameter variations were generally made in smaller increments and changed over a wider range. The numerous landing gear, pilot dependents, and hydraulic system parametric changes which were included in the previous sensitivity tests (Reference 1) were excluded, because they are not realistic and/or relevant operational test conditions.

SECTION IV
TEST RESULTS

1. BASELINE

A baseline airplane was defined for each of the three aircraft studied. The baseline configuration is meant to represent a typical aircraft during its landing phase. The numerical values of the baseline parameters are listed in Table 2. The values, when used in the brake control simulation, establish a unique distance versus ground friction relation for each airplane.

Figure 3 relates the braking distance and peak available ground friction (peak available mu) for each of the three baseline airplanes. The data is associated with the braking segment only, the distances shown represent only braked distances, approach, flare, and transition distances are excluded. Peak available mu (such as shown in Figure 3) is a computer input that defines the maximum value of friction available between the tire and ground during a test condition. The value of peak available friction was held constant throughout the entire braking run to generate the distance-friction data of Figure 3.

An ideal brake system should operate at the peak available friction value during the entire stop. For an actual brake system, the instantaneous coefficient of friction at the tire-runway interface depends on the condition of the runway, tire properties, tire slippage and antiskid system characteristics. Consequently, the brake system actually functions over a range of friction somewhat lower than the peak value. Since the actual antiskid system has been used in the brake control simulation the distances produced reflect the efficiency of the braking system.

Figure 4 is a plot of baseline braking distance efficiency as a function of peak available friction for each of the three test airplanes. Braking distance efficiency is the ratio (in percent) of perfect braking distance to actual braking distance The efficiency curves were determined using the data of Figure 3. A detailed definition of braking distance efficiency and perfect braking distance is given in Section V.

The KC-135 and F-111 efficiency curves are quite typical of second generation (early 1960's) brake control systems. The B-52 efficiency curve is unique and requires explanation. The B-52 brake control system is a first generation (early 1950's) system. The system was designed as a tire saver (preventing tire blow-out due to wheel lockup) with little attention to braking efficiency. The efficiency curve has three distinct regions; .05 to .225 mu, .225 to .3 mu, and .3 to .6 mu. Each of the three regions is characterized by a unique form of brake control operation. At values of friction above .3 the B-52 is torque limited during the entire braking run (Figure 5a). Torque limiting occurs when the torque due to friction force at the tire-runway interface (ground torque) exceeds the available brake torque. This is typical of an undersized brake.

In the region of .225 to .3 mu a combination of brake control activity and torque limiting occurs (Figure 5b). Skidding activity occurs during the first portion of the braking segment, when insufficient ground friction and/or vertical tire load exists so as to cause torque limiting. As lift decreases, tire loading increases to the point where ground torque exceeds brake torque

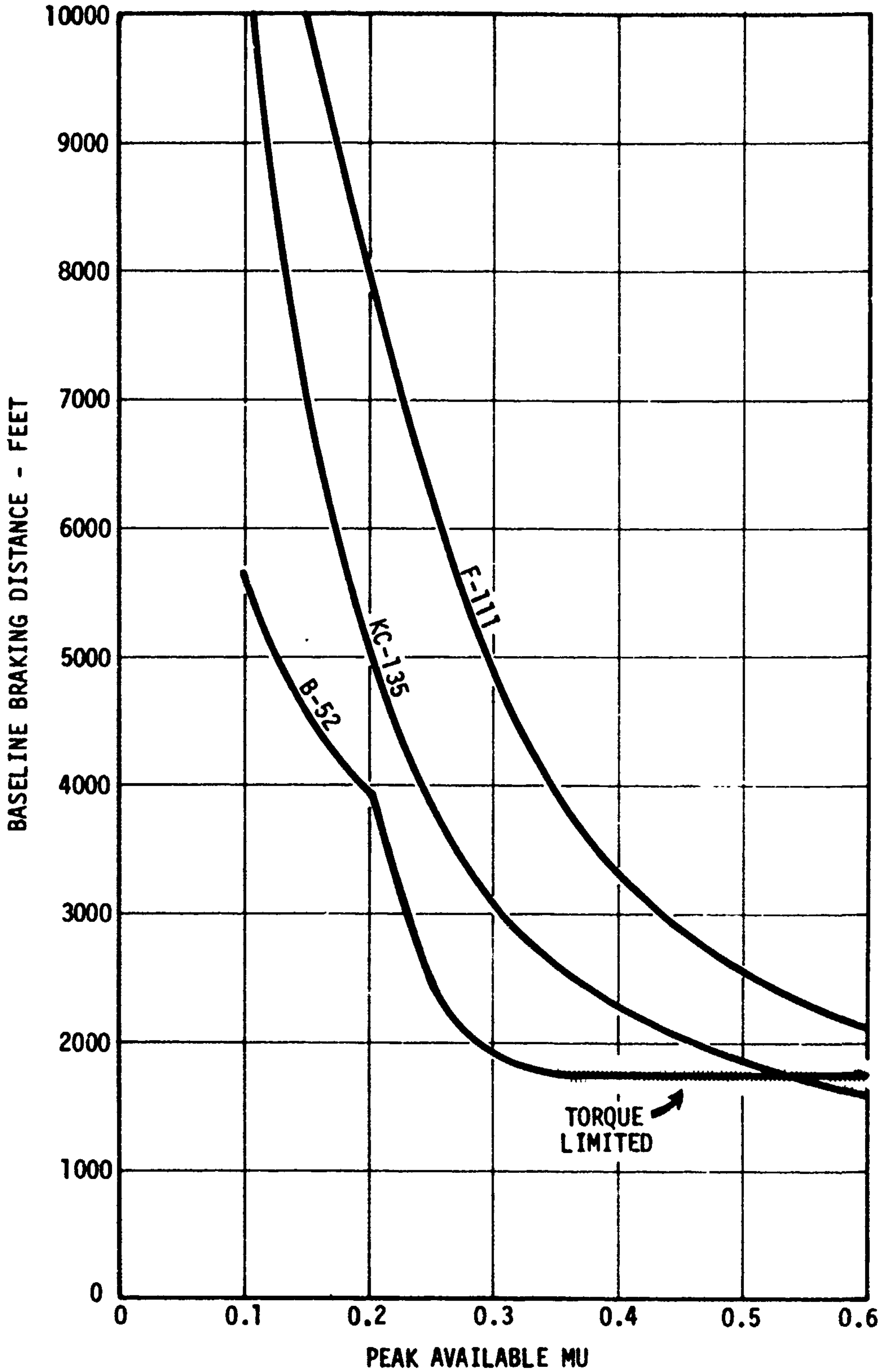

Figure 3.—Baseline Braking Distance vs. Peak Available Mu

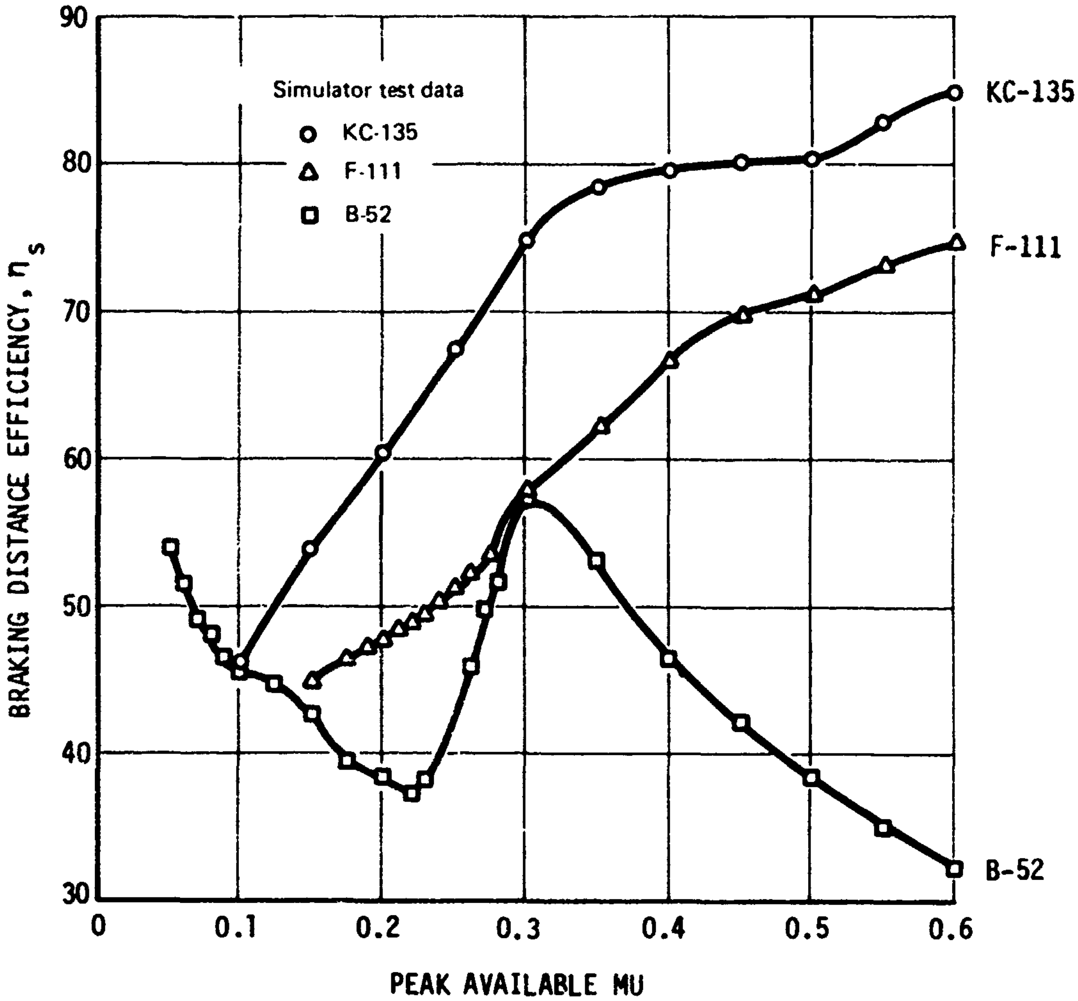

Figure 4.—Baseline Braking Efficiency vs. Peak Available Mu

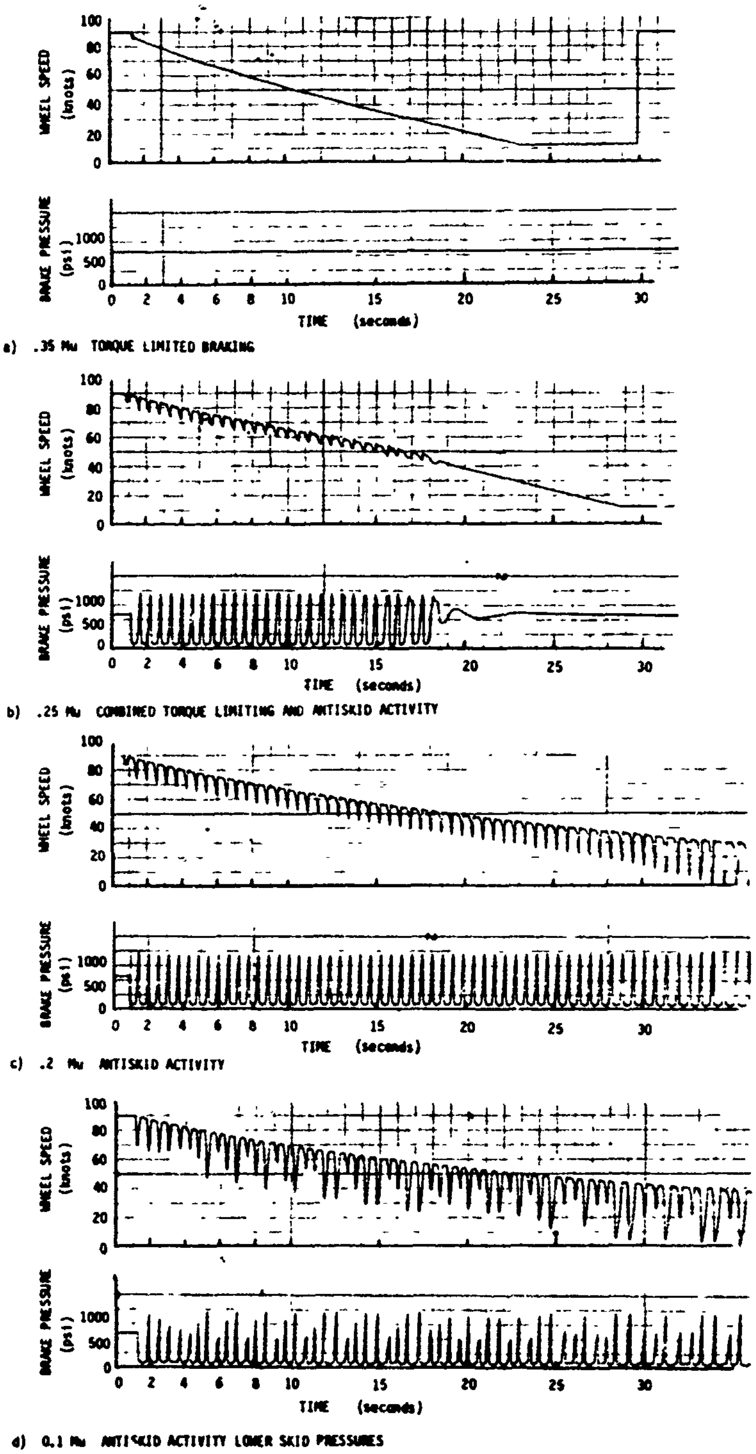

Figure 5.—B-52 H Braking Activity Comparison

resulting in torque limiting and the elimination of skid activity. The duration of the initial skid activity increases as ground friction decreases, and results in decreased braking distance efficiency. The decrease in efficiency is due to the excessively long time between skids, when brake pressure is zero.

From 0.05 to .225 mu antiskid activity occurs during the entire braking segment. In this region stopping efficiency increases with decreasing ground friction. This phenomenon is a result of the decreased level of pressure (brake torque) that is required to cause a tire to skid. As friction decreases the system is able to make more efficient use of available brake pressure.

2. SENSITIVITY

The sensitivity study of the three airplanes involved changing a parameter, or group of parameters, and observing the effect on braking distance. The braking distance associated with a change was then compared to the baseline airplane distance at the same value of peak available mu. In this manner, the effect of a specific change could be analyzed quantitatively.

The braking data obtained from the brake control simulator represents an absolute distance. To facilitate the analysis of a parameter change, a normalized distance has been introduced. It is termed "percent baseline braking distance". The use of a normalized distance allows the three airplanes to be compared simultaneously. Percent baseline braking distance is defined in Section V.

Each airplane uses its own baseline distances as normalizing factors. Distances longer than baseline are greater than 100% and shorter distances are reflected as less than 100%.

The braking distance results from the sensitivity study have been reduced to bar charts, Figure 6, pages 22 through 26. The test conditions corresponding to each bar chart are given to the left and below the chart. On each graph, the baseline braking distance percentage for the three airplanes has been plotted for four values of peak available mu: 0.6, 0.4, 0.2, and 0.1, (0.15 for F-111). During initial testing of the F-111 it was found that antiskid system operation on low mu runways (less than .15) was sporadic (See Volume II, Section X). In an attempt to produce consistent data, .15 mu was selected as the minimum runway friction coefficient for testing.

A brief analysis of the results follows. The raw data along with the associated performance indices can be found in Volume II, Section VIII.

A. AIRPLANE FLIGHT CHARACTERISTICS

1. Landing Weight with Initial Velocity Variation (Tests 1a through 1d, Figure 6, page 22)

Landing weight, initial airplane velocity, and mass pitching moment were changed in these tests. The velocity was adjusted to reflect changes in stall speed resulting from a landing weight variation. The mass pitching moment was varied to reflect changes in load distribution. In each test, brake application occurred 0.75 seconds after initiation of a computer run. These tests were not applicable to the B-52 since it is not normal operating procedure to vary brake application velocity.

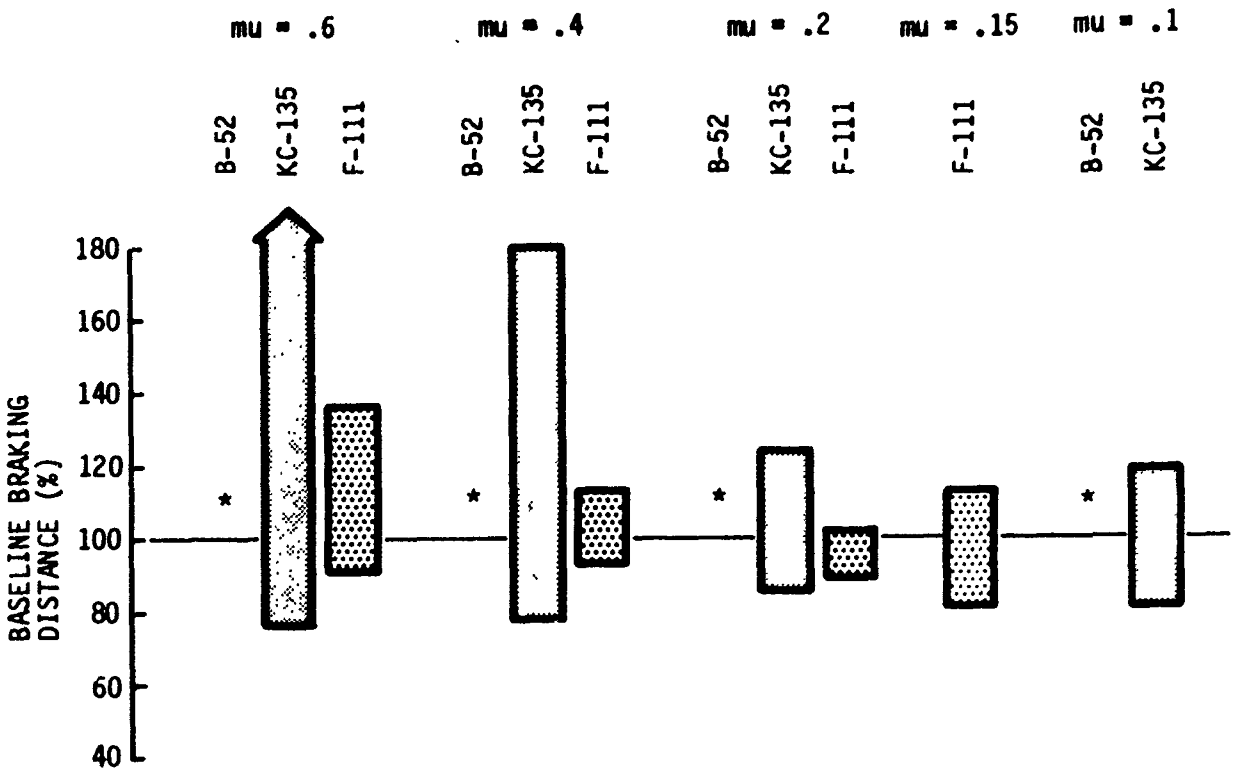

1. LANDING WEIGHT WITH INITIAL VELOCITY VARIATION (Tests 1a through 1b)

* TEST NOT COMPATIBLE WITH STANDARD B-52H OPERATING PROCEDURE

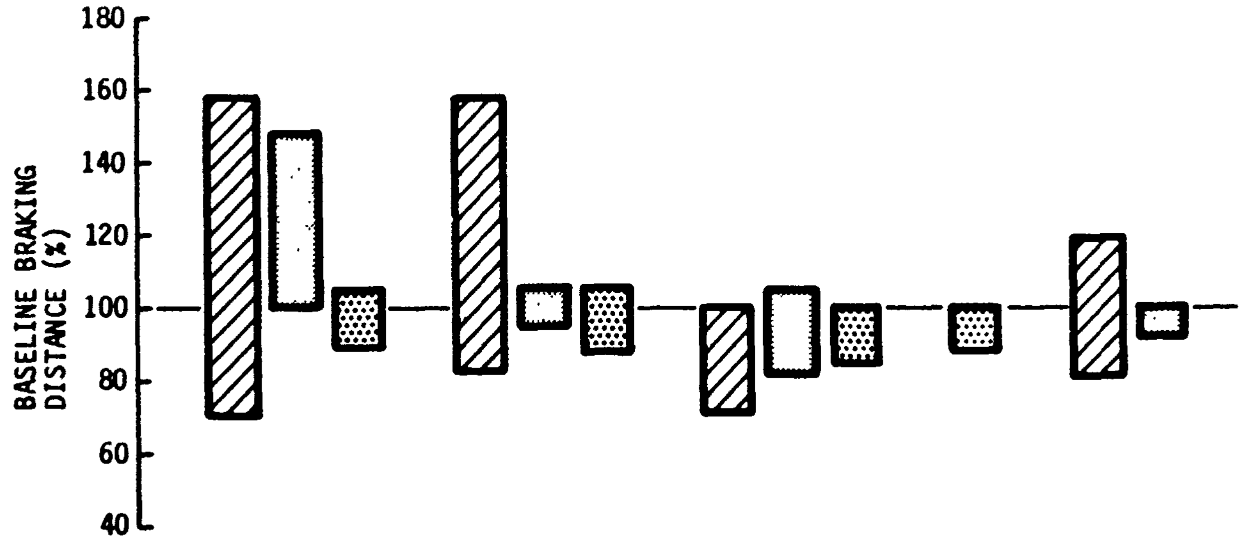

2. LANDING WEIGHT WITHOUT INITIAL VELOCITY VARIATION (Tests 1e through 1h)

Figure 6.—Sensitivity Study Test Results

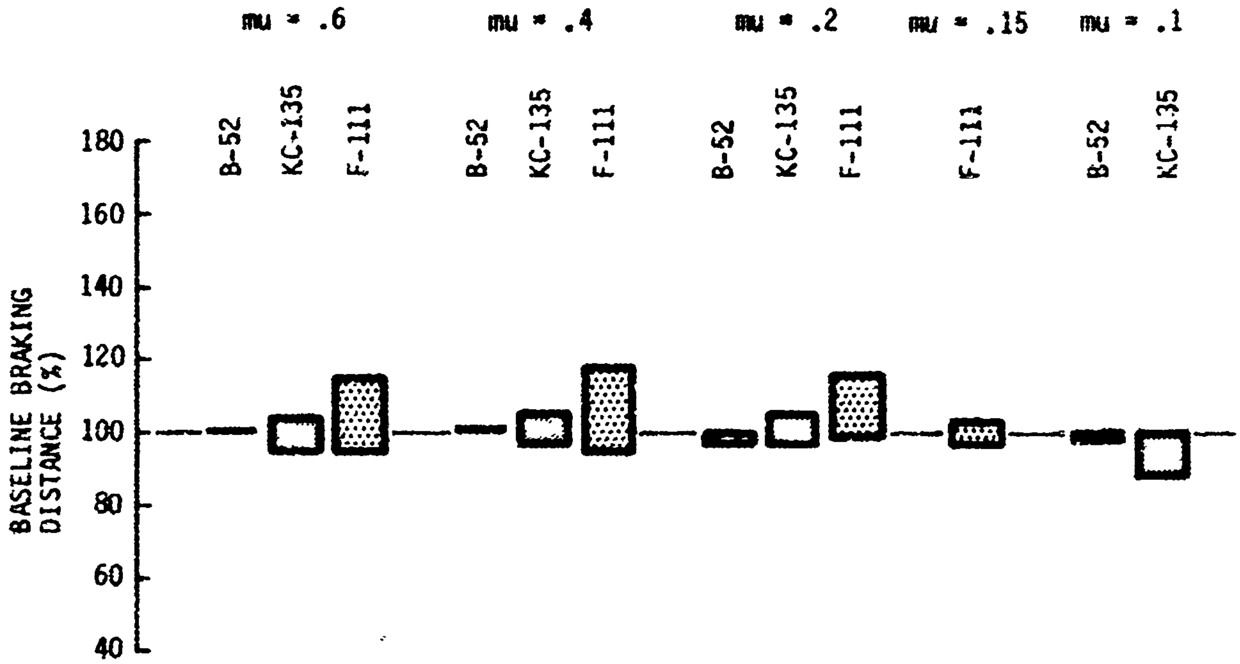

3. CENTER OF GRAVITY (Tests 2a and 2b)

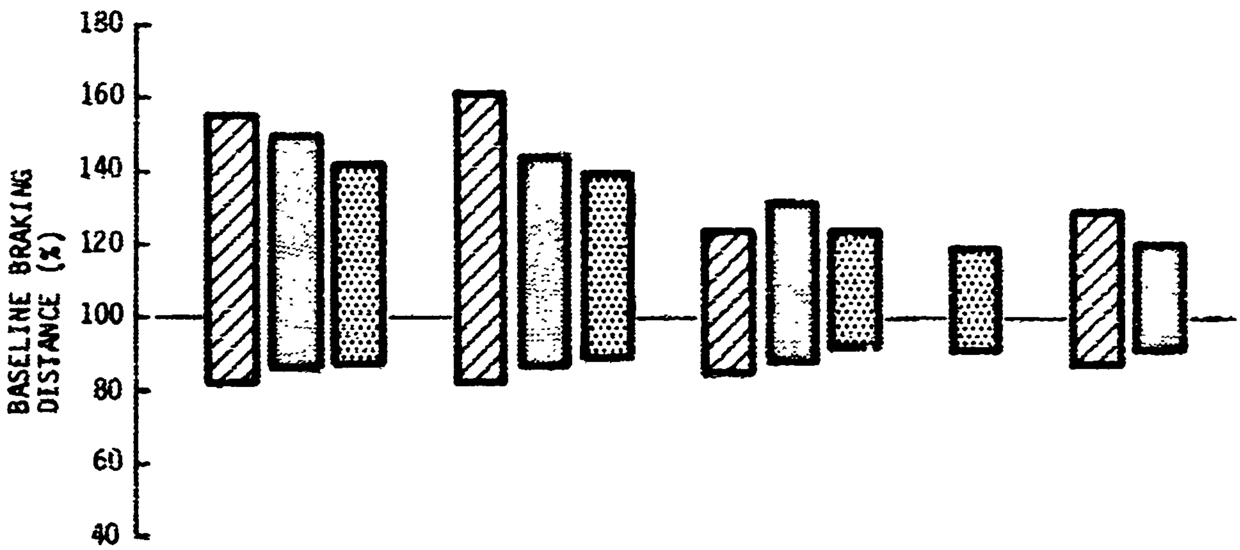

4. BRAKE APPLICATION SPEED (Tests 3a through 3f)

Figure 6.—Sensitivity Study Test Results (Continued)

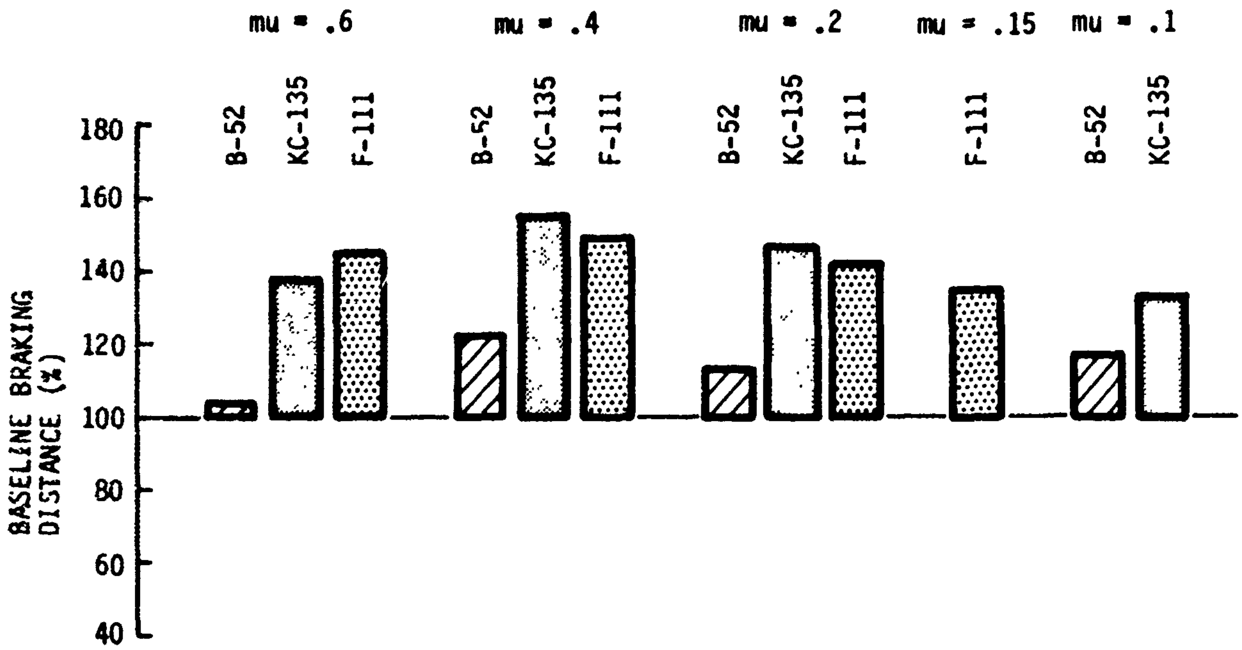

5. SPOILER EFFECTIVENESS (Tests 4a through 4e)

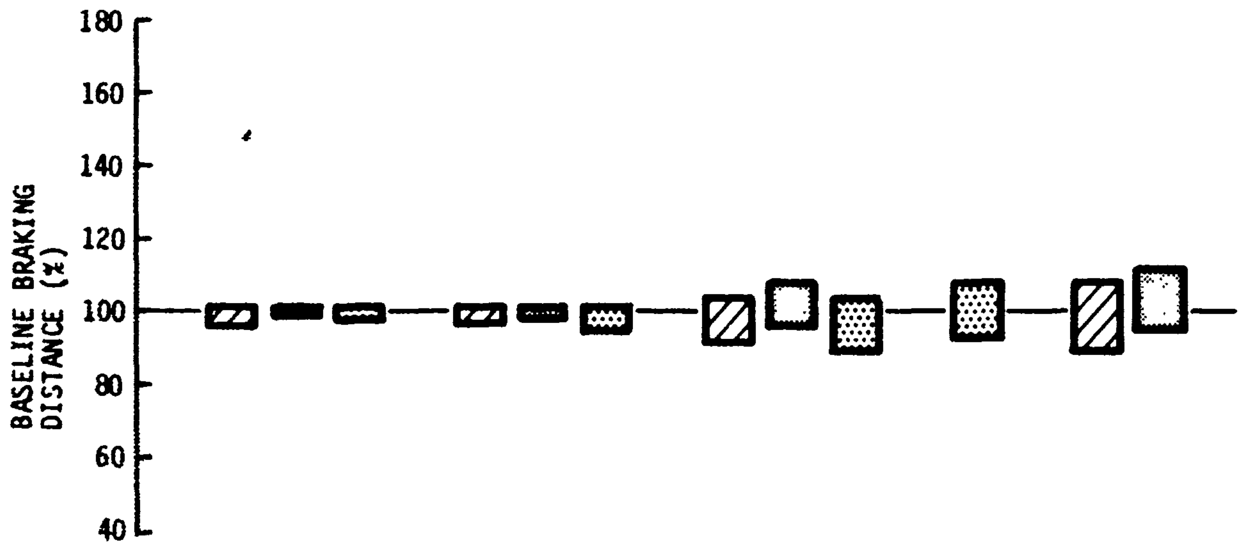

6. ENGINE IDLE THRUST (Tests 4f through 4i)

Figure 6.—Sensitivity Study Test Results (Continued)

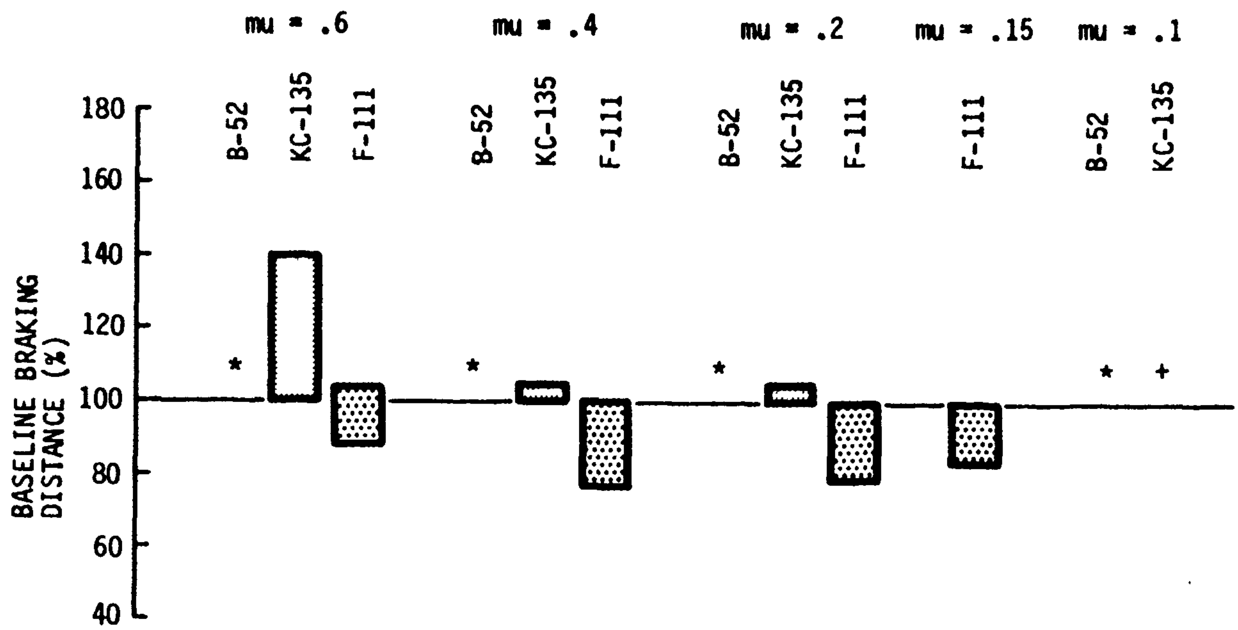

7. METERED PRESSURE (Tests 5a and 5b)

* TEST NOT RUN

+ ANTISKID ACTIVITY WITH VIRTUALLY NO AIRPLANE DECELERATION

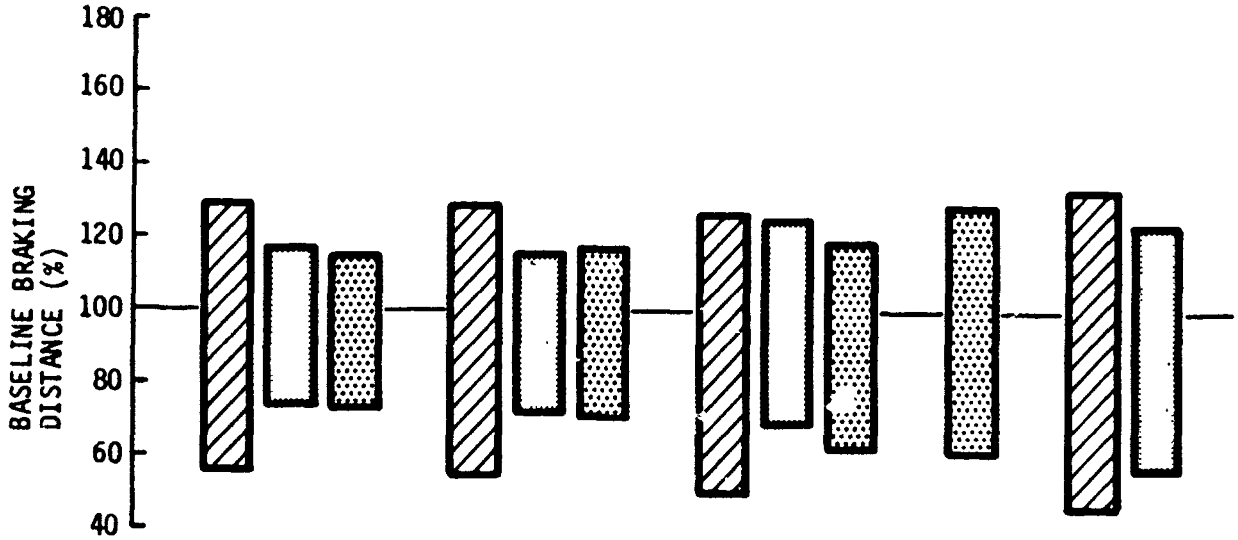

1. WIND (Tests 1a through 1f)

Figure 6.—Sensitivity Study Test Results (Continued)

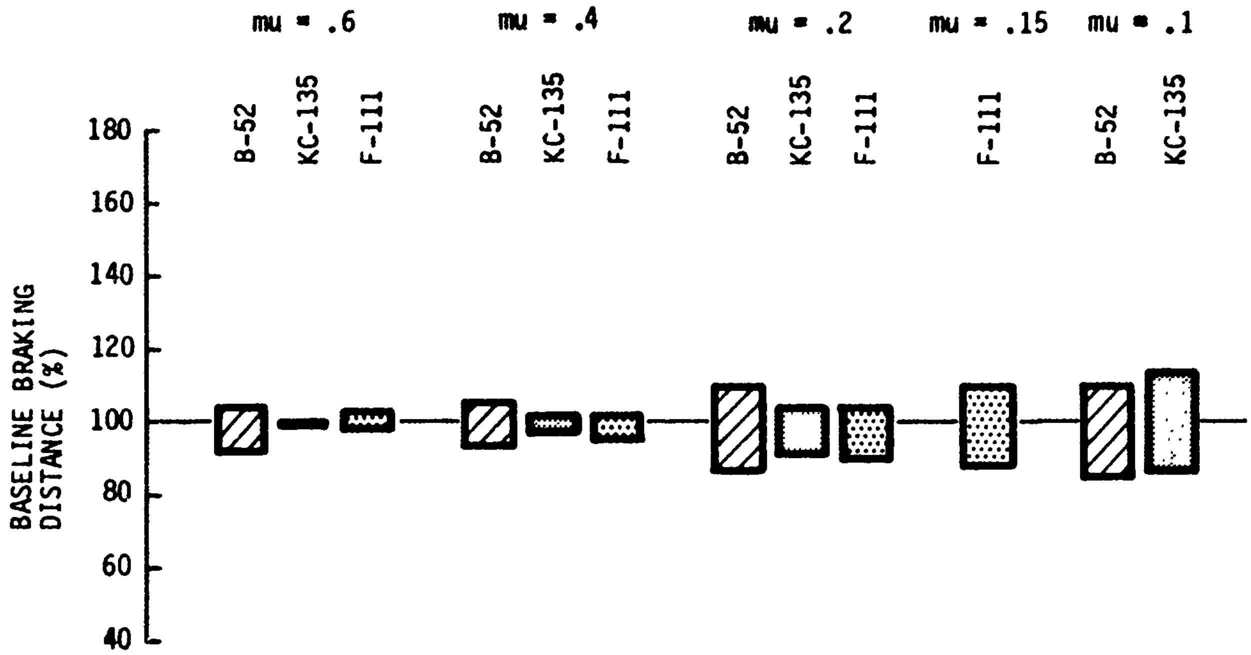

2. AIR DENSITY (Tests 2a and 2b)

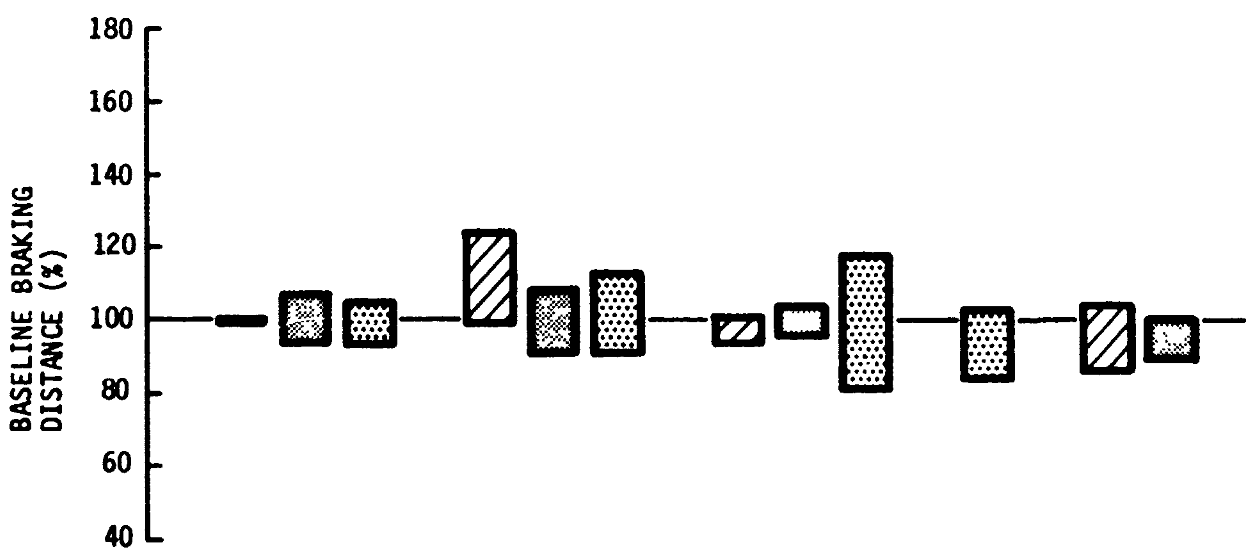

1. MU-SLIP CURVES (Tests 1a through 1d)

Figure 6.—Sensitivity Study Test Results (Continued)

As shown in the bar charts, combined weight, velocity and pitch moment changes resulted in large braking distance variations. The distance variations result from a change in the kinetic energy dissipated during braking.

2. Landing Weight Without Initial Velocity Variation (Tests 1e thru 1h, Figure 6, page 22)

Tests similar to 1a thru 1d were run however the initial airplane velocity was held at its appropriate baseline value. These tests indicate that the airplane weight (and load distribution) has a large effect on braking distance.

3. Center of Gravity (Tests 2a and 2b, Figure 6, page 23)

Results indicate that the aft location of center of gravity causes a decrease in braking distance. This is due to the increased load placed on the main gear, which increased the available braking force. The F-111 appears to be more sensitive to CG changes. This, however, is due in part to the larger range over which the F-111 CG can move. The B-52 has braked nose and main gears, consequently, fore and aft load transfer has no effect on total available braking force (as it does with a brake main gear airplane)

4. Brake Application Speed (Tests 3a thru 3f, Figure 6, page 23)

Brake application speed was varied during these tests. Results indicate that additional braking distance was required to dissipate the increased kinetic energy of the aircraft.

5. Spoiler Effectiveness (4a thru 4e, Figure 6, page 24)

Lift and drag coefficients were varied between full landing spoilers and no spoilers conditions. Braking distance increases as the spoilers become less efficient. The increased braking distance results from: (1) loss of braking force due to increased lift and (2) loss of effective drag force due to lower drag.

6. Engine Idle Thrust (Tests 4f through 4i, Figure 6, page 24)

Increasing engine idle thrust increases the kinetic energy to be dissipated during braking The results indicate that this resulted in longer stopping distances.

7. Metered Pressure (Tests 5a and 5b, Figure 6, page 25)

The results from the metered pressure tests do not show a general stopping distance trend. The variation between aircraft are attributable to valve characteristics, torque limiting characteristics of the brake and skid control system adaptation to conditions. The braking distance of the F-111 was generally reduced as pressure was lowered. The dynamic response of the hydraulic system is slower at lower pressures reducing antiskid cycling, increasing system efficiency and reducing braking distance. The KC-135, however, was largely unaffected by metered pressure changes except at .6 mu where torque limiting occurred.

Metered pressure testing of the B-52 was not done due to an inability to obtain constant lower metered pressures.

B. ENVIRONMENTAL PARAMETERS

1. Wind (Tests 1a through 1f, Figure 6, page 25)

During these tests the relative wind-airplane velocity was maintained, while the airplane-ground velocity and lift and drag forces were changed. Headwinds decrease the airplane kinetic energy to be dissipated during braking resulting in shorter braking distances.

2. Air Density (Tests 2a and 2b, Figure 6, page 26)

Air density was varied to change the lift and drag forces on the airplane. On hot days, both lift and drag decrease, on cold days, they increase. Results indicate that drag has the greater effect on braking distance. On hot days, the distances are longer because of reduced aerodynamic drag.

C. LANDING GEAR SYSTEM

1. Mu-Slip Curves (Test 1a through 1d, Figure 6, page 26)

Variations in the shape of the Mu-slip curves were made to analyze how the wheel, brake and antiskid system reacts to various mu-slip characteristics. The randomness between the different aircraft results from the basic control characteristics of each antiskid system, however it may be generalized that braking distance decreased as the time spent on the backside (negative slope) of the mu-slip curve increased.

SECTION V
PARAMETER EVALUATION CRITERIA

1. PERFORMANCE INDICES

To evaluate the performance of a system, four parameters were used. These performance parameters were

- Airplane braking distance
- Perfect braking distance
- Braking distance efficiency
- % baseline braking distance

A. AIRPLANE BRAKING DISTANCE

Airplane braking distance, X_A, as measured on the analog computer is the distance the airplane travels from brake application to a low-velocity turn-off speed with the brake control system operating.

B. PERFECT BRAKING DISTANCE

Perfect braking distance, X_P, is the distance required to stop an airplane when the friction coefficient at the tire runway interface is at its peak available value during the entire braking run. This is the minimum distance in which the airplane can be stopped at a given friction value. Peak available friction is an input to the computer which can be a fixed value (.05 to .6 typically) or variable (a function of velocity simulating a wet runway).

Friction has been found to be a function of tire slippage at the tire-runway interface (see Figure 7). Maximum braking is realized only when the percent of available friction is 100, this occurs at about 10% slip. A typical antiskid system allows slip to vary from 0 to 100%, resulting in friction values less than peak. Perfect braking distance is produced on the computer by artifically maintaining the percentage of maximum friction at 100.

C. BRAKING DISTANCE EFFICIENCY

Braking distance efficiency, n_s, is the ratio of the perfect braking distance to the braked airplane distance.

$$n_s = X_p/X_A \times 100\%$$

where:

n_s = braking distance efficiency

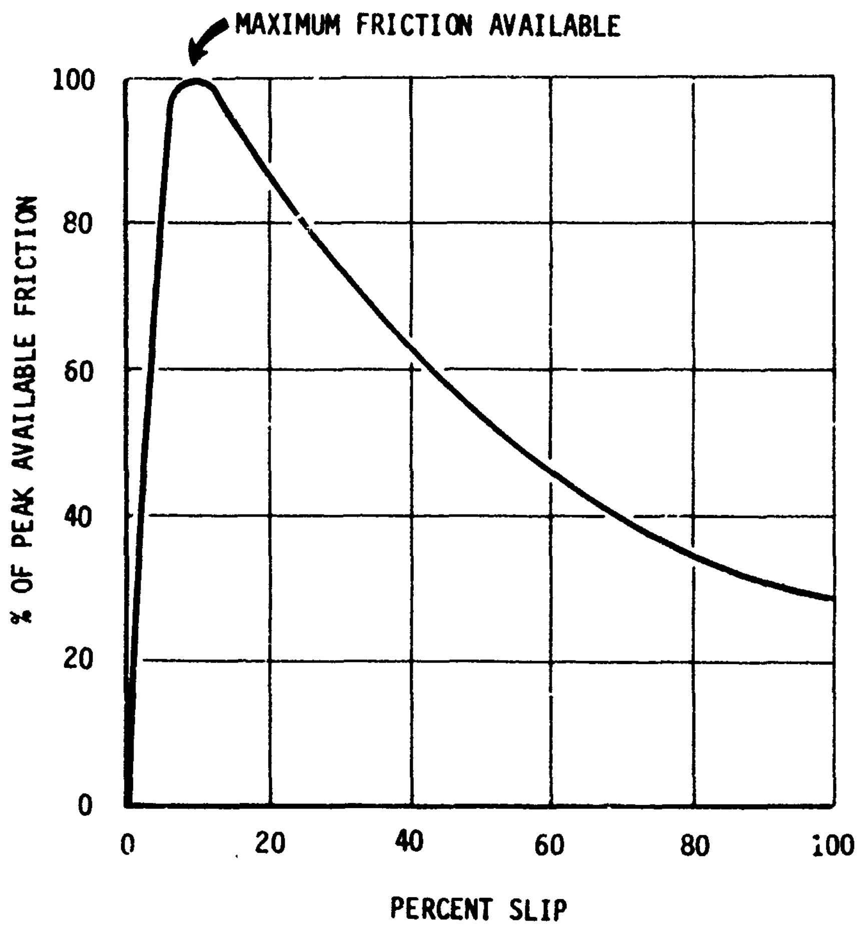

Figure 7.—Mu-Slip Curve

X_p = perfect braking distance

X_A = airplane braking distance

Braking distance efficiency indicates the degree to which the system meets its primary requirement of stopping the aircraft.

D. PERCENT BASELINE BRAKING DISTANCE

Percent baseline braking distance is a dimensionless distance ratio which facilitates the comparison of sensitivity test results. It is the ratio of the braking distance resulting from a parametric change to the baseline braking distance. The baseline braking distance of each aircraft as a function of peak available friction is given in Figure 3.

2. SYSTEM STABILITY

In addition to the four performance indices, a measure was made of the ability of an antiskid system to contribute to system stability. The criterion used to determine system stability was that the system is termed unstable if the main gear strut oscillations diverge and/or strut oscillations cause a reduction in brake pressure. The stability of the system was measured by determining the damping ratio necessary to cause instability.

3. PARAMETER RATING SYSTEM

The final step in the sensitivity analysis of aircraft braking performance was to rate each parameter. To facilitate the rating of a parameter change a normalized distance referred to as "baseline braking distance percentage" was used. The use of this term allows the three airplanes to be analyzed as a group. In order to uniformly and quantitatively rate a parameter change, the following formula was used:

$$PRI = \sum_{i=1}^{n} \frac{\text{Percent baseline braking distance}_i - 100\%}{n}$$

PRI = parameter rating index
n = total number of data points for a particular parameter change

Percent baseline braking distance$_i$ = the baseline braking distance percentage value for the ith data point

The parameter rating index (PRI) as calculated above is the average percentage deviation from the baseline braking distance. Thus, the value of the PRI increases when a parameter change causes larger deviations from the baseline braking distance. The data used in the calculation of the PRI are given in Volume II. Also included are the final PRI values for the dry-stabilized landing conditions.

SECTION VI
SIMULATOR TO AIRPLANE CORRELATION

Meaningful results from a simulator can be obtained only when the dynamic performance duplicates that of the actual system. The brake control simulator used during this study is the culmination of considerable effort including model development, subsystem testing and evaluation, correlation with flight tests, and operational usage.

Verification of a simulated aircraft's performance consists of comparing computer results with results obtained from similar tests conducted during actual airplane flight tests. Typical data required to simulate a specific test condition includes airplane weight, C. G. location, brake application speed, environmental conditions, etc. Key parameters within the simulation can be adjusted until the desired level of correspondence is obtained. The following items are key points that were considered during this study in evaluating and obtaining simulator-to-airplane correlation.

- Stopping distance
- Skidding pressure
- Number of skids
- Depth of skids
- Rate in and out of skids
- General control

No attempt was made to duplicate airplane stopping distance exactly. Instead, emphasis was placed on producing the same basic control characteristics.

The aircraft data and flight test data used for formulation and verification of each airplane simulation was supplied by the Air Force. The data provided for use in the simulation was adequate, the flight test data and associated records used for correlation purposes were, however, limited. Ideally, a number of actual flight test records with documentation of aircraft configuration, initial conditions, stopping distance, etc., are needed to ensure adequate airplane to simulator correlation. In the case of the B-52 no flight test records were available, however, limited records were provided on the KC-135 and F-111. The specific test conditions (KC-135 and F-111) used for correlation are listed in Table 6. The following paragraphs briefly describe correlation procedures for each airplane simulation.

1. B-52

The B-52 brake control system posed unique problems during simulator setup and correlation. The major concern during setup was the locked wheel and skid detector. The detector is the major control element in the brake system. The mechanical nature of the device required that it be simulated on an analog computer. To correctly simulate the unit, an actual aircraft

Table 6.—Correlation Tests

Airplane	Test program or reference document	Test number	Test conditions
F-111A	F-111A Initial Category II Landing Performance Evaluation (See reference 21)	Flight #4 (Dry runway)	WA = 53800 VI = 226.7 fps LA = 20.95 VSTOP = 38.2 fps LB = 3.44 RHO = .00222 FEO = 950 KE = 1.28
		Flight #6 (Wet runway)	WA = 55600 VI = 228 VSTOP = 35.3 LA, LB, FEO, KE, RHO UNCHANGED FROM FLIGHT #4
KC-135	Evaluation of a 5-rotor Brake and Modulated Antiskid System installed on a KC-135A (See reference 21)	2-7 (Dry runway)	WA = 135,200 %MAC = 19.9 VI = 199.62 fps C_L = .30 FEO = 2304 C_D = .155 KE = 5.24
B-52	B-52H flight manual: (See reference 8)	T.0 1B-52H-1-1 Figure A8.11	Case #1 WA = 200,000 Case #2 WA = 290,000 Case #3 WA = 370,000

locked wheel and skid detector was tested in the laboratory to determine its performance. A detailed description of the device, test results and the analog simulation may be found in Volume II, Section III. In addition, stopping procedure for the B-52 is unique and required special consideration. The landing ground run consists of two distinct segments, a pre-braking section and a braking section as shown in Figure 8. Operating manuals for the B-52H instruct the pilot to apply the brakes at 90 knots. Thus, the pre-braking run extends from touchdown to 90 knots. During this segment aerodynamic drag and rolling friction decelerate the airplane until the drag chute is deployed at 135 knots.

Flight test traces, pertaining to performance of the B-52 brake control system, were not available. As a result, the basic control characteristics could not be accurately checked. Verification of the simulator was, however, obtained by comparison of landing distances found in the B-52H flight manual (Reference 8) with distances generated by the simulation. Three aircraft weights were considered, a .02 rolling mu was assumed for the prebrake landing segment. Table 7 shows the simulator results and the flight manual data. The results are not directly comparable (since the flight manual's RCR classification is a qualitative measure of friction), however the range and lower limit of stopping distance are comparable.

The general control performance of the B-52 antiskid system is typical of a first generation skid control system. The control performance is characterized by a series of skids at a rate of about 1 to 2 skids per second. When a skidding wheel is sensed, brake pressure is removed, allowing the wheel to spin-up. However, the wheel goes into another skid as soon as brake pressure is reapplied. This skid cycling and pressure dump-fill pattern is typical of the skid-control operation. Figures 9 and 10 are sample simulator records of antiskid activity occurring during the braking run on intermediate and low friction runways. It was found that the B-52 brake becomes torque limited (see ASD-TR-77-6, Volume II, Section X) at higher values of friction coefficient and/or aircraft weight. This characteristic is noted in the B-52 Flight Manual (Reference 6, page 7-39). Torque limiting results in a constant stopping distance as runway friction increases. This point is alluded to in the B-52 performance data (reference 8), when stopping distance becomes a constant, even though the RCR increases.

2. KC-135

Airplane to simulator correlation was aided by use of an Air Force brake and antiskid system report (Reference 15). This document provides actual flight test data and sample records of wheel and brake pressure time histories for both wet and dry runways. It must be noted that numerous inconsistencies exist in the time histories. Specifically the wheel speed, antiskid voltage and brake pressure for the wet runway conditions do not appear to be compatible with one another. Additionally, the antiskid voltage level in both the wet and dry cases is not consistent with previous experience and current results. Consequently, only the brake pressure and wheel speed time histories along with the braking distances reported in Reference 15, and previous experience with the Mark II antiskid system (found on the KC-135) were used to evaluate simulator correlation.

A portion of flight number 2-7, dry runway, (Reference 15) is shown in Figure 11, along with an equivalent condition obtained from the simulator. The skid control performance

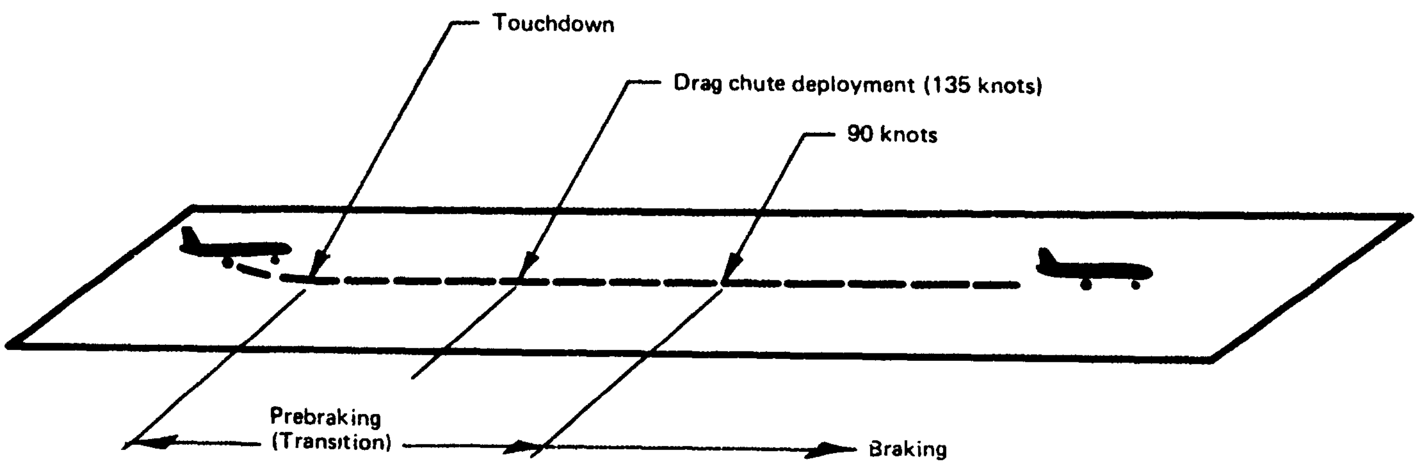

Figure 8.—B-52H Stopping Procudure

Table 7.—Simulator to Airplane Correlation Results, B-52

200,000 LB. LANDING WEIGHT				290,000 LB.				370,000 LB.			
AIRPLANE *		COMPUTER **		AIRPLANE *		COMPUTER **		AIRPLANE *		COMPUTER **	
RCR	X (FT)	MU	X (FT)	RCR	X (FT)	MU	X (FT)	RCR	X (FT)	MU	X (FT)
3	-	.05	7332	3	11400	.05	10891	3	12900	.05	13139
4	8000	.1	6087	4	9400	.1	8666	4	11200	.1	10701
5	6600	.15	5123	5	8400	.15	7377	5	10200	.15	9247
6	5750	.2	4482	6	7500	.2	6755	6	9300	.2	7159
7	5200	.25	4118	7	6900	.25	5249	7	8600	.25	6641
8	4750	.3	3790	8	6500	.3	4823	8	8200	.3	6437
9	4450	.35	2860	9	6200	.35	4685	9	7800	.35	6365
10	4200	.4	2647	10	5800	.4	4632	10	7600	.4	6401
11	3950	.45	2539	11	5600	.45	4616	11	7300	.45	6351
12	3800	.5	2469	12	5400	.5	4596	12	7100	.5	6341
14	3450	.55	2455	14	5100	.55	4563	14	6800	.55	6345
16	3100	.6	2388	16	4800	.6	4564	16	6500	.6	6352
18	2750			18	4500			≥18	6350		
20	2600			≥20	4400						
23	2400										

X = STOPPING DISTANCE FROM TOUCHDOWN
RCR = RUNWAY CONDITION READING
* = DATA COMPILED FROM TO 1B-52H-1-1 FIGURE A8-11
** = COMPUTER GENERATED DISTANCE ASSUMED A ROLLING MU OF .02 PRIOR TO BRAKING, DURING BRAKING MU IS AS SPECIFIED IN THE TABLE

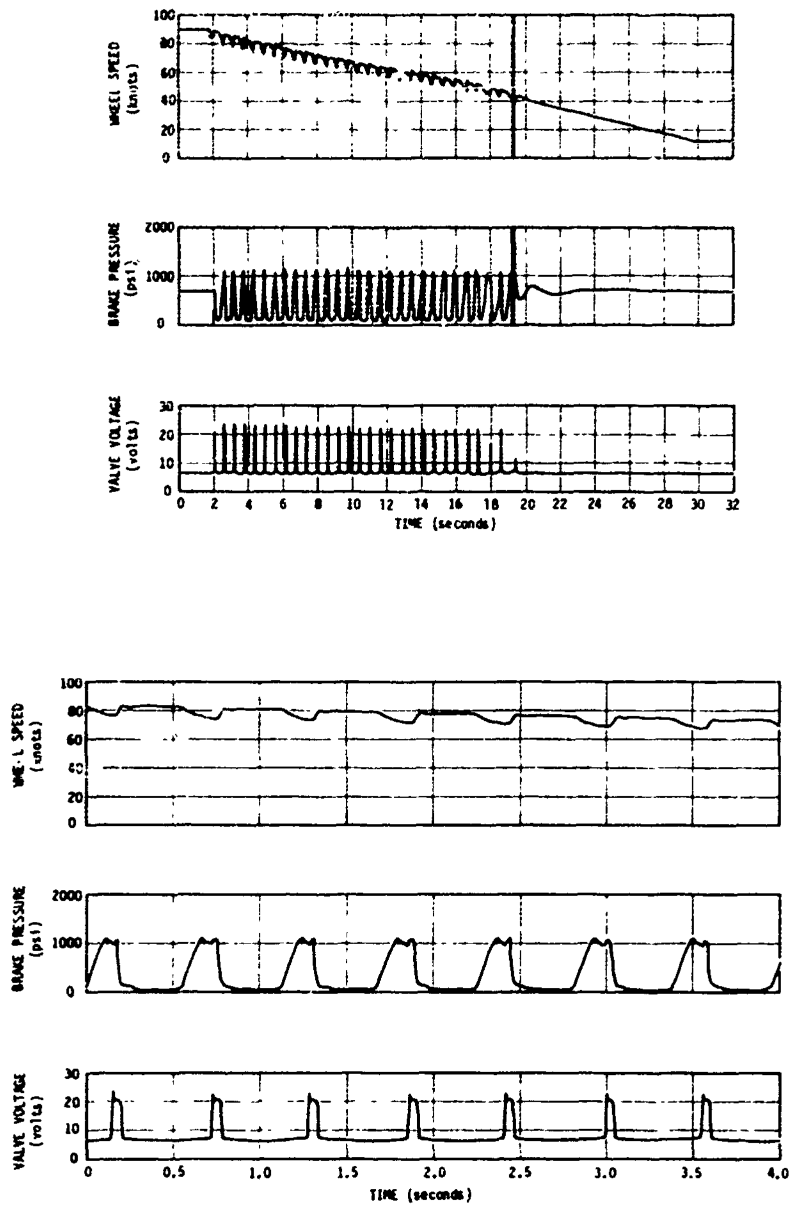

Figure 9.—B-52H Simulator Performance (Baseline Airplane) Intermediate Mu (.25)

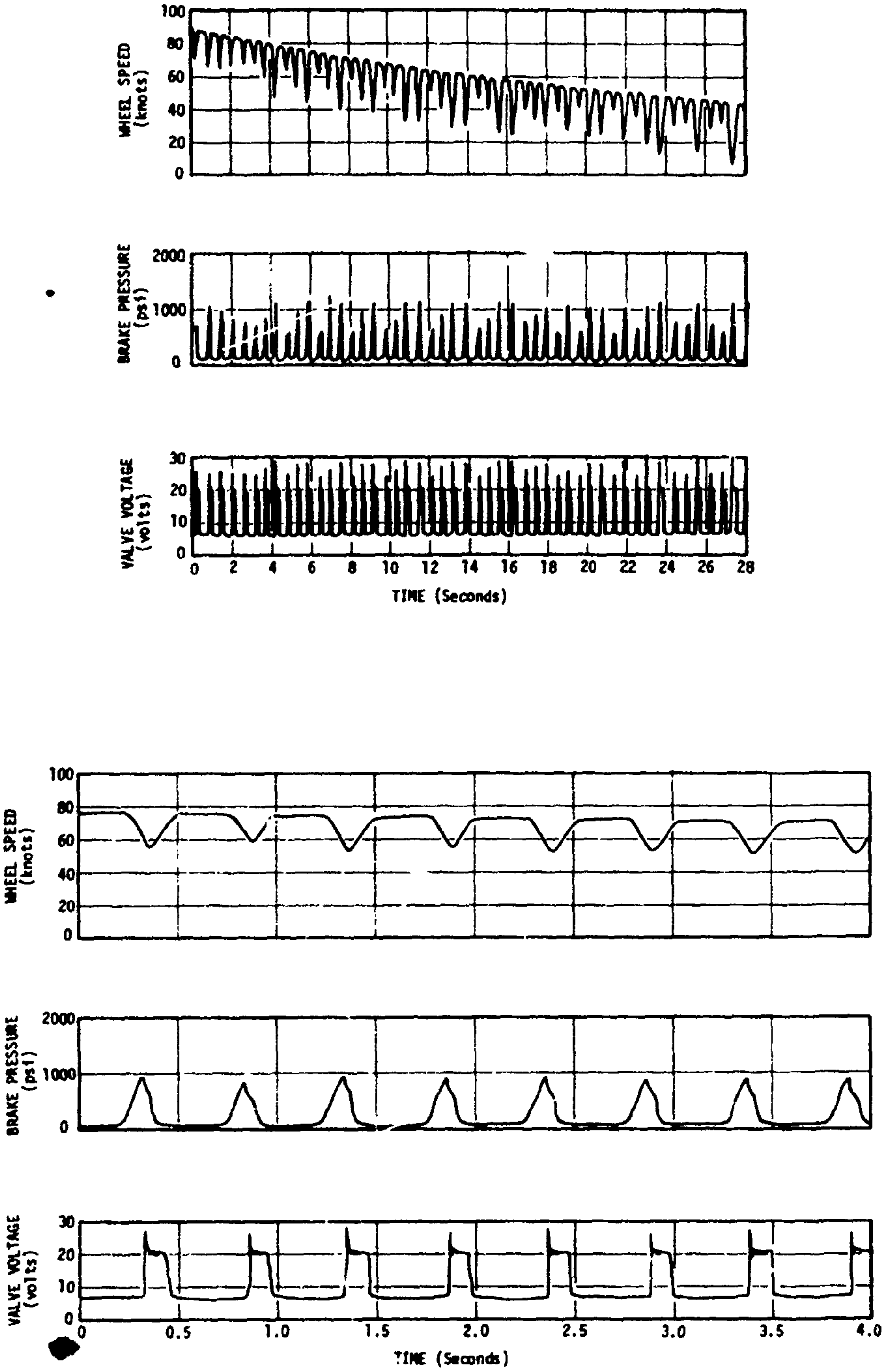

Figure 10.—B-52H Simulator Performance (Baseline Airplane) Low Mu (.10)

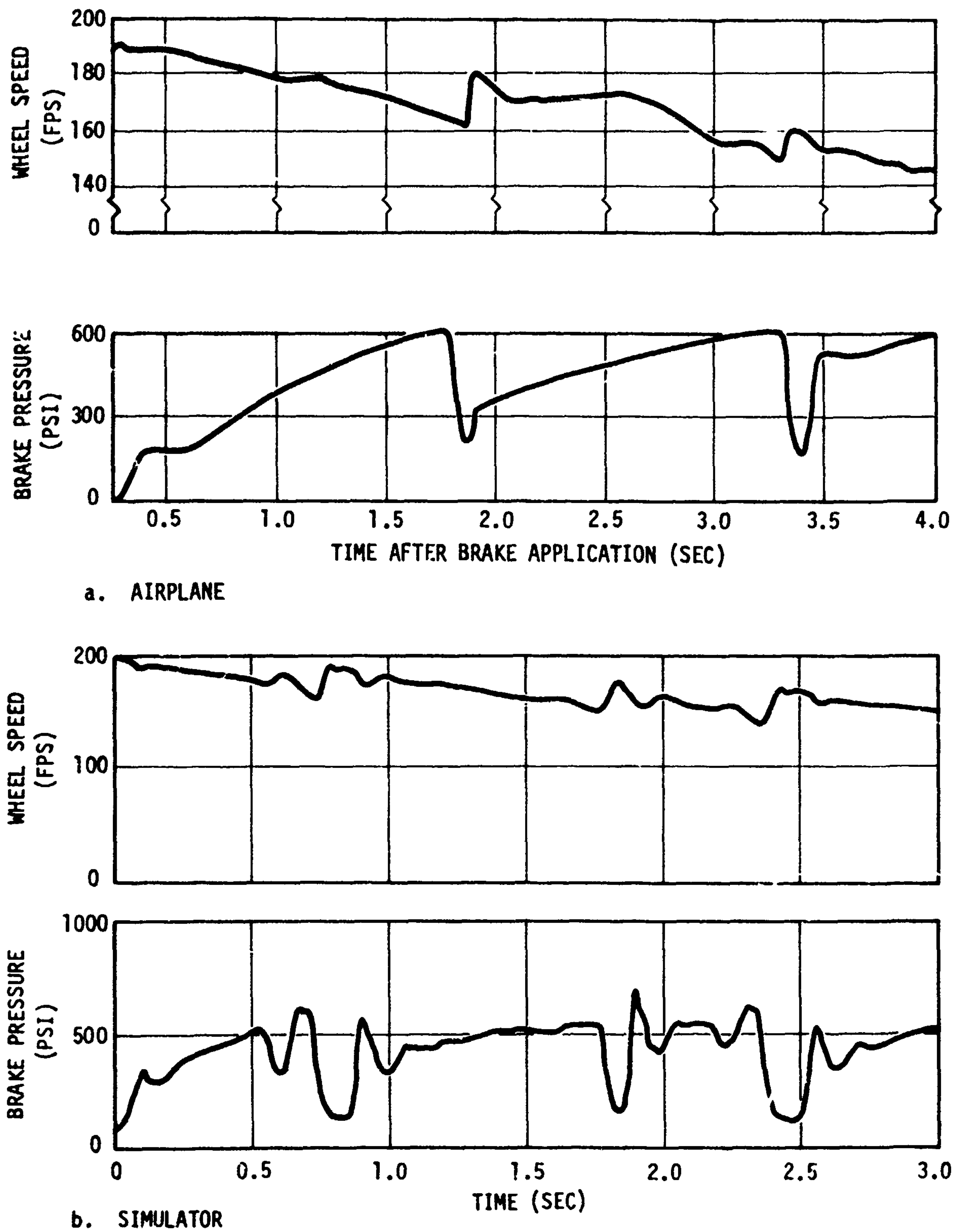

Figure 11.—KC-135 Dry Runway (Flight 2-7)

is characterized by skidding activity at regular intervals. The skid rate is about one per second. Between skid cycles pressure is ramped on by the system at a rate of about 200 to 250 psi/sec. Skidding occurs at approximately 600 psi. Both the simulator and flight test data show these characteristics. The airplane braking distance was 1750 feet, while the distance obtained on the simulator was 1772.

3. F-111

The F-111 simulator performance was compared with flight tests 4 through 7 (Reference 21). Portions of tests 4 and 6 are shown in Figures 12 through 14, along with an equivalent condition obtained from the simulator. It should be noted that the wheel speed signals in the flight test traces do not reflect skidding activity consistent with the antiskid signal and brake pressure traces. The wheel speed traces would appear to be heavily filtered. It is a common instrumentation practice to filter signals to reduce noise. However, this practice also attenuates the amplitude of a rapidly changing signal (such as a skid). A comparison of the traces in Figures 12 and 13 shows that the skid and recovery pressure levels, antiskid value voltage levels and general control characteristics of the actual aircraft are reproduced by the simulator. In the dry runway example, major skid cycling occurs at a rate of about one skid every 1 to 2 seconds; in addition, a higher frequency skid cycling (about 10 cps) has also been reproduced, Figure 13. Resulting skid cycling pressures are about 1200 to 1400 psi. The actual stopping distance of flight 4 was 1753, while the corresponding simulator distance was 1748. Pressure and antiskid signal voltage levels and cycling rate, are reproduced in the wet runway condition (flight 6) shown in Figure 14. The simulator braking distance for this condition was 6006 feet, while the aircraft distance was 5956.

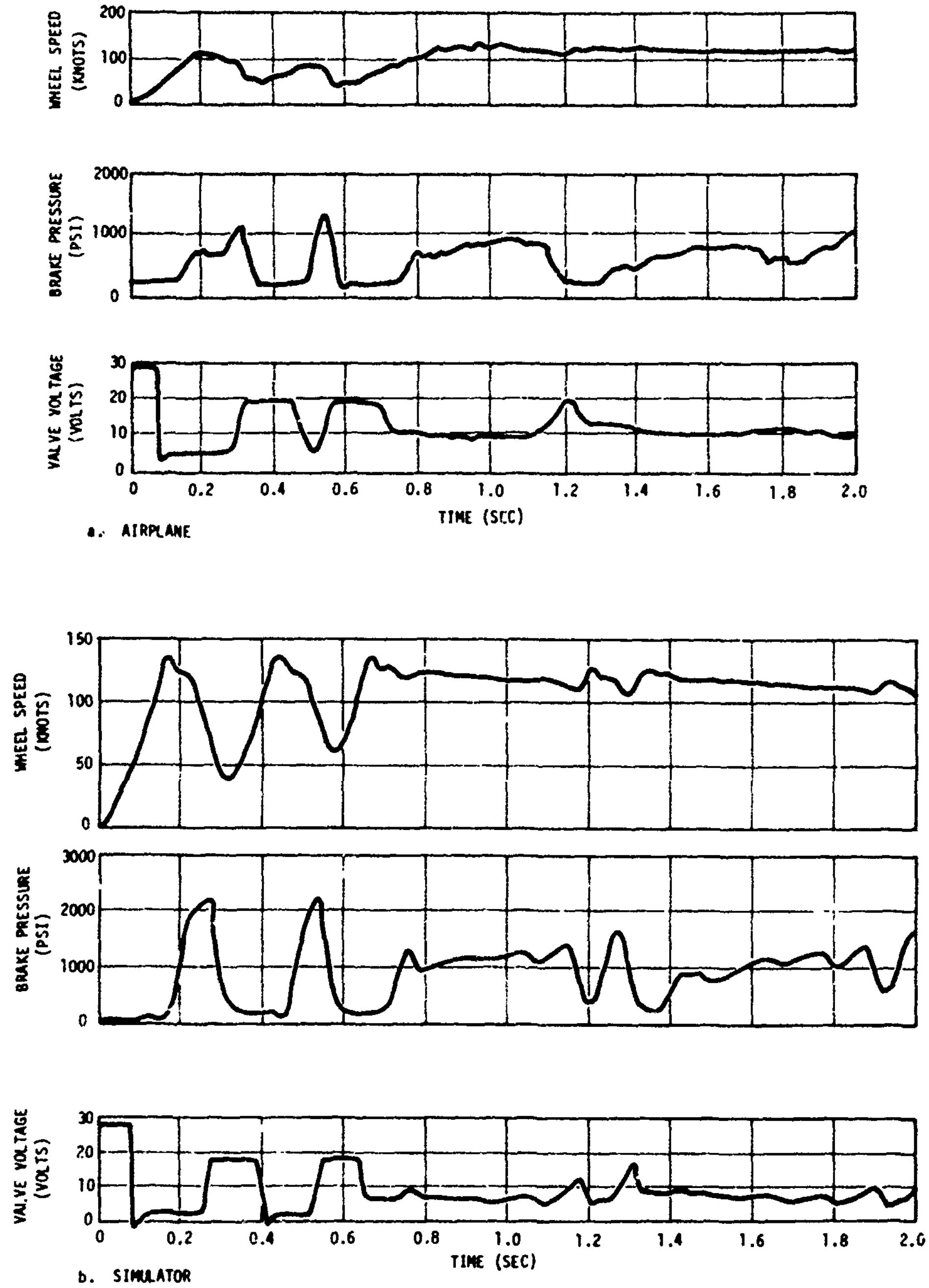

Figure 12.—F-111 Dry Runway (Flight #4)

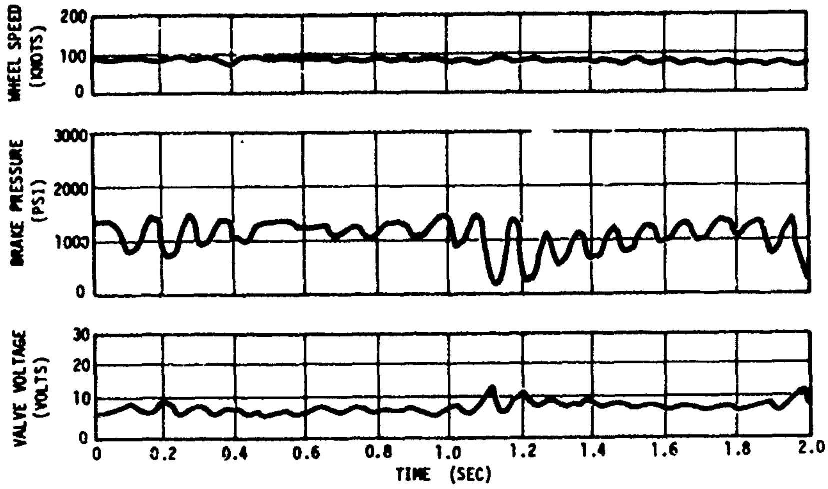

a. AIRPLANE

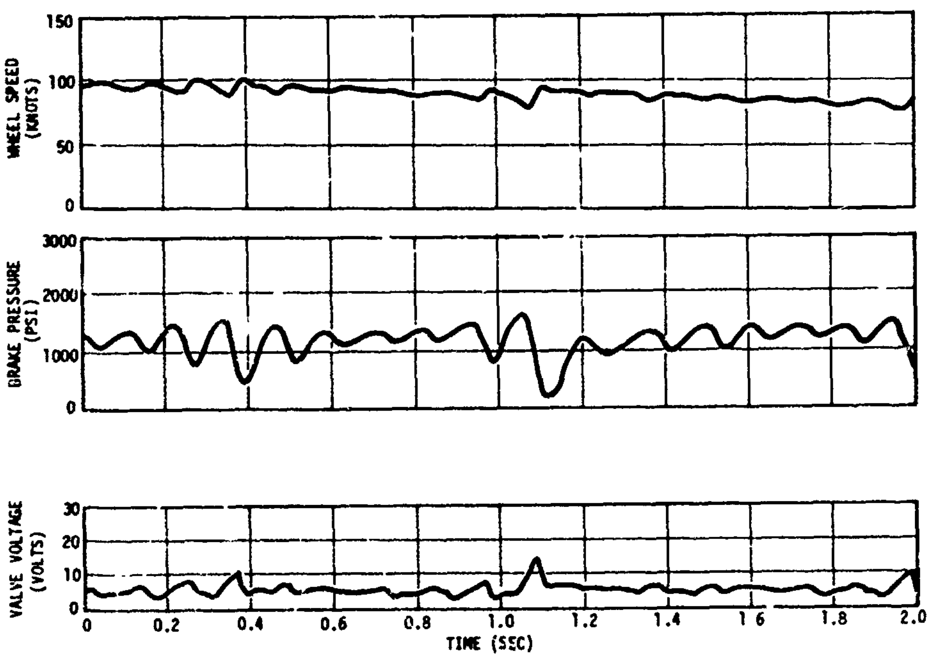

b. SIMULATOR

Figure 13.—F-111 Dry Runway (Flight #4)

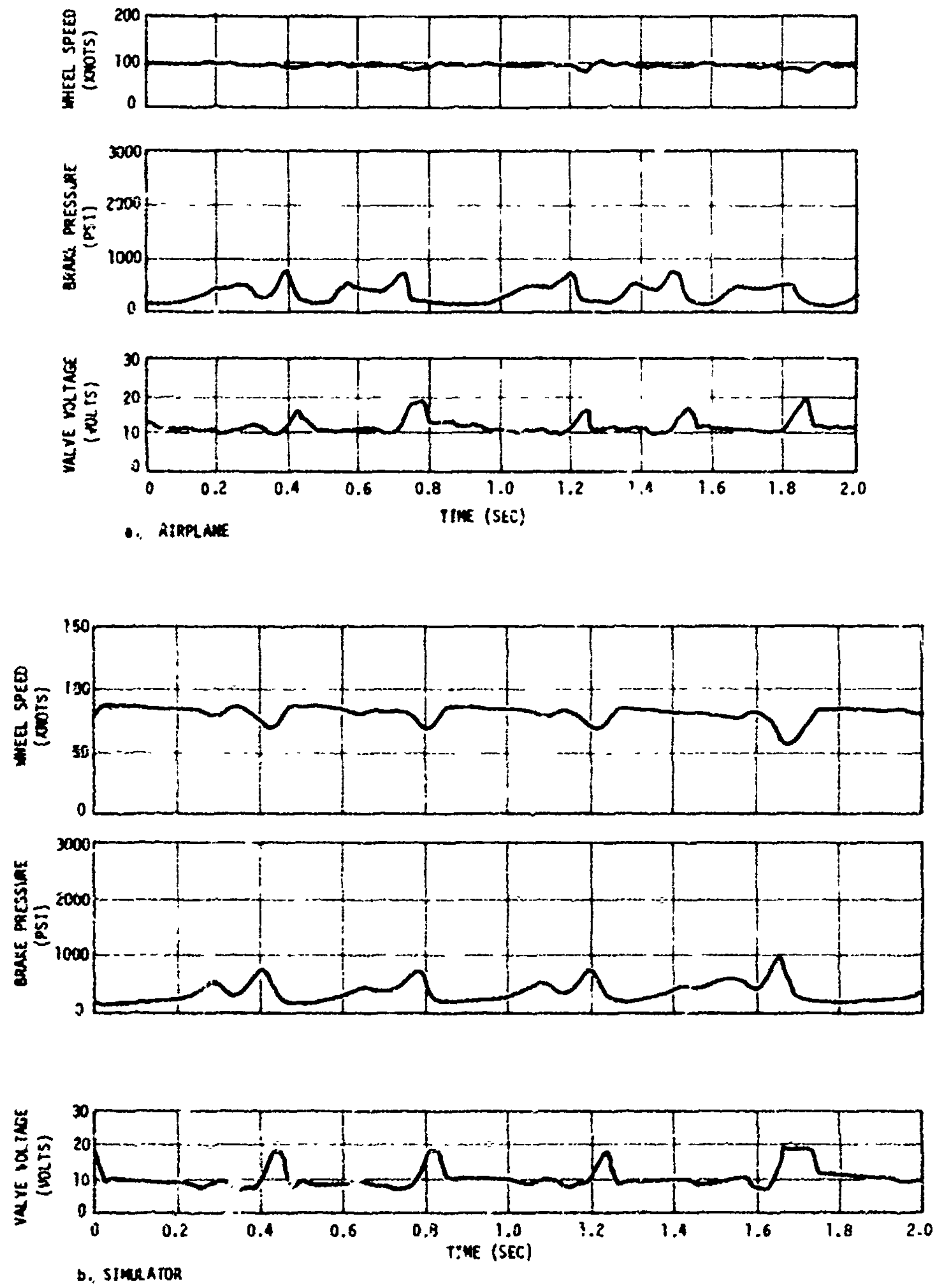

Figure 14.—F-111 Wet Runway (Flight #6)

SECTION VII
DETERMINATION OF SIGNIFICANT PARAMETERS

1. PARAMETER RATINGS

The parameter rating index (PRI) was used to rank the parameter changes according to their effect on braking distance. The value of the PRI is the average percentage deviation from the baseline braking distance. Thus, the larger the PRI, the greater impact the parameter has on airplane braking distance. Based on the PRI, the parameter changes have been arranged in numerical order, and the results are listed in Table 8. The table presents the average PRI for the three aircraft tested. Although the tire-ground friction coefficient (mu) is a predominant influence on airplane braking performance, it is not included in these tables because the PRI rating methodology was used to determine variable significance for a range of mu values.

2. SIGNIFICANT PARAMETERS

The second step in the rating of parameters was to determine which parameter changes have a significant effect on stopping distance. It was decided to consider all parameters having a PRI greater than 2.0 as being significant. A value of 2.0 represents a 2% change in the baseline braking distance. The repeatability fo the analog-hardware simulation itself results in 1% variations.

Based on the above criteria, Table 8 has been reduced and peak available mu included. In addition, the parameter changes have been summarized by combining related tests under a general heading. The resulting list of parameters having a significant effect on braking distance is given in Table 9.

Table 8.—Parameter Rating

Composite F-111, B-52, KC-135

RANK	TEST CONDITION	DESCRIPTION	PRI
1	1a	MAXIMUM LANDING WEIGHT WITH VI	43.88
2	1d	20 KNOT WIND	37.67
3	3d	BRAKE APPLICATION SPEED + 30 KNOTS	35.92
4	4a	NO SPOILERS	33.50
5	1c	15 KNOT WIND	29.75
6	1e	MAXIMUM LANDING WEIGHT WITHOUT VI	23.42
7	1f	-10 KNOT WIND	23.33
8	3c	BRAKE APPLICATION SPEED + 20 KNOT	23.25
9	4e	20% EFFECTIVE SPOILERS	22.42
10	1b	10 KNOT WIND	20.50
11	5b	50% OF FULL METERED PRESSURE	15.71
12	1b	HIGH INTERMEDIATE LANDING WEIGHT WITH VI	15.25
13	4d	40% EFFECTIVE SPOILERS	14.95
14	1d	MINIMUM LANDING WEIGHT WITH VI	13.50
	1h	MINIMUM LANDING WEIGHT WITHOUT VI	13.50
16	1f	HIGH INTERMEDIATE LANDING WEIGHT WITHOUT VI	13.08
17	3f	BRAKE APPLICATION SPEED -10 KNOTS	12.75
18	3d	BRAKE APPLICATION SPEED + 10 KNOTS	11.83
19	1e	-5 KNOT [illegible]	11.33
20	1a	5 KNOT WIND	11.17
21	1c	LOW INTERMEDIATE LANDING WEIGHT WITH VI	10.63
22	4c	60% EFFECTIVE SPOILERS	8.83
23	1a	FLAT MU-SLIP PEAK	8.58
24	2b	COLD DAY	8.17
25	5a	75% OF FULL METERED PRESSURE	8.14
26	3e	BRAKE APPLICATION SPEED - 5 KNOTS	7.00
27	1g	LOW INTERMEDIATE LANDING WEIGHT WITHOUT VI	6.75
28	1b	LOW TIRE HEATING	6.58
29	2a	FORWARD CENTER OF GRAVITY	6.50
30	1c	TIRE INFLATION PRESSURE 80% OF NORMAL	6.33
31	3a	BRAKE APPLICATION SPEED + 5 KNOTS	5.82
32	2a	HOT DAY	5.75
33	1d	TIRE INFLATION PRESSURE 120% OF NORMAL	5.42
34	4i	80% ENGINE IDLE THRUST	5.25
35	4b	80% EFFECTIVE SPOILERS	3.75
36	2b	AFT CENTER OF GRAVITY	3.67
37	4f	120% ENGINE IDLE THRUST	3.58
38	4h	90% ENGINE IDLE THRUST	2.75
39	4g	110% ENGINE IDLE THRUST	2.00

Table 9.—Significant Parameters

Parameters affecting braking distance by more than 2%
(Listed in decreasing order of significance)

1. Peak available ground friction
2. Landing weight with initial velocity changes
3. Wind
4. Brake application speed
5. Spoiler effectiveness
6. Landing weight without initial velocity changes
7. Metered pressure level
8. Mu-slip curve shape
9. Air density
10. Fore and aft center of gravity
11. Engine idle thrust

SECTION VIII
SELECTION OF PERTINENT PARAMETERS

Figure 15 is a flow chart where each block represents a major step of analysis in the formulation of the prediction equation. Figure 16 shows the breakdown of the entire Task II.

Table 10 lists those significant parameters remaining after excluding, from Table 9, the parameters that depend on pilot technique, or are design constraints and/or are outside the scope of present work. The following paragraphs present the reasoning for further refinement to the list.

1. PEAK AVAILABLE MU AND MU-SLIP CURVES

Parameter number 11 in Table 9, namely mu-slip curve shapes, are not independent variables and therefore are inherent parts of or dependent upon the peak available mu at the tire-runway interface. One of the a priori requirements when forming dimensionless groups is that each term or group be independent. Therefore, Mu-slip curve shapes are not listed on Table 10.

2. AERODYNAMIC LIFT AND DRAG

Lift and drag coefficients are interdependent variables. Therefore, the ratio C_L/C_D was chosen as an independent variable. Wherever applicable, drag-chute caused drag was added to the aerodynamic drag and the sum treated as the total aerodynamic drag.

3. HEAD OR TAIL WIND

In the previous sensitivity study report, reference (1), it was pointed out that a single curve would suffice to describe the variation of both wind velocity and brake application speed. Thus, a five knot wind velocity was the same as a five knot change in the brake application velocity. This comparison was made for the aircraft considered in present study and the results are shown in figures 17, 18, and 19. Clearly the aforementioned axiom does not apply at all for the B-52 and holds only at high mu (0.4μ and higher) conditions for the KC-135 and F-111 airplanes. Although the above axiom does not apply in this case, the wind component can be converted to a velocity change and therefore cannot be considered as an independent variable apart from the brake application velocity. A correction factor is therefore needed to convert a given wind component into an equivalent velocity component to be used in the prediction equation/model. These correction factors were computed, based on the sensitivity study data and are discussed in detail in Appendix A.

4. LANDING WEIGHT AND BRAKE APPLICATION VELOCITY

Nominally, the touchdown speed and, consequently, the brake application speed are a direct function of gross weight; the higher the weight the higher the touchdown speeds. The pilot technique and/or training (e.g., see the later paragraph/discussion on B-52 operations) may, however, result in situations where the pilot applies brakes at the same speed regardless of the gross weight or touchdown speed. It is thus interesting to study the effect of weight variation (without velocity variation) upon the stopping distance.

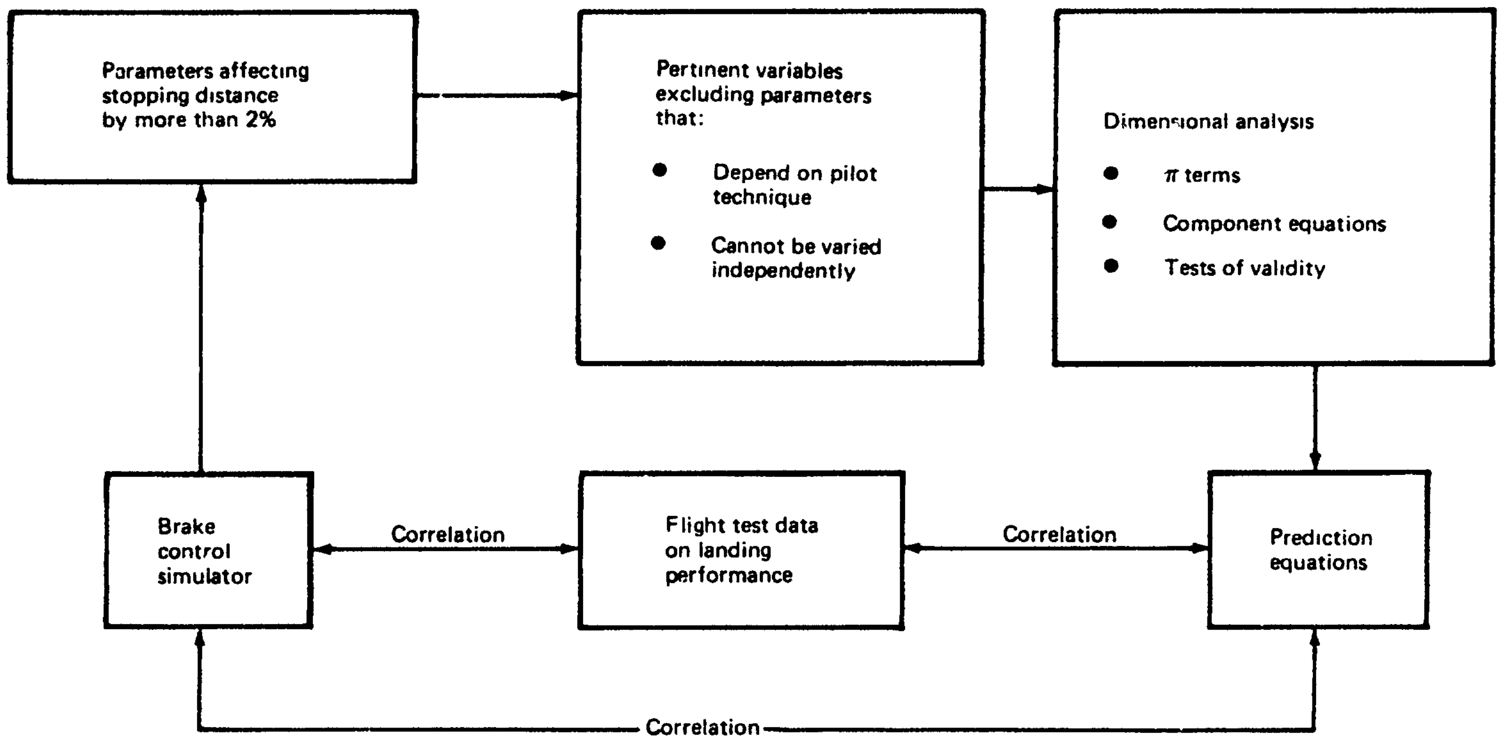

Figure 15.—Block Diagram for Task II Analysis

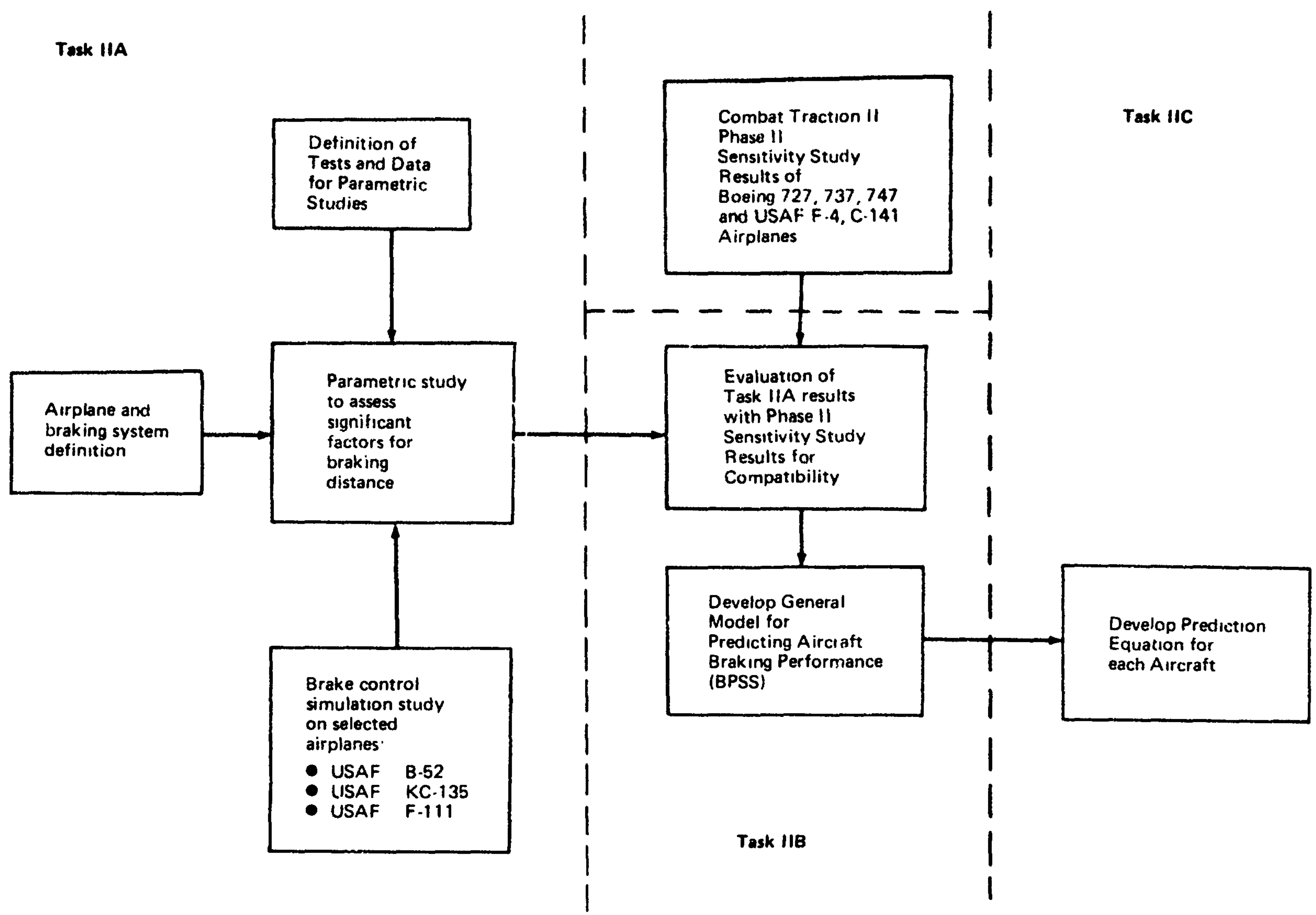

Figure 16.—Sensitivity Analysis and Braking Prediction Subsystem (BPSS)

Table 10.—Significant Parameters

1.	Peak available mu
2.	Drag device effectiveness
3.	Head or tail wind
4.	Brake application speed
5.	Landing weight
6.	Air density
7.	Engine idle thrust
8.	Center-of-gravity location

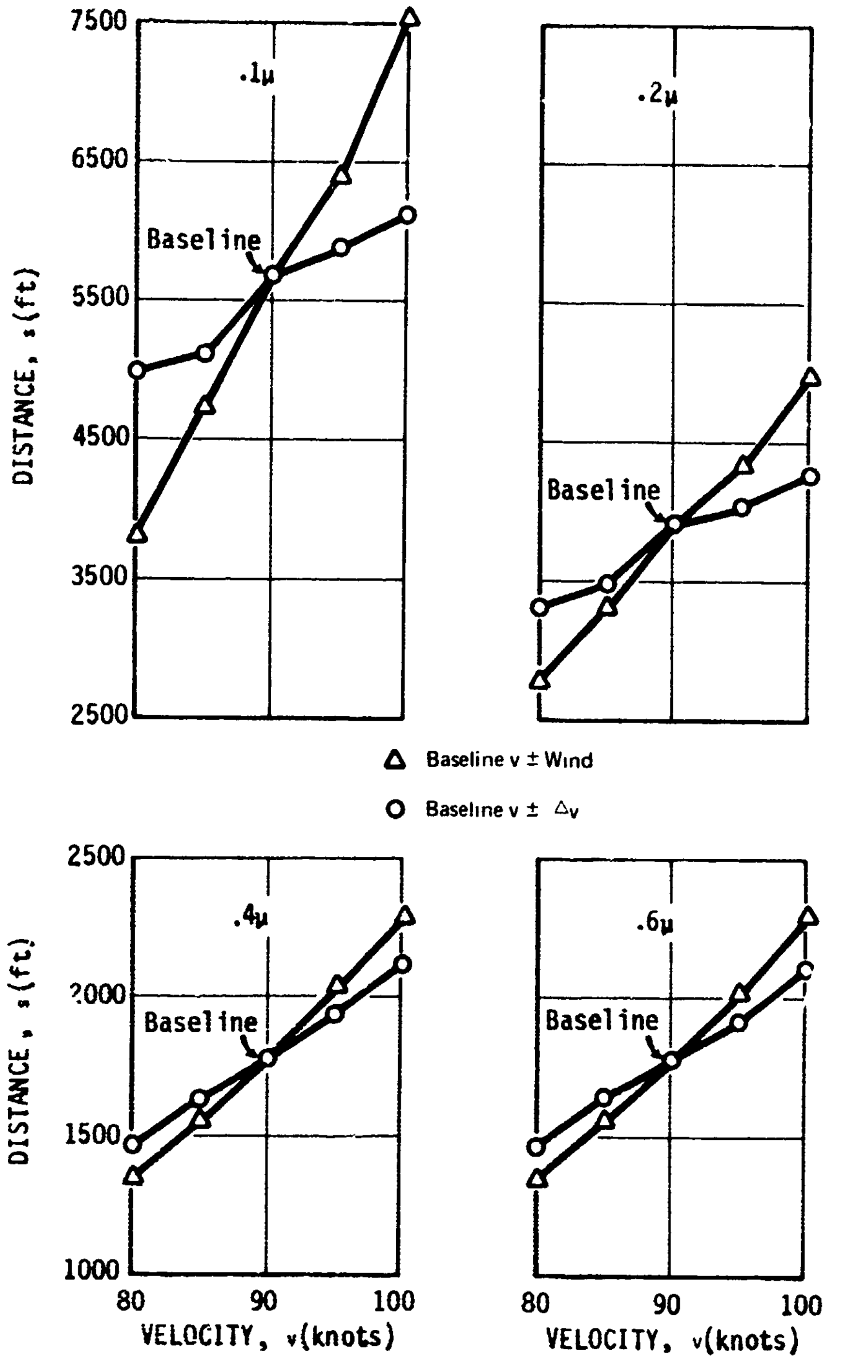

Figure 17.—Effect of Wind and Brake Application Velocities on Stopping Distance, B-52

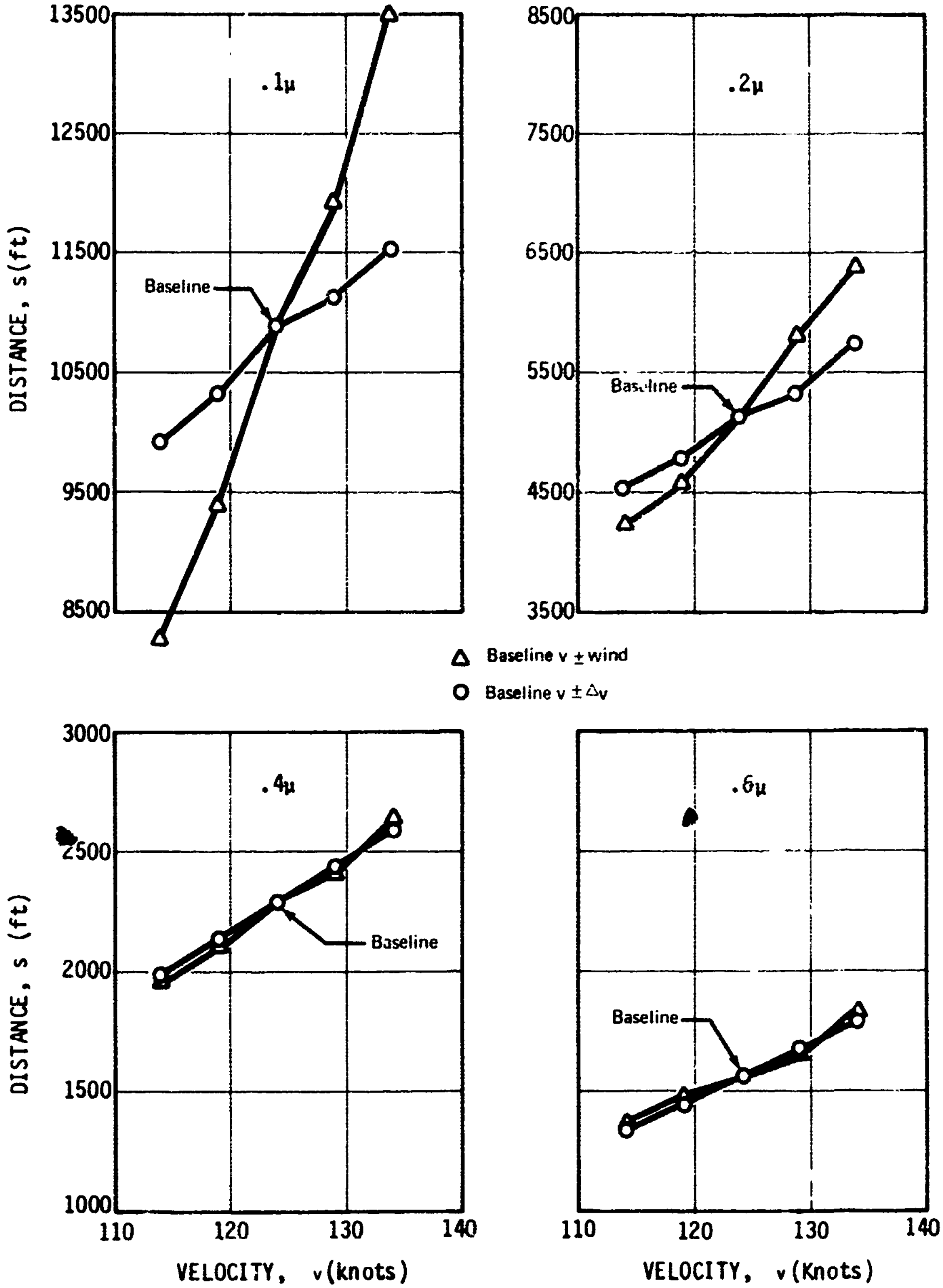

Figure 18.—Effect of Winds and Brake Applicati n Velocities on Stopping Distance (KC-135)

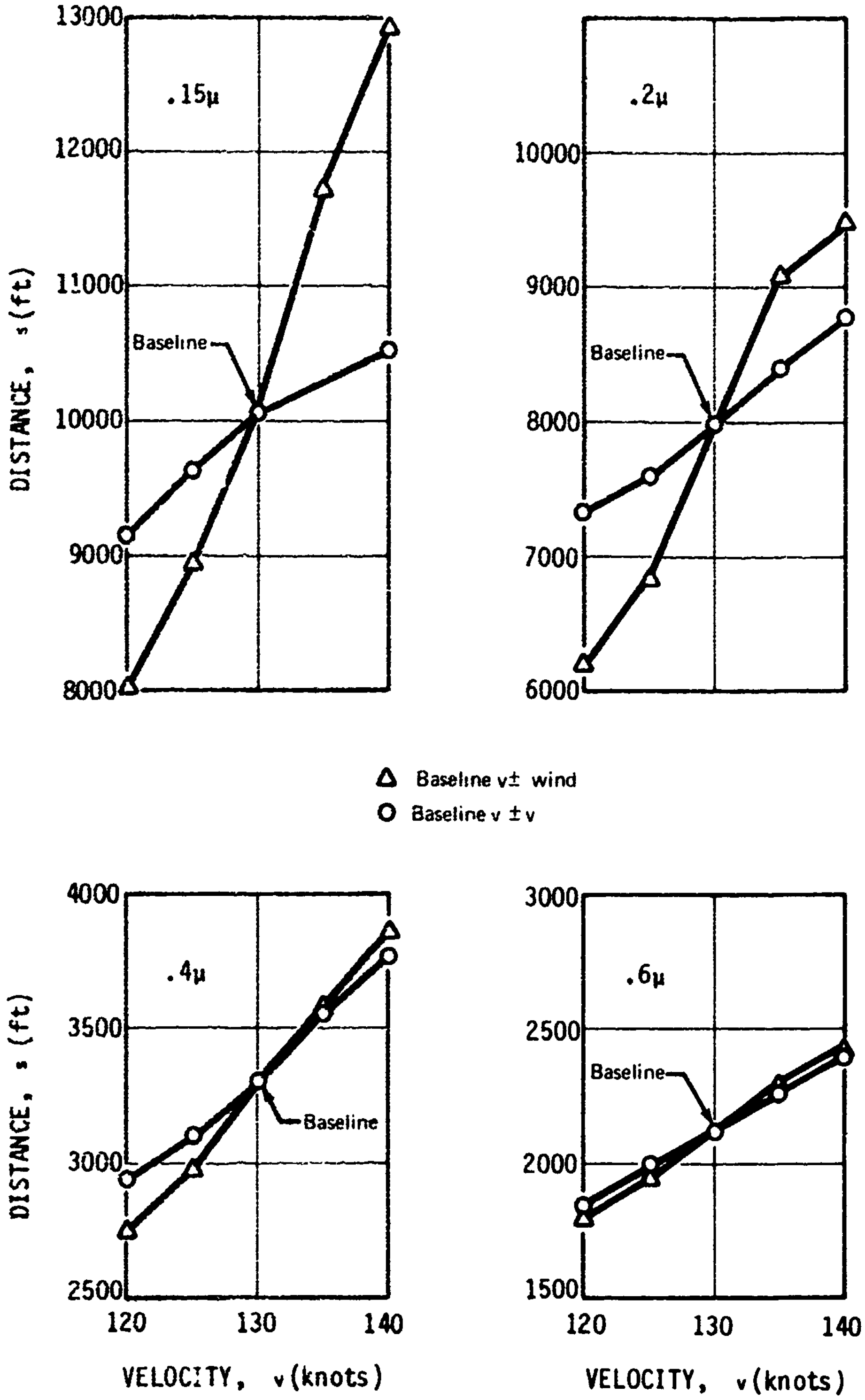

Figure 19.—Effect of Wind and Brake Application Velocities on Stopping Distance, F-111

A USAF contract study, reference (24), had shown that for the F-4 airplane this effect was less than one percent in terms of stopping distance. In the previous sensitivity study, references (1) and (2), the tests on the B-747 simulator showed this effect to be less than two percent. The matter was therefore not pursued any further at that time, as the criteria for selecting significant parameters was to detect a change in the stopping distance of more than two percent.

In the current study it was noted that the flight manuals for the B-52, reference (8), instruct the pilot to apply brakes at the same speed regardless of the landing weight or touchdown speed, e.g., 90 knots for B-52 G/H models (70 knots for earlier versions). This necessitated generation of B-52 simulator data in a fashion so as to duplicate the actual aircraft operation It was, however, decided to obtain simulator data for all three airplanes (B-52, KC-135 and F-111) to study the weight-alone variation effect. These data have been plotted, figures 20 to 22, as percent change in weight, % Δw, versus percent change in braking distance, % Δs; the change being calculated as ± percentage values from the defined baseline (see section II for baseline definition).

The data for the B-52, figure 20, is consistent, except for two data points at 0.2 mu. It shows a direct relationship between weight and distance; an increasing weight resulting in higher braking distance and vice versa. The deviations at 0.2 mu are due to torque limiting operation as well as the skid control system transients at that particular friction level. This will become more clear when mu-braking efficiency plots are discussed in a later section (see section X).

The data for KC-135 and F-111, figures 21 and 22, show a mixed trend in that an increase in weight does not necessarily cause an increase in distance and vice versa. The skid control system efficiency, available friction level, the landing gear foot print (geometry), the transfer/distribution of airplane weight among the gears and the strut stability, could individually or collectively influence the resulting braking distance from one landing weight to another. The data, however, can be grouped together into shaded areas and certain trends established when the torque limited braking cases (designated TL in the figures) are excluded.

It was explained in reference (1), page 78, as to why only brake application velocity and not both the landing weight and velocity were chosen as significant independent parameters. In the case of B-52, however, a special handling of the weight variation (without velocity variation) data was necessary as weight does not appear as a separate variable in the nondimensional terms. An equivalent velocity change was, therefore, calculated for each weight change. This will be demonstrated by an example in Appendix B. The weight-alone variation data for KC-135 and F-111, figures 21 and 22, were not included in the prediction model analysis as the data for weight and velocity varying together (normal approach) was also obtained on the simulator and accordingly, used in the analysis. Due to the unique B-52 operating procedures of delaying brake application until 90 knots, the rolling distance or the prebraking distance from touchdown to brake application amounts to a considerable value, and should be calculated separately and added to the braking distance to obtain the needed runway length/ground roll. Typical prebraking roll distances were calculated for the B-52 and are shown in figure 23. The mathematical expression used for these calculations is explained in Appendix C.

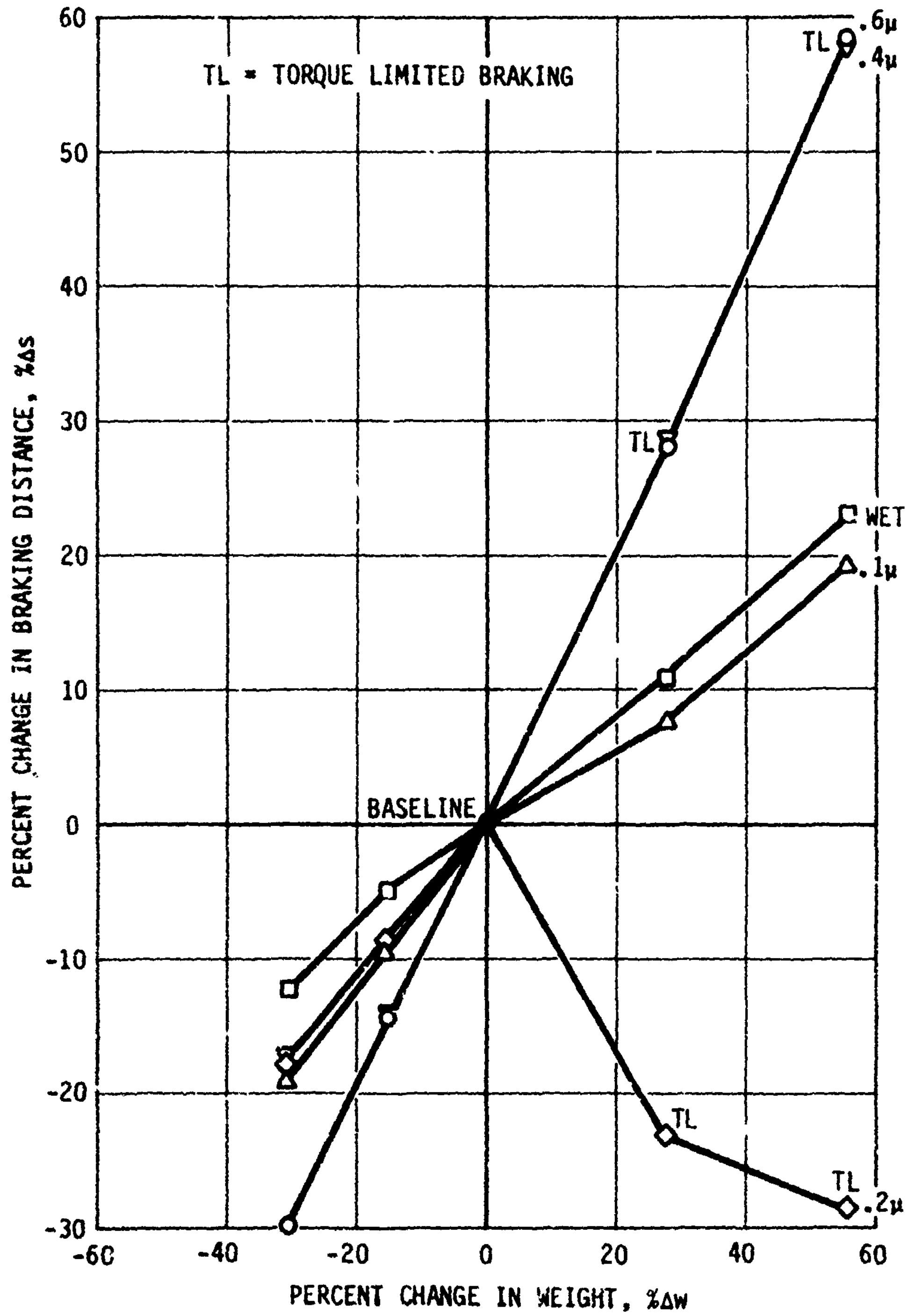

Figure 20.—Effect of Weight Variation Without Velocity Variation , B-52

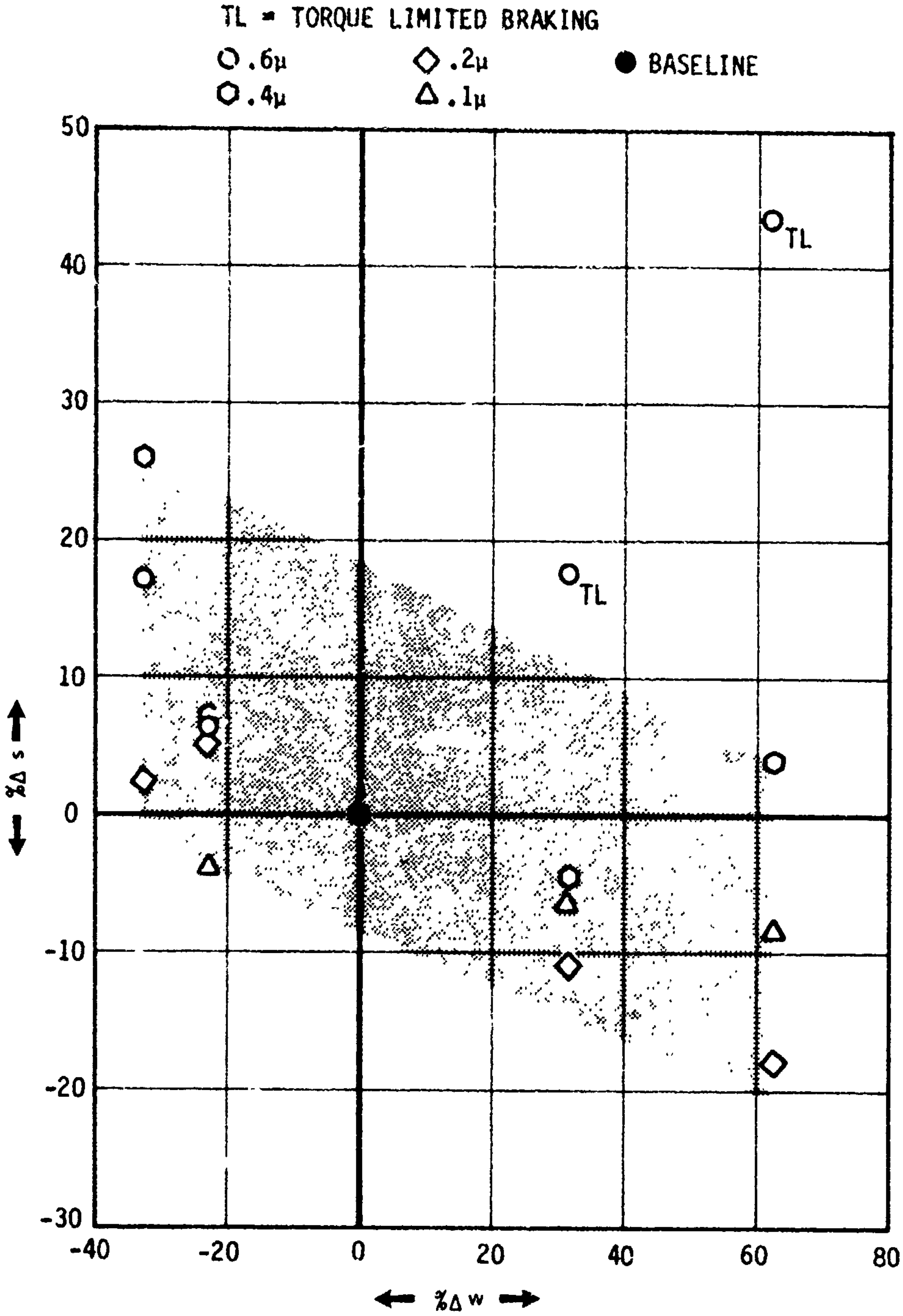

Figure 21.—Effect of Weight Variation Without Velocity Variation , KC-135

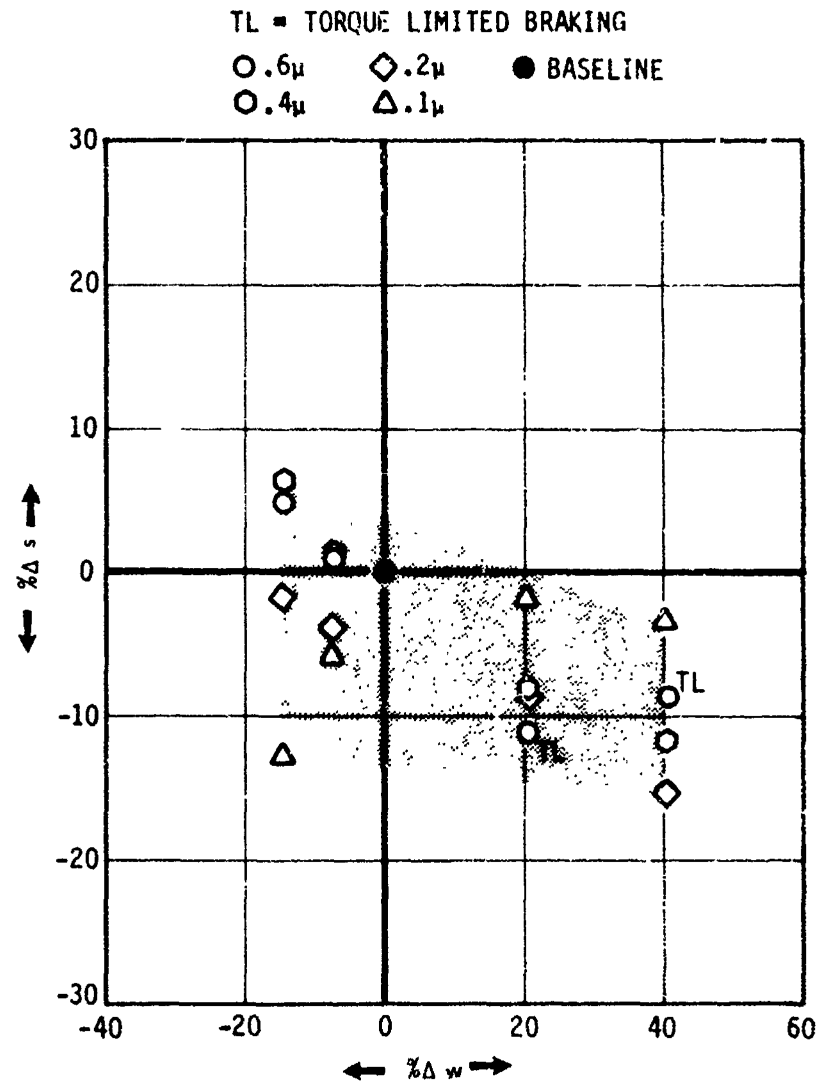

Figure 22.—Effect of Weight Variation Without Velocity Variation, F-111

ASSUMPTIONS:

1 Rolling μ = 0.02

2 Drag chute deployment speed = 135 Knots

3 C_D = .152 for $V_{Touchdown}$ to 135 Knots

4 C_D = .321 for 135 Kn to 90 Kn

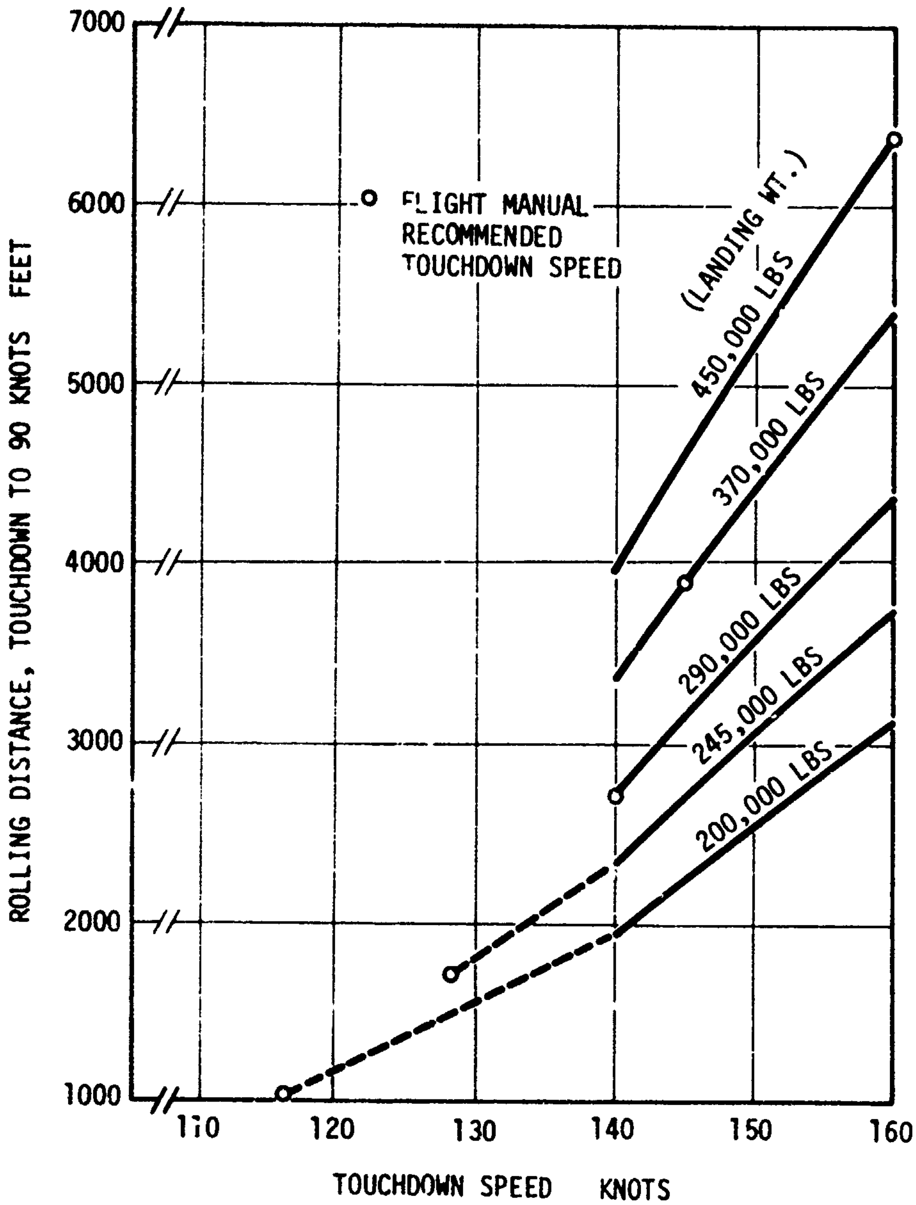

Figure 23.—Prebraking Roll Distance, B-52

5. CENTER-OF-GRAVITY

The CG location effect considered in the analog simulation was of the form:

$$\Psi = \frac{\mu \cdot LA}{LA + LB + \mu \cdot HB}$$

where LA, LB, and HB are geometric distances (see Table 2), and μ is the coefficient of available friction. The parameters Ψ and $(1-\Psi)$ thus determine the respective loads carried by the main and nose gears for given c.g. locations. Because the CG variation of any correlation ground vehicle would be minimal, and because geometric similarity with an airplane would be almost impossible to achieve, it was decided to consider only the coefficient of available friction as the independent variable.

6. OTHER PARAMETERS

The remaining parameters (ρ and F_e) are independent variables and require no discussion. From the preceding paragraphs, it follows that the pertinent variables are.

- Braking distance (s)
- Available mu (μ)
- C_L/C_D ratio (C_L/C_D)
- Brake application speed (v)
- Air density (ρ)
- Engine idle thrust (F_e)

where (s) is the dependent variable and all others are independent variables.

SECTION IX
DEVELOPMENT OF PREDICTION MODEL

1. COMPONENT EQUATIONS

The first step in forming a prediction model is to identify the pertinent and independent variables. This step is by far the most important because the validity of the results depends on the correctness with which the pertinent factors are selected. For this study, as explained in Section VIII. This required the combining of some of the interdependent variables listed in Table 10. The list of resultant independent variables is shown in Table 11.

The second step is to express the secondary quantity (dependent variable) as a function of the primary quantities (independent variables), so that:

$$s = F(g, v, \rho, F_e, \mu, C_L/C_D) \qquad (1)$$

where:

s = braking stop distance

g = acceleration caused by gravity.

The dimensional matrix that can be formed for the fundamental units (mass, length, and time) of the seven parameters in Equation 1 is of rank 3, so that, according to Buckingham's π theorem, these would yield four independent π terms. By inspection and analysis, they can be written (sg/v^2), (μ), (C_L/C_D), and $(\rho v^6/F_e g^2)$. Thus:

$$(sg/v^2) = F(\mu, C_L/C_D, \rho v^6/F_e g^2) \qquad (2)$$

or,

$$(\pi_1) = F(\pi_2, \pi_3, \pi_4) \qquad (2a)$$

where.

$\pi_1 = sg/v^2$

$\pi_2 = \mu$

$\pi_3 = C_L/C_D$

$\pi_4 = \rho v^6/F_e g^2$

Appendix C, reference (1), shows the detailed analysis of arriving at Eq. 2 and Eq. 2a. Section XII, Volume II of this report (ASD-TR-77-6) shows the calculations of π terms (numerics) using raw data from Task IIA simulation. The application of dimensional analysis, including the pi theorem, leads to a type of equation involving an unknown function, of which

Table 11.—Pertinent Independent Variables

Variable	Notation
Available mu	μ
Brake application speed	v
Drag device effectiveness	C_L/C_D
Engine idle thrust	F_e
Air density	ρ

Eq. 2 is an example. Before a prediction equation can be formulated, the nature of the function must be determined. This cannot be accomplished by dimensional analysis, but it can be done from analysis of laboratory observations.

The best procedure for evaluating a function is to arrange the observations so that all but one of the pi terms containing the independent variables in the function remain constant. Then the remaining independently variable pi term is varied to establish a relationship between it and the dependent variable (π_1 term). Section XIII, Volume II of this report (ASD-TR-77-6) shows this arrangement of experimental observations (π terms) for all three airplanes under consideration. This procedure is repeated for each of the pi terms in the function; the resulting relationships between π_1 and the other individual pi terms are called component equations. Statistical curve fitting computer programs were used to generate the component equations (see Appendix D). A summary of the equations is listed in Table 12. It should be noted that in some of the component equations, the exponent for the (π_4) term has been modified by a $\Delta\rho$ term where $\Delta\rho$ equals [ρ(std-day) - ρ(non-std-day)] in lb-sec^2/ft^4, the terms standard day and non-standard day are defined in Appendix E. This was necessary to arrive at a satisfactory relationship between (π_1) and (π_4) where satisfactory implies an acceptable correlation error between the actual and predicted values, e.g., ±5%. This modification of the (π_4) exponent was needed at all μ conditions for the B-52 and only at 0.2μ or less for the KC-135 and the F-111 airplanes. The mechanism for arriving at the numerical value of the modifier ($\Delta\rho$ term) is explained by an example calculation in Appendix E.

An examination of the previous sensitivity study, reference (1) showed that even though air density (ρ) had been included as an independent variable (as part of the π_4 term) the density change data collected on the simulator had inadvertently been left out when formulating component and prediction equations in the numerical form. This caused some concern as to the accuracy of the previously reported prediction equations for the Boeing 727, 737, 747 and the USAF C-141 and F-4 airplanes, reference (1). All the component equations and the corresponding prediction equations were, therefore, recalculated by including the data points for density variation. A check of the correlation errors showed that a modified (π_4) exponent would be needed for F-4 at all μ conditions and only for wet runways for the other four airplanes. The accuracy of the remaining prediction equations and their application range were not affected. Accordingly, the revised prediction equations with modified exponents are shown in Table 13.

2. GENERALIZED FUNCTIONS

When the component equations have been determined, they are combined in a certain manner to give a general relationship. It is possible for some of the component equations to be combined by multiplication, while others require addition in the formation of the resultant prediction equation. In general, these two methods are adequate for the majority of engineering problems. For the stopping distance problem, the analysis showed that the prediction equation should be formed by multiplication. The necessary and sufficient conditions to be met for the function to be a product were developed and translated into tests of validity. All aspects of the development of prediction equations discussed in this paragraph are detailed in Appendix E, reference (1). The major equations of interest are repeated in succeeding paragraphs.

Table 12.—Summary of Component Equations

Airplane model	μ*	Equation	Eq. No.
B-52	0.6	$(\pi_1) = 2.3931\ (\pi_2)^{-.0400}$	(3)
		$(\pi_1) = 2.4772\ (\pi_3)^{.03021-.01786\%\ SP^{**}}$	(4)
		$(\pi_1) = 4.4960\ (\pi_4)^{9.05\Delta\rho\ -\ .06803}$	(5)
	0.4	$(\pi_1) = 2.3931\ (\pi_2)^{-.04007}$	(3)
		$(\pi_1) = 2.4815\ (\pi_3)^{.1285\ -\ .2227\%SP}$	(6)
		$(\pi_1) = 4.0297\ (\pi_4)^{8.48\Delta\rho\ -\ .0554}$	(7)
	0.23	$(\pi_1) = .1747\ (\pi_2)^{-2.2504}$	(8)
		$(\pi_1) = 4.8081\ (\pi_3)^{.13006\ -\ .07741\%SP}$	(9)
		$(\pi_1) = 24.5495\ (\pi_4)^{17.75\Delta\rho\ -\ .1836}$	(10)
	0.2	$(\pi_1) = 2.3637\ (\pi_2)^{-.5166}$	(11)
		$(\pi_1) = 5.4324\ (\pi_3)^{.09091-.07014\%SP}$	(12)
		$(\pi_1) = 26.3742\ (\pi_4)^{12.5\Delta\rho\ -\ .1803}$	(13)
	0.1	$(\pi_1) = 2.3637\ (\pi_2)^{-.5166}$	(11)
		$(\pi_1) = 7.9153\ (\pi_3)^{.11144-.1367\%SP}$	(14)
		$(\pi_1) = 43.8256\ (\pi_4)^{16.11\Delta\rho\ -\ .1962}$	(15)

*Baseline value of μ used in the data set

**% SP is the percentage of the spoiler configuration.

Table 12.—Summary of Component Equations (Continued)

Airplane model	μ*	Equation	Eq. No.
KC-135	0.6	$(\pi_1) = .71355\ (\pi_2)^{-.9420}$	(16)
		$(\pi_1) = 1.1046\ (\pi_3)^{.19028-.10895\%SP}$	(17)
		$(\pi_1) = 2.1672\ (\pi_4)^{-.05414}$	(18)
	0.4	$(\pi_1) = .71355\ (\pi_2)^{-.9420}$	(16)
		$(\pi_1) = 1.68155\ (\pi_3)^{.22326-.20718\%SP}$	(19)
		$(\pi_1) = 4.39388\ (\pi_4)^{-.08228}$	(20)
	0.2	$(\pi_1) = .5893\ (\pi_2)^{-1.1410}$	(21)
		$(\pi_1) = 3.38793\ (\pi_3)^{.25766-.02665\%SP}$	(22)
		$(\pi_1) = 22.44915\ (\pi_4)^{3.5\Delta\rho-.15208}$	(23)
	0.1	$(\pi_1) = .5893\ (\pi_2)^{-1.1410}$	(21)
		$(\pi_1) = 8.0898\ (\pi_3)^{.1485-.1643\%SP}$	(24)
		$(\pi_1) = 82.26867\ (\pi_4)^{12.65\Delta\rho-.200863}$	(25)

Table 12.—Summary of Component Equations (Concluded)

Airplane model	μ^*	Equation	Eq. No.
F-111	.6	$(\pi_1) = .7760\ (\pi_2)^{-1.1411}$	(26)
		$(\pi_1) = 1.3973\ (\pi_3)^{.1890\ -.1286\%SP}$	(27)
		$(\pi_1) = 2.9702\ (\pi_4)^{-.05843}$	(28)
	.4	$(\pi_1) = .7760\ (\pi_2)^{-1.1411}$	(26)
		$(\pi_1) = 2.1722\ (\pi_3)^{.2060-.1448\%SP}$	(29)
		$(\pi_1) = 5.1797\ (\pi_4)^{-.06742}$	(30)
	.2	$(\pi_1) = .9467\ (\pi_2)^{-1.0490}$	(31)
		$(\pi_1) = 5.2212\ (\pi_3)^{.1885-.1185\%SP}$	(32)
		$(\pi_1) = 42.8987\ (\pi_4)^{-.1648}$	(33)
	.15	$(\pi_1) = .9467\ (\pi 2)^{-1.0490}$	(31)
		$(\pi_1) = 6.6120\ (\pi_3)^{.1656-.0698\%SP}$	(34)
		$(\pi_1) = 66.2844\ (\pi_4)^{8.8\Delta\rho\ -\ .1797}$	(35)

Table 13.—Revised Prediction Equations for 727, 737, 747, C-141 and F-4 Airplanes

Revised Prediction Equations for F-4

μ^*	Equation	Eq.* No.
0.6	$(\pi_1) = 1.7679\,(\pi_2)^{-0.9236}\,(\pi_3)^{[.3485-.1185\%\,SP]}\,(\pi_4)^{[6.1\,\Delta\rho-.0468]}$	(56)
0.4	$(\pi_1) = 2.2932\,(\pi_2)^{-0.9236}\,(\pi_3)^{[0.5259-.0783\%\,SP]}\,(\pi_4)^{[12.26\,\Delta\rho-.0649]}$	(57)
0.2	$(\pi_1) = 21.5085\,(\pi_2)^{-1.1580}\,(\pi_3)^{[.6829-.0039\%\,SP]}\,(\pi_4)^{[12.81\,\Delta\rho-.2419]}$	(58)

* The original prediction equations are listed in Reference (1), Table 14, p.92.

Revised Prediction Equations - Wet Runways

Air-plane	μ^*	Equation	Eq.** No.
727	.167	$(\pi_1) = 1.9647\,(\pi_2)^{-1.16}\,(\pi_3)^{[.1346-.001\%\,SP]}\,(\pi_4)^{[18.18\,\Delta\rho-.1108]}$	(14)
737	.141	$(\pi_1) = 0.6595\,(\pi_2)^{-.7626}\,(\pi_3)^{[.2344-.1271\%\,SP]}\,(\pi_4)^{[18.36\,\Delta\rho+.0160]}$	(15)
747	.125	$(\pi_1) = 0.6704\,(\pi_2)^{-.8104}\,(\pi_3)^{[.3568-.07\%\,SP]}\,(\pi_4)^{[21.6\,\Delta\rho-.0143]}$	(16)
C-141	.225	$(\pi_1) = 2.4953\,(\pi_2)^{-1.0326}\,(\pi_3)^{[.0569-.0002\%\,SP]}\,(\pi_4)^{[13.48\,\Delta\rho-.0979]}$	(17)
F-4	.278	$(\pi_1) = 4.6672\,(\pi_2)^{-1.1665}\,(\pi_3)^{[.7498-.0257\%\,SP]}\,(\pi_4)^{[18.29\,\Delta\rho-.1320]}$	(18)

** The original prediction equations are listed in Reference (2), Table 60, p.206.

When the component equations (see Table 12) are combined by multiplication, the prediction equation is of the form:

$$\pi_1 = (C)\,(\pi_1)_{\bar{3},\bar{4}}\,(\pi_1)_{\bar{2},\bar{4}}\,(\pi_1)_{\bar{2},\bar{3}} \tag{36}$$

where the bar denotes a constant (held) value.

The analysis shows that the value of the constant term C is of the form

$$C = \frac{1}{[F(\bar{\pi}_2, \bar{\pi}_3, \bar{\pi}_4)]^2} \tag{37}$$

Thus the prediction equation is of the form:

$$F(\pi_2, \pi_3, \pi_4) = \frac{F(\pi_2, \bar{\pi}_3, \bar{\pi}_4)\, F(\bar{\pi}_2, \pi_3, \bar{\pi}_4)\, F(\bar{\pi}_2, \bar{\pi}_3, \pi_4)}{[F(\bar{\pi}_2, \bar{\pi}_3, \bar{\pi}_4)]^2} \tag{38}$$

The equations constituting a test for the validity of Eq. 38 are shown to be (see Appendix E, Reference (1).

$$\frac{F(\bar{\pi}_2, \pi_3, \bar{\pi}_4)\, F(\bar{\pi}_2, \bar{\pi}_3, \pi_4)}{[F(\bar{\pi}_2, \bar{\pi}_3, \bar{\pi}_4)]^2} = \frac{F(\bar{\bar{\pi}}_2, \pi_3, \bar{\pi}_4)\, F(\bar{\bar{\pi}}_2, \bar{\pi}_3, \pi_4)}{[F(\bar{\bar{\pi}}_2, \bar{\pi}_3, \bar{\pi}_4)]^2} \tag{39}$$

or $$\frac{F(\pi_2, \bar{\pi}_3, \bar{\pi}_4)\, F(\bar{\pi}_2, \bar{\pi}_3, \pi_4)}{[F(\bar{\pi}_2, \bar{\pi}_3, \bar{\pi}_4)]^2} = \frac{F(\bar{\pi}_2, \bar{\bar{\pi}}_3, \bar{\pi}_4)\, F(\bar{\pi}_2, \bar{\bar{\pi}}_3, \pi_4)}{[F(\bar{\pi}_2, \bar{\bar{\pi}}_3, \bar{\pi}_4)]^2} \tag{39a}$$

The values $\bar{\bar{\pi}}_2$ and $\bar{\bar{\pi}}_3$ are values of π_2 and π_3 held constant at some value other than $\bar{\pi}_2$ and $\bar{\pi}_3$. Thus from the observed data:

$\bar{\pi}_2 = 0.6$ — the primary set of data, for example

$\left.\begin{array}{l} \bar{\bar{\pi}}_2 = 0.4 \\ \bar{\bar{\pi}}_2 = 0.2 \\ \text{etc.} \end{array}\right\}$ supplementary sets of data

If the supplementary sets of data satisfy either Eq. 39 or 39a, the general equation can be formed by multiplying the component equations together and dividing by the constant, as indicated in Eq. 38.

This test was applied to all available data (component equations); the results are shown in Table 14 clearly indicating the validity of the approach. Table D-1 contains the details of this calculation.

Table 14.—Test of Validity for the Function to be a Product

Airplane Model	Value of Function in Eq -39				Ideal Value of Function in Eq -39	Deviation Percentage			
	L.H.S. π_2 =0.6	R.H.S. π_2 =0.4	R.H.S. π_2 =0.2	R.H.S. π_2 =0.1*		L.H.S. π_2 =0.6	R.H.S. π_2 =0.4	R.H.S. π_2 =0.2	R.H.S. π_2 =0.1*
B-52	1.018	0.995	0.976	1.011	1.000	1.8	-0.5	-2.4	1.1
KC-135	1.008	0.998	0.963	1.031	1.000	0.8	-0.2	-3.7	3.1
F-111	0.971	1.014	1.022	0.972	1.000	-2.9	1.4	2.2	-2.8

* π_2 = 0.15 for F-111

Another test of validity was to calculate the value of the constant term C of Eq. 36 The test requires that any of the three component equations should yield an identical value for C. This test was also applied to all the test data; the results are shown in Table15. Again, the accuracy achieved is satisfactory. Table D-2 contains details of this calculation.

The two validity tests were successful, thus permitting the writing of the prediction equations. Example calculations for formulating prediction equations are shown in Section XIV, Volume II of ASD-TR-77-6. A summary of all prediction equations is listed in Table 16. Equation 40 is a combination of Eq. 3.4,5 and corresponding C. Equation 41 is a combination of Eq. 3,6,7 and corresponding C, and so on.

Table 15.—Test of Validity for Constant Term

Airplane Model	$C = \left[1/F(\bar{\pi}_2, \bar{\pi}_3, \bar{\pi}_4)\right]^2$			Ideal Value of C	Average Deviation (%)	Value of $\bar{\pi}_2$
	Component Equation Used					
	π_1 vs π_2	π_1 vs π_3	π_1 vs π_4			
B-52	.1675	.1631	.1660	.1630	1.59	0.6
	.1622	.1609	.1651	.1636	-.53	0.4
	.03394	.03395	.0356	.0338	2.07	0.2
	.01658	.01592	.01689	.01591	3.70	0.1
KC-135	.7496	.7641	.7470	.7654	-1.54	0.6
	.3493	.3489	.3485	.3539	-1.40	0.4
	.0732	.0715	.0694	.0707	0.99	0.2
	.01504	.01549	.01553	.01556	-1.33	0.1
F-111	.5176	.5023	.5030	.5059	0.34	0.6
	.2051	.2077	.2081	.2070	0.00	0.4
	.03812	.03583	.03614	.03553	3.29	0.2
	.02085	.02216	.02227	.02231	-2.46	0.15

Table 16.—Summary of Prediction Equations

Airplane model	μ*	Prediction Equation	Eq. No.
B-52	C.6	$(\pi_1) = 4.4138\ (\pi_2)^{-.04007}\ (\pi_3)^{.03021-.01786\%SP}\ (\pi_4)^{9.05\Delta\rho\ -\ .06803}$	(40)
	0.4	$(\pi_1) = 3.8935\ (\pi_3)^{.04007}\ (\pi_3)^{.1285-.2227\%SP}\ (\pi_4)^{8.48\Delta\rho\ -\ .0554}$	(41)
	0.23	$(\pi_1) = 0.9009\ (\tau_2)^{-2.2504}\ (\pi_3)^{.13006-07741\%SP}\ (\pi_4)^{17.75\Delta\rho\ -\ .1836}$	(42)
	0.2	$(\pi_1) = 11.6824\ (\pi_2)^{-.5165}\ (\pi_3)^{.09091-1.07014\%SP}\ (\pi_4)^{12.5\Delta\rho\ -\ .1203}$	(43)
	0.1	$(\pi_1) = 13.5275\ (\pi_2)^{-.5165}\ (\pi_3)^{.11144-.1367\%SP}\ (\pi_4)^{16.11\Delta\rho\ -\ .1954}$	(44)
KC-135	0.6	$(\pi_1) = 1.28745\ (\pi_2)^{-.9420}\ (\pi_3)^{.1903-.1090\%SP}\ (\pi_4)^{-.05414}$	(45)
	0.4	$(\pi_1) = 1.83884\ (\pi_2)^{-.9420}\ (\pi_3)^{.2233-.2072\%SP}\ (\pi_4)^{-.08228}$	(46)
	0.2	$(\pi_1) = 3.1969\ (\pi_2)^{-1.1410}(\pi_3)^{.2577-.0267\%SP}\ (\pi_4)^{3.5\Delta\rho\ -\ .15208}$	(47)
	0.1	$(\pi_1) = 6.0204\ (\pi_2)^{-1.410}\ (\pi_3)^{.1485-.1643\%SP}\ (\pi_4)^{12.65\Delta\rho\ -\ .20086}$	(48)
F-111	0.6	$(\pi_1) = 1.643\ (\pi_2)^{-1.1411}\ (\pi_3)^{.1840\ -\ 1.1286\%SP}(\pi_4)^{-.05843}$	(49)
	0.4	$(\pi_1) = 1.8069\ (\pi_2)^{-1.1411}(\pi_3)^{.2060-1.448\%SP}\ (\pi_4)^{-.06742}$	(50
	0.2	$(\pi_1) = 7.7773\ (\pi_2)^{-1.0490}(\pi_3)^{.1885-.1184\%SP}\ (\pi_4)^{-.1643}$	(51)
	.15	$(\pi_1) = 9.0207\ (\pi_2)^{-1.0490}(\pi_3)^{.1656-.0698\%SP}\ (\pi_4)^{8.8\Delta\rho\ -\ .1797}$	(52)

* Value used to derive the equation

SECTION X
MODEL-TO-SIMULATOR CORRELATION

The prediction equations were next used to correlate back with the stopping distance data collected in the Task IIA simulation. A summary of errors in correlation is listed in Table 17. The model to simulator correlation tables for all μ conditions are included in Section XIV, Volume II, ASD-TR-77-6.

The limitations (range of validity) of the prediction equations are:

- Equations 40, 41, 45, 46, 49, and 50 are applicable for μ values of 0.3 to 0.6.
- Equation 42 is applicable for μ range of 0.2 to 0.3 only.
- Equations 43, and 44 are applicable for μ range of 0.05 to 0.2 only.
- Equations 47, and 48 are applicable for μ range of 0.1 to 0.3 only.
- Equations 51, and 52 are applicable for μ range of 0.15 to 0.3 only.

For a given airplane model, the prediction equations are interchangeable (alternate solutions) if their range of applicability and validity is common. Thus, Eq. 40 and 41 are interchangeable, so are 43 with 44, 45 with 46 and 49 with 50. Eq. 42 is a unique solution and not interchangeable with any of its counterparts, Eqs. 40, 41, 43 or 44. Equations 47 and 48 should have been interchangeable; however, the wide-variation in the simulator baseline data (as explained in Section IV) prevented the achievement of a ± 5% correlation accuracy, i.e., ability of one equation to correlate with the data of the counterpart equation. By same reasoning Eq. 51 and 52 should have been, but are not, interchangeable.

Some airplane systems need only one prediction equation to define the entire range of μ values tested on the simulator; others needed more than one equation. The reason for this can be comprehended by studying braking distance efficiency curves for the various systems as shown by Figure 24.

Braking distance efficiency, n_s, is defined as the ratio of the perfect braking distance to the braked airplane distance resulting from the simulation.

$$n_s = X_p/X_a \times 100\%$$

where

n_s = braking distance efficiency
X_p = perfect braking distance
X_a = airplane braking distance

The perfect braking distance is the distance required to stop the airplane if it is braked for the entire stop with maximum available braking force. Braking distance efficiency indicates the degree to which the system meets its primary requirement of stopping the aircraft.

Table 17.—Summary of Percentage Errors

AIRPLANE MODEL	USINC PRED. EQ. FOR $\bar{\pi}_2$	APPLIED TO DATA @ $\bar{\pi}_2$	ERROR RANGE
B-52	0.6	0.6	-1.24 to +1.53
	(40)	0.4	-2.96 to +2.94
	0.4	0.4	-2.41 to +2.51
	(41)	0.6	-4.70 to +4.16
	0.23	0.23	-2.98 to + 3.58
	(42)		
	0.20	0.2	-4.50 to +2.77
	(43)	0.1	-1.86 to +4.65
	0.1	0.1	-4.81 to +4.73
	(44)	0.2	-4.56 to +2.29
KC-135	0.6	0.6	-2.96 to +4.53
	(45)	0.4	-5.51 to +4.26
	0.4	0.4	-1.88 to +4.03
	(45)	0.6	-3.95 to +3.28
	0.2	0.2	-5.09 to +5.03
	(47)		
	0.1	0.1	-4.43 to +4.91
	(48)		
F-111	0.6	0.6	-0.77 to +2.08
	(49)	0.4	-4.71 to +1.91
	0.4	0.4	-3.00 to +1.66
	(50)	0.6	-1.22 to +3.49
	0.2	0.20	-4.85 to +4.86
	(51)	0.15	-9.95 to +0.00
	0.15	0.15	-4.58 to +3.58
	(52)	0.20	-0.50 to +9.56

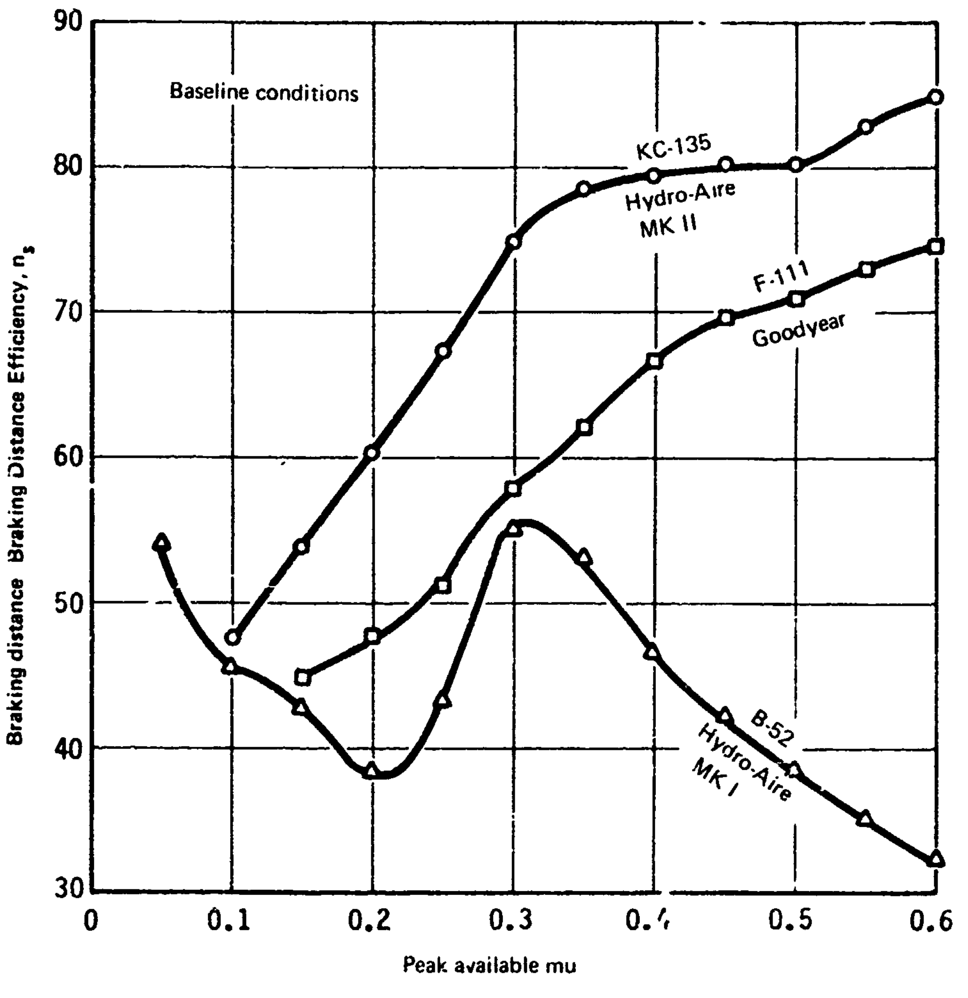

Figure 24.—Mu-Efficiency Curves

The skid control systems for the three subject airplanes encompass two enerations of technology namely, the old, and an intermediate type (see reference 1 page 93). The B-52, Hydro-Aire MK I system was developed under the old technology, the KC-135, Hydro-Aire MK II System from the intermediate technology while the F-111, Goodyear System is very similar to the Hydro-Aire MK II system in design. Two well defined discontinuities occur in the curve for the B-52 for reasons related to torque-limited-braking, weight and velocity combination and the resulting skid activity from being in a particular region of mu-slip curve (see Section IV of this report) while sharp changes in slope appear in the curves for the other two systems at μ values of 0.3. Piecemeal linearization is required when writing mathematical relationships for curves of this nature. This in turn leads to several/multiple prediction equations for each of the curves shown.

The sudden drop in the efficiency at 0.3μ for the B-52 airplane is the result of torque limited braking experienced at mu levels of 0.3 and higher; the torque limiting being the result of an under designed brake. Under torque limiting conditions there is no antiskid cycling because the brake does not have the capability to counteract the maximum available ground force fully. The prediction equation then becomes independent of the π_2 (i.e., mu) term and equation 2a takes the form:

$$(\pi_1) = F(\pi_3, \pi_4)$$

or

$$(\pi_1) = K(\pi_3)^{\alpha}(\pi_4)^{\beta} \qquad (2b)$$

The data generated on the simulator for cases where torque limiting was experienced could be handled by this simplified form of prediction equation; however, the general prediction equations provided in the report for B-52 would also handle these cases. Torque limiting was experienced only at very high weight and high friction (μ) value combinations for both the KC-135 and the F-111 airplanes. The torque limiting cases for the KC-135, and F-111 were therefore excluded from the formulation of equations and the correlation.

The correlation data error summary (Table17)indicates that, for almost all conditions, a prediction accuracy of ± 5% can be achieved.

Even though in the correlation process, comparison was made between predicted and actual π_1 values, that is:

$$(sg/V^2)_{pred} \text{ versus } (sg/V^2)_{actual}$$

it is tantamount to comparing the braking stop distances since both terms use identical g and v values and the distance term has no exponent.

SECTION XI

ADDITIONAL CORRELATION AND WET RUNWAY ANALYSIS

1. PREDICTED MU FROM FLIGHT TEST DATA

The credibility of the simulator procedure was established by comparing the simulator and airplane flight test data and showing that similar trends were obtained under identical conditions (see Section VI). The credibility of the prediction model has been established by obtaining a ± 5% correlation accuracy in predicting simulator stopping distances. The next logical step is to determine if the airplane flight test data could be correlated to the prediction model. This three way correlation process is depicted graphically in figure 25. The results of this exercise are shown in Table18. From the type of information available on the flight test data (Table18)the only parameter that could be calculated by the prediction equation was the friction coefficient. The predicted values, for both dry and wet runway conditions, compare rather well.

2. WET-RUNWAY ANALYSIS

During Task IIA simulation testing, a wet runway was simulated so that the available ground mu was programmed to vary with speed. (See Figure 26). The mu values (end points) used were 0.05 at brake application speed and 0.5 at the end of the stop. Additional wet runways were also simulated with end points being 0.05 to 0.4 and 0.05 to 0.3.

The average value of peak available mu for the braking system was unknown, so it was decided to use the component equations formed earlier (the π_1 versus π_2 relationships) to calculate peak available mu. Based on calculations for wet runways, prediction equations were generated for each wet runway. With these prediction equations, a correlation prediction accuracy analysis was conducted as before and satisfactory results were obtained. The component equations, the prediction equations, and the correlation error tables for the wet runways tested, are included in this section, (see Tables 19 through 23). The details of this analysis are reported in ASD-TR-77-6, Volume II, Section XV. The results show that the wet runway data based prediction equations relate with each other with the same accuracy as the fixed mu prediction equations, and give additional confidence to the selected methodology for forming prediction equations.

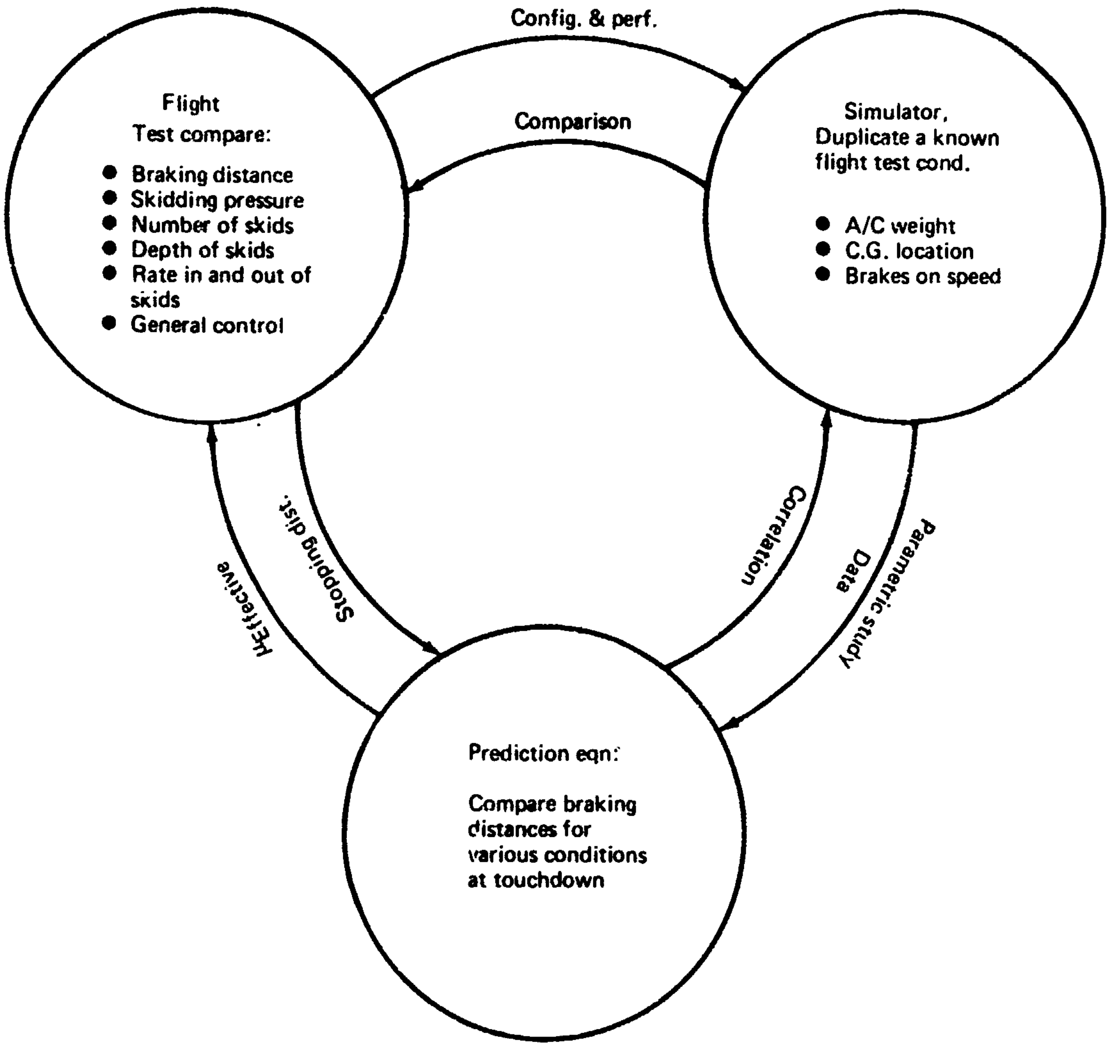

Figure 25.—Correlation Process

Table 18.—Comparison with Flight Test Data

AIRPLANE	FLIGHT NO. (REF. NO.)	TYPE OF RUNWAY	FLIGHT TEST DATA: BRAKING DURATION (FPS)	FLIGHT TEST DATA: BRAKING DISTANCE (FT)	FLIGHT TEST DATA: CALCULATED MU*	SIMULATOR "MU" VALUE**	USING FLIGHT TEST DATA: PREDICTED MU	USING FLIGHT TEST DATA: PREDICTION EQ. USED @ $\bar{\pi}_2$
KC-135	2 - 7 (15)	DRY CONCRETE	199.6-24.0	1750	.505	.52	.503 .502	.6 .4
	9 - 2 (15)	WET CONCRETE	234.9-24.0	5021	.257	.26	.243 .240	.2 .05 to .5
F-111	4 (21)	DRY CONCRETE	226.73 - 38.17	1753	Not Available	.760	.743	.6
	5 (21)	WET CONCRETE	225.53 - 57.27	5128	N/A	N/A	.30 .31	.3 .05 to .5
	6 (21)	WET CONCRETE	228.0 - 35.3	5[illegible]56	N/A	.260	.267 .277	.3 .06 to .5
	7 (21)	WET CONCRETE	233 90.65	7756	N/A	N/A	.295 .297	.3 .05 to .5

** VALUE OF PEAK AVAILABLE MU USED ON SIMULATOR FOR CORRELATION WITH FLIGHT TEST DATA

* CALCULATED MU = $\mu_{AVG.}/n_{BRAKING}$

WHERE $\mu_{avg.}$ IS THE VALUE TAKEN FROM TABLE I, REFERENCE (15).

AND $n_{BRAKING}$ IS THE BRAKING DISTANCE EFFICIENCY DETERMINED BY SENSITIVITY STUDY

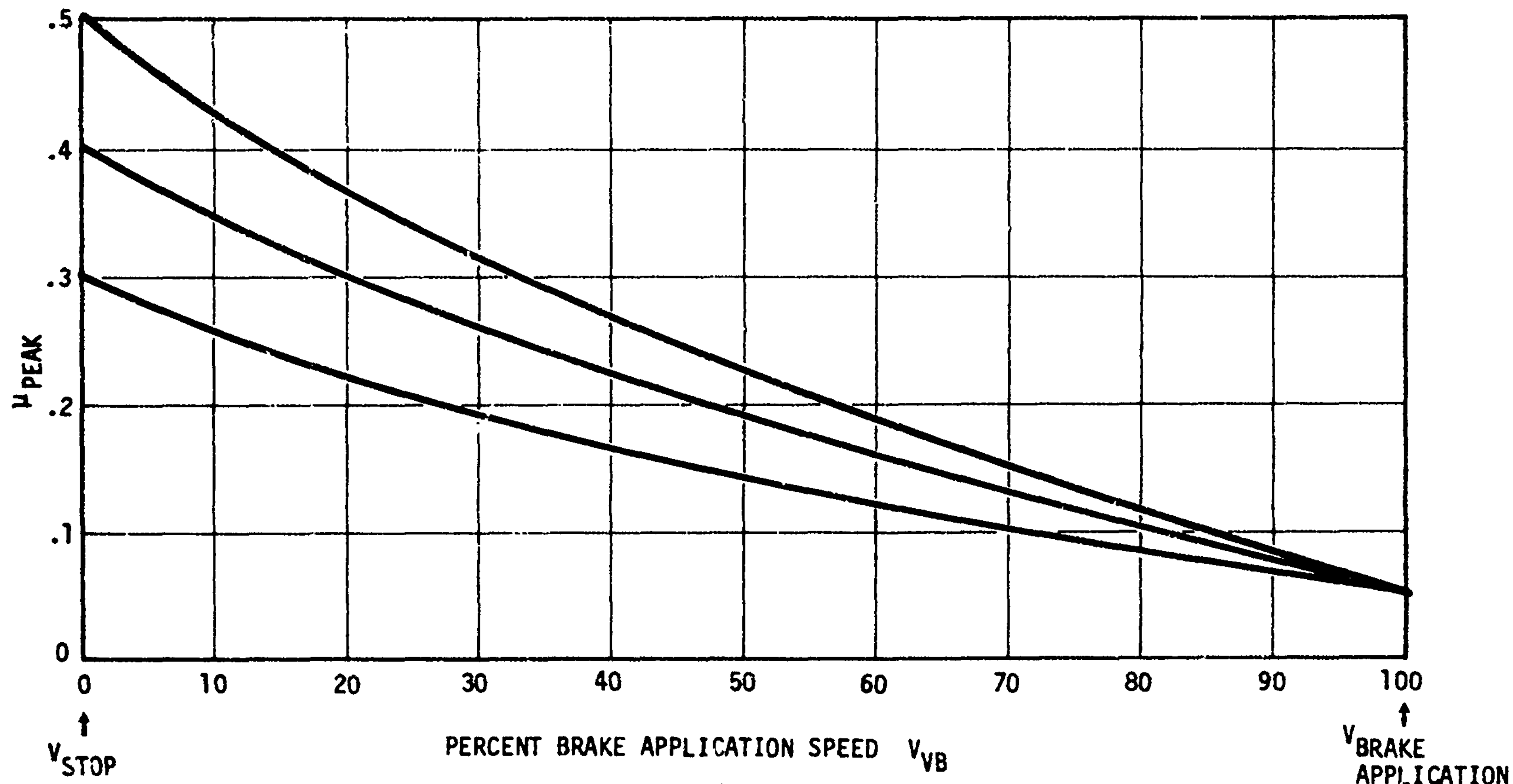

Figure 26.—Mu-Velocity Curves for Wet Runways

Table 19.—Summary of Component Equations - Wet Runways

Airplane model	μ	Equation	Eq. No.
B-52	.05 to .5 (23)	$(\pi_1) = .1747\ (\pi_2)^{-2.2504}$	(8)
		$(\pi_1) = 4.8081\ (\pi_3)^{.13006-.07741\%SP}$	(9)
		$(\pi_1) = 24.5495\ (\pi_4)^{17.75\Delta\rho\ -\ .1836}$	(10)
	.05 to .4 (.175)	$(\pi_1) = 2.3524\ (\pi_2)^{-.5188}$	(11)*
		$(\pi_1) = 5.8154\ (\pi_3)^{.1275-.1258\%SP}$	(53)
		$(\pi_1) = 32.7278\ (\pi_4)^{19.60\Delta\rho\ -.1991}$	(54)
	.05 to .3 (.127)	$(\pi_1) = 2.3524\ (\pi_2)^{-.5188}$	(11)*
		$(\pi_1) = 6.8597\ (\pi_3)^{.1049-.1243\%SP}$	(55)
		$(\pi_1) = 37.7863\ (\pi_4)^{20.97\Delta\rho\ -\ .19788}$	(56)
KC-135	.05 to 0.5 (.166)	$(\pi_1) = .5893\ (\pi_2)^{-1.1410}$	(21)
		$(\pi_1) = 4.4163\ (\pi_3)^{.1994-.1225\%SP}$	(57)
		$(\pi_1) = 15.2166\ (\pi_4)^{18.00\Delta\rho\ -\ .1063}$	(58)
	.05 to 0.4 (.154)	$(\pi_1) = .5893\ (\pi_2)^{-1.1410}$	(21)
		$(\pi_1) = 4.8494\ (\pi_3)^{.2161-.1412\%SP}$	(59)
		$(\pi_1) = 11.1128\ (\pi_4)^{21.00\Delta\rho\ -\ .07158}$	(60)
	.05 to 0.3 (.137)	$(\pi_1) = .5893\ (\pi_2)^{-1.1410}$	(21)
		$(\pi_1) = 5.6794\ (\pi_3)^{.1913-.1781\%SP}$	(61)
		$(\pi_1) = 15.3497\ (\pi_4)^{17.54\Delta\rho\ -.06797}$	(62)

* was calculated with Eq. (11) data plus wet runway data.

Table 19.—Summary of Component Equations - Wet Runways (Concluded)

Airplane model	μ	Equation	Eq. No.
F-111	.05 to .5 (.231)	$(\pi_1) = .9467\ (\pi_2)^{-1.0490}$	(31)
		$(\pi_1) = 4.3767\ (\pi_3)^{.1790-.0834\%SP}$	(63)
		$(\pi_1) = 33.7671\ (\pi_4)^{8.0\Delta\rho-.1606}$	(64)
	.05 to .4 (.218)	$(\pi_1) = .9467\ (\pi_2)^{-1.0490}$	(31)
		$(\pi_1) = 4.6220\ (\pi_3)^{.1976-.1046\%SP}$	(65)
		$(\pi_1) = 46.5388\ (\pi_4)^{7.75\Delta\rho-.1804}$	(66)
	.05 to .3 (.193)	$(\pi_1) = .9467\ (\pi_2)^{-1.0490}$	(31)
		$(\pi_1) = 5.2915\ (\pi_3)^{.1973-.1296\%SP}$	(67)
		$(\pi_1) = 55.0660\ (\pi_4)^{-.1827}$	(68)

Table 20.—Test of Validity for the Function to be a Product - Wet Runways

Airplane Model	Value of Function in Eq.39			Ideal Value of Function in Eq.39	Deviation Passage		
	L.H.S. $\pi_2 = .05$ to .5	R.H.S. $\pi_2 = .05$ to .4	R.H.S. $\pi_2 = .05$ to .3		L.H.S. $\pi_2 = .05$ to .5	R.H.S. $\pi_2 = .05$ to .4	R.H.S. $\pi_2 = .05$ to .3
B-52	0.9910	1.0268	1.0563	1.000	-0.89	2.68	5.63
KC-135	1.0148	1.0165	1.0147	1.000	1.48	1.65	1.47
F-111	0.9964	1.0002	0.9859	1.000	-.36	0.02	-1.41

Table 21.—Test of Validity for Constant Term - Wet Runways

Airplane Model	$C = \left[1/_F(\pi_2, \pi_3, \pi_4)\right]^2$ Component Equation Used			Ideal Value of C	Average Deviation (%)	Value of π_2
	π_1 vs π_2	π_1 vs π_3	π_1 vs π_4			
B-52	.04395	.04349	.04362	.04373	0.10	.023
	.02954	.02957	.03112	.02954	1.83	.175
	.02124	.02121	.02373	.02123	3.62	.127
KC-135	.04782	.04801	.04906	.04788	0.88	.166
	.04000	.03987	.04146	.40000	1.10	.154
	.03065	.03065	.03156	.03065	0.99	.137
F-111	.05158	.05057	.05224	.05096	0.99	.231
	.04568	.04538	.04599	.04338	0.67	.218
	.03537	.03491	.03483	.03506	0.06	.193

Table 22.—Summary of Prediction Equations - Wet Runways

Airplane model	μ*	Equation	Eq. No.
B-52	.23	$(\pi_1) = .9009\,(\pi_2)^{-2.2504}\,(\pi_3)^{.13006-07741\%SF}\,(\pi_4)^{17.75\Delta\rho-.1836}$	(42)
	.175	$(\pi_1) = 13.4764\,(\pi_2)^{-.5188}\,(\pi_3)^{.1275-.1258\%SP}\,(\pi_4)^{19.60\Delta\rho-.1991}$	(69)
	.127	$(\pi_1) = 13.4145\,(\pi_2)^{-.5188}\,(\pi_3)^{.1049-.1243\%SP}\,(\pi_4)^{20.97\Delta\rho-.1979}$	(70)
KC-135	.166	$(\pi_1) = 1.9123\,(\pi_2)^{-1.1410}\,(\pi_3)^{.1995-.1225\%SP}\,(\pi_4)^{18.00\Delta\rho\,-.10629}$	(71)
	.154	$(\pi_1) = 1.2841\,(\pi_2)^{-1.1410}\,(\pi_4)^{.2161-.1412\%SP}\,(\pi_4)^{21.0\Delta\rho\,-.07158}$	(72)
	.137	$(\pi_1) = 1.5899\,(\pi_2)^{-1.1410}\,(\pi_3)^{.1913-.1781\%SP}\,(\pi_4)^{17.54\Delta\rho-.08797}$	(73)
F-111	.231	$(\pi_1) = 7.1987\,(\pi_2)^{-1.0490}\,(\pi_3)^{.1790-.0834\%SP}\,(\pi_4)^{8.0\Delta\rho\,-.1606}$	(74)
	.218	$(\pi_1) = 9.3190(\pi_2)^{-1.0490}\,(\pi_3)^{.1976-.1046\%SP}\,(\pi_4)^{7.75\Delta\rho\,-.1804}$	(75)
	.193	$(\pi_1) = 9.6663(\pi_2)^{-1.0490}\,(\pi_3)^{.1973-.1296\%SP}\,(\pi_4)^{6.85\Delta\rho-.1827}$	(76)

Table 23.—Summary of Percentage Errors - Wet Runways

AIRPLANE MODEL	USING PRED. EQ. FOR $\bar{\pi}_2$ (EQ. NO.)	APPLIED TO DATA @ $\bar{\pi}_2$	ERROR RANGE
B-52	0.23 (42)	0.23	-2.98 to +3.58
	0.175 (69)	0.175	-4.25 to +4.05
		0.127	-7.08 to +2.64
	0.127 (70)	0.127	-7.95 to +2.76
		0.175	-5.40 to +4.69
KC-135	0.166 (71)	0.166	-4.76 to +4.73
		0 154	-9.88 to +7.30
		0.137	-5.30 to +6.00
	0.154 (72)	0.154	-4.04 to +5.58
		0.166	-5.68 to +6.47
		0.137	-6.46 to +5.69
	0.137 (73)	0.137	-5.32 to +5.13
		0.166	-7.46 yo +5.91
		0.154	-6.24 to +5.37
F-111	0.231 (74)	0.231	-4.68 to +3.67
		0.218	-1.93 to +4.34
		0.193	-0.75 to +5.84
	0.218 (75)	0.218	-2.21 to +4.69
		0.231	-5.50 to +3 79
		0.193	-4.43 to +3.17
	0.193 (76)	0.193	-3.92 to +2 98
		0.231	-6.13 to +3.38
		0.218	-3.15 to +1.34

Table 23.—Summary of Percentage Errors - Wet Runways

AIRPLANE MODEL	USING PRED. EQ. FOR $\bar{\pi}_2$ (EQ. NO.)	APPLIED TO DATA @ $\bar{\pi}_2$	ERROR RANGE
B-52	0.23 (42)	0.23	-2.98 to +3.58
	0.175 (69)	0.175	-4.25 to +4.05
		0.127	-7.08 to +2.64
	0.127 (70)	0.127	-7.95 to +2.76
		0.175	-5.40 to +4.69
KC-135	0.166 (71)	0.166	-4.76 to +4.73
		0 154	-9.88 to +7.30
		0.137	-5.30 to +6.00
	0.154 (72)	0.154	-4.04 to +5.58
		0.166	-5.68 to +6.47
		0.137	-6.46 to +5.69
	0.137 (73)	0.137	-5.32 to +5.13
		0.166	-7.46 yo +5.91
		0.154	-6.24 to +5.37
F-111	0.231 (74)	0.231	-4.68 to +3.67
		0.218	-1.93 to +4.34
		0.193	-0.75 to +5.84
	0.218 (75)	0.218	-2.21 to +4.69
		0.231	-5.50 to +3 79
		0.193	-4.43 to +3.17
	0.193 (76)	0.193	-3.92 to +2.98
		0.231	-6.13 to +3.38
		0.218	-3.15 to +1.34

SECTION XII
TBPS COMPLETENESS AND VERIFICATION

1. COMPATIBILITY VERIFICATION

Under Task I analysis the Friction Prediction Subsystem concept was developed and is shown here in figure 27. Validation of the Braking Performance Prediction Model was established under Task II and the resulting Braking Prediction Subsystem concept is depicted in figure 28. These two subsystems, when integrated, will form the Total Braking Prediction System as shown in figure 29. The compatibility between the output of the FPSS and the input to the BPSS is solely dependent upon the tire-model verification which in turn is based upon conducting the recommended tire testing. However, based on our engineering judgment and available tire test data, there is no reason to believe that this compatibility will not be achieved.

Assuming that the recommended tire test data will be obtained and that the output of the FPSS will be in the form of a family of mu-velocity curves, we can proceed to the TBPS analysis of the simulator conditions. As explained in section XI, wet runway analysis, the wet runway curve was input to the simulator as a mu-velocity curve (figure 26). In accordance with the suggested TBPS and its subsystems, three wet runway curves (.05 to .5, .05 to .4, .05 to .3) forming the so-called family of curves were input for each of the three airplanes studied. The sensitivity tests were run and the data analyzed, as already explained in section XI. The prediction equations obtained for each of these wet runways and their cross-correlation accuracy were shown to be in conformity with the fixed mu equations and correlation for each of the respective airplanes. This clearly establishes that when the required significant parameters are input into the BPSS, the correct stopping prediction will result.

2. FINALIZATION OF TBPS SPECIFICATION

The specification for the TBPS is comprised of the FPSS performance specification, the general BPSS model and the tire correlation model. The basic concept of the FPSS is shown in Figure 27. The FPSS performance specification was established under Task I of this contract and discussed in detail in ASD-TR-77-7. The FPSS specification also covered the system fabrication criteria. The general BPSS model was established and validated by a sensitivity study of eight different airplane braking systems. The general concept of the BPSS is depicted in Figure 28. Certain hardware and data are required for a successful simulation of any given aircraft braking system.

Basic vehicle system parameters and brake system hardware are incorporated into the computer/hardware simulation for each of the airplanes being evaluated. The basic data are available from existing specifications, qualification reports, and flight handbooks, and are generally no cost items.

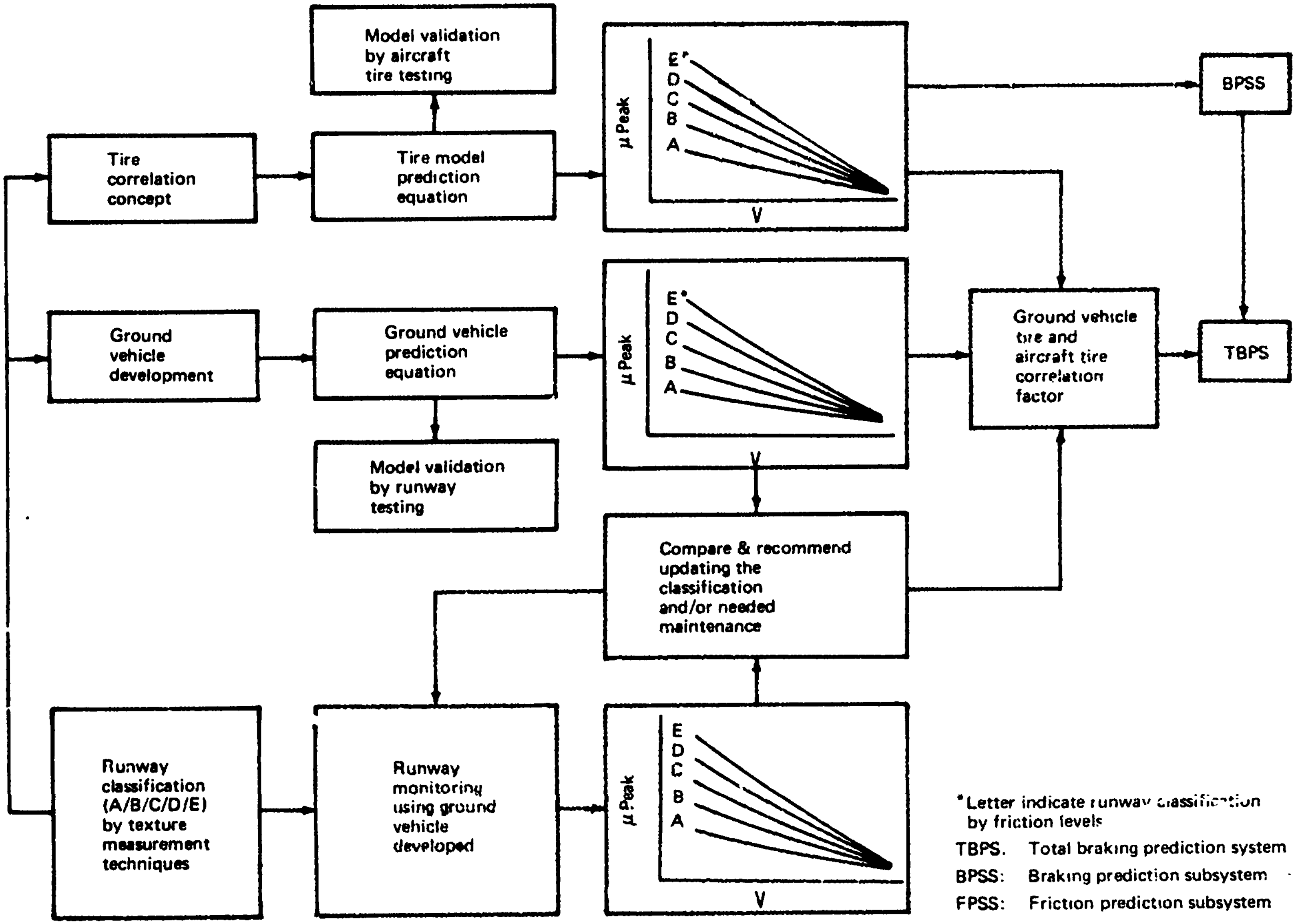

*Letter indicate runway classification by friction levels

TBPS. Total braking prediction system

BPSS: Braking prediction subsystem

FPSS: Friction prediction subsystem

Figure 27.—Friction Prediction Subsystem (FPSS)

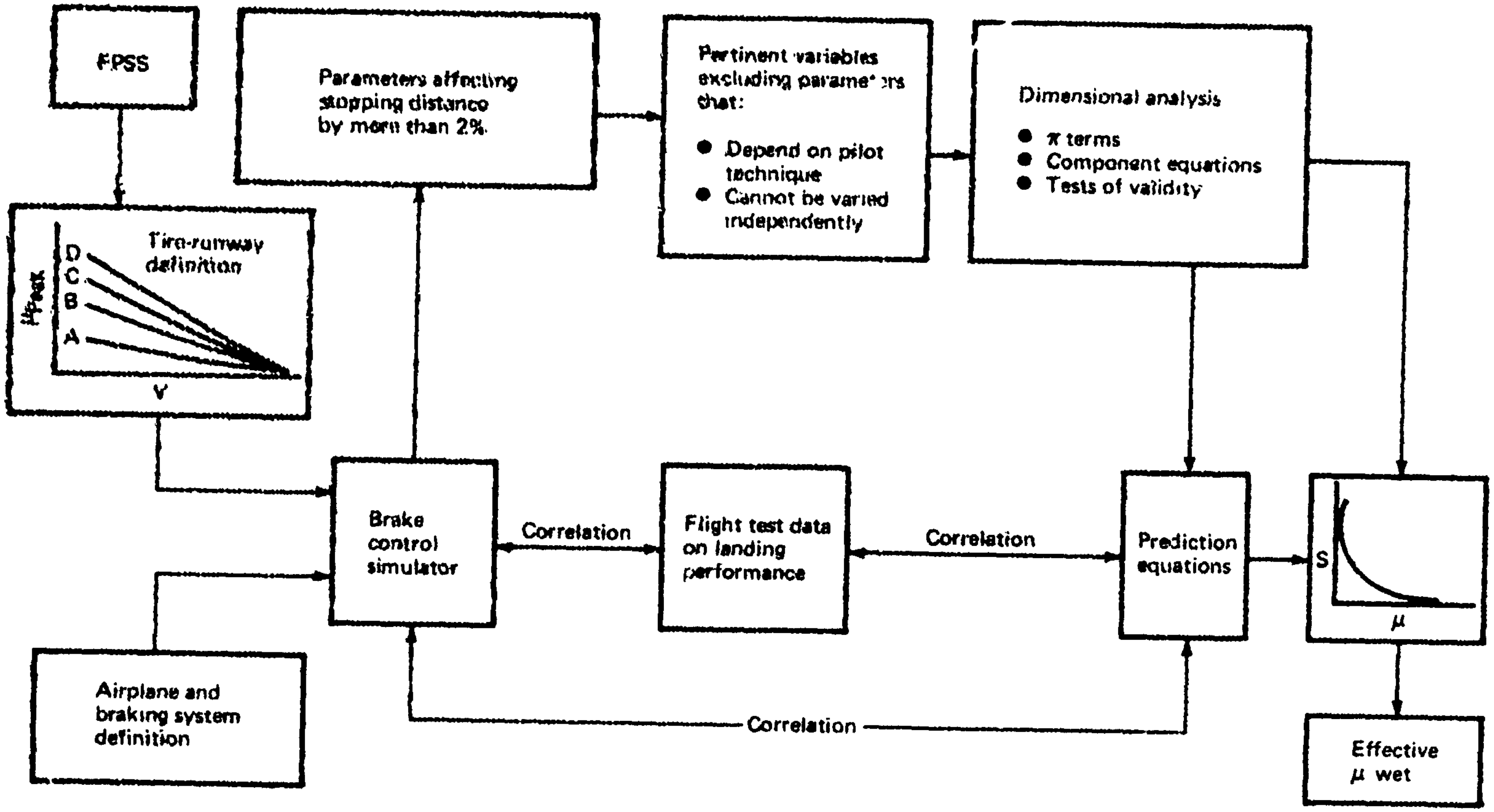

Figure 28.—Braking Prediction Subsystem (BPSS)

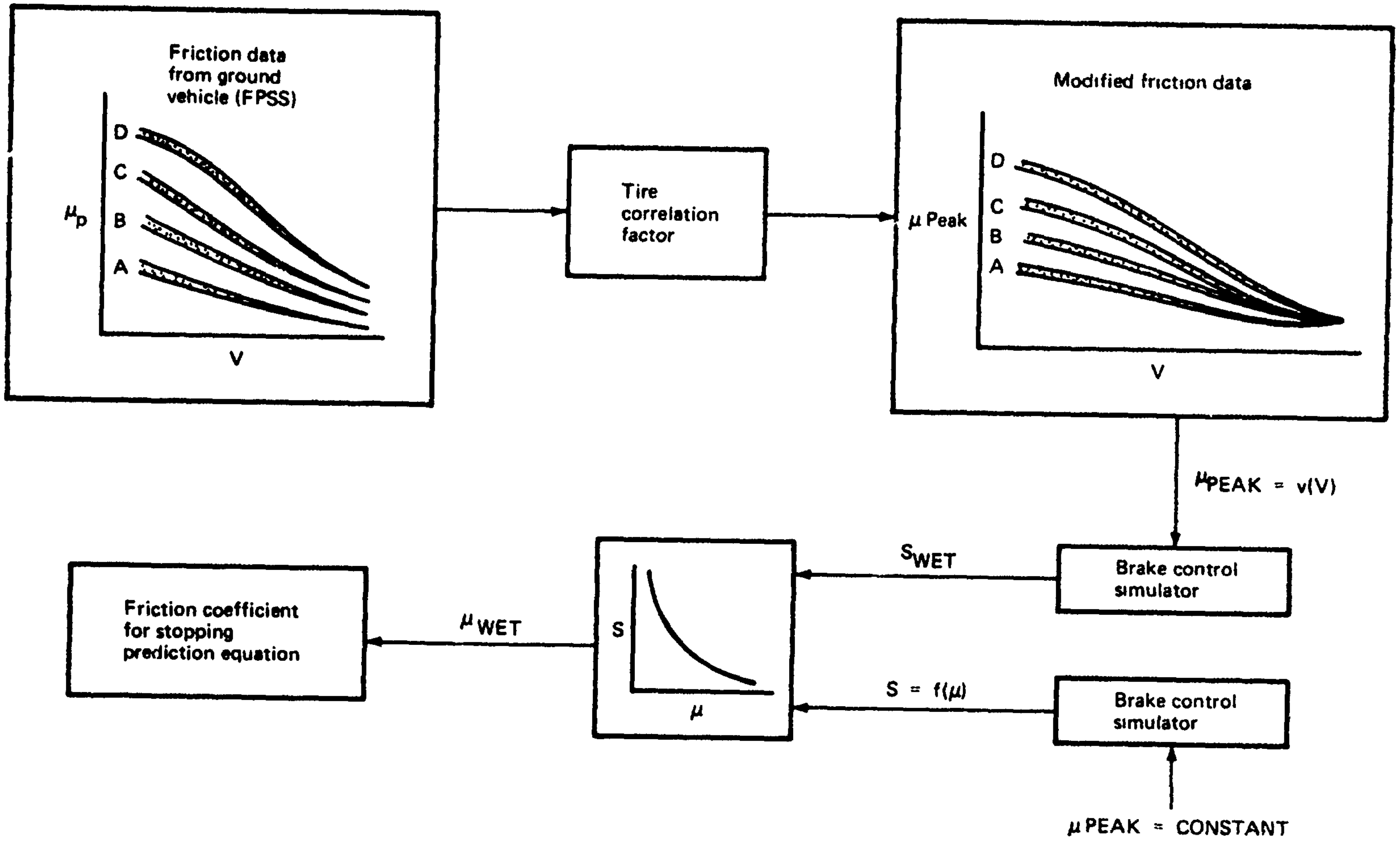

Figure 29.—Total Braking Prediction System (TBPS)

The requirements can be divided into three categories as follows:

- Basic vehicle parameters
- Landing gear strut parameters
- Tire, wheel and brake system parameters

The specific requirements for each category are listed in Table 24. Any of the less critical parameters which are not available can be estimated for the simulation.

Brake system hardware required for the USAF-F-4, C-141, B-52, KC-135, and F-111 simulations are listed in Table 25. Items unique to each skid control system are checked accordingly.

In addition to the above requirements, airplane flight test records showing brake pressure, wheel speed valve voltages and strut loads are very helpful and necessary for establishing the credibility of the individual simulation.

The tire correlation model was also established under Task I analysis and the concept is shown here in figure 30. The integration of the three subsystem concepts has already been discussed and shown in figure 29. The information provided herein and in ASD-TR-77-7, together should be sufficient to allow total system fabrication and development.

3. VERIFICATION TEST PROGRAM

An extensive test program must be conducted for the verification of the Total Braking Prediction System. It involves the use of the Friction Prediction Subsystem (ground vehicle), the Prediction Equation, Tire Correlation Method, and at least one suitable aircraft. The overall goal is, of course the prediction of braking distance with the methods and tools recommended during the course of this program. Comparison of predicted braking distance to the value measured from actual airplane tests will give a measure of correlation. Measurements taken with the ground vehicle and actual airplane braking test must be conducted within a few minutes of each other so that runway and environmental conditions can vary the least possible amount. The major tasks which must be accomplished are shown on Figure 31. A ground vehicle which is configured and performs according to the Friction Prediction Subsystem specification is used to conduct friction evaluation tests on the runway. With the use of the previously developed prediction equation for the vehicle a friction coefficient can be determined. Due to the physical and operational differences between vehicle and airplane tires a correction factor must be applied to the friction coefficient calculated from the ground vehicle test before it can be applied to the airplane braking distance prediction equation. The airplane conditions at brake application are to be used in the prediction equation. Hence in this verification program a braking distance comparison can only be made after the airplane and ground vehicle tests are performed. In actual operational use the anticipated condition at touchdown will be used for a prediction of braking distance. The sensitive parameters such as brake application speed and friction coefficients can then be varied to determine the margin of the runway.

Table 24.—Basic Airplane Data Required

- Airplane parameters

  1. Location of the landing gear relative to the center of gravity.
  2. Airplane landing gross weight range, (including corresponding stall speeds).
  3. Airplane center of gravity range (vertical and horizontal).
  4. Effective wing area.
  5. Aerodynamic coefficients—lift and drag (nominal landing flaps, spoilers, up and down).
  6. Total engine idle thrust versus speed.
  7. Airplane mass moment of inertia about the center of gravity in the pitch direction.

- Tire, wheel and brake system parameters

  1. Weight
     a) Main gear tire and wheel assembly.
     b) Total brake assembly.
     c) Brake heat sink.
  2. Brake mean torque versus pressure.
  3. Number of braked wheels.
  4. Tire size and ply rating.
  5. Tire mechanical properties.
  6. Brake hydraulic system diagrams showing line sizes, line lengths, and materials.
  7. Mass moment of inertia of the wheel, brake and tire assembly about the axle centerline.

- Landing gear strut parameters

  1. Vertical spring rate of the main gear oleo.
  2. Vertical spring rate of the nose gear oleo.
  3. Effective length of the main gear strut.
  4. Fore-aft spring rate of the strut.
  5. Strut fore-aft natural frequency range.
  6. Total effective mass of the strut.
  7. Main landing gear layout drawing showing basic dimensions.
  8. Truck size, weight, center of gravity and pitch moment of inertia (where applicable).
  9. Fore-aft mass moment of inertia of main gear strut.

Table 25.—Hardware Required for Brake Control Simulator (BPSS)

ITEM DESCRIPTION	AIRPLANE AND APPLICABILITY				
	C-141	F-4	B-52	KC-135	F-111
SKID CONTROL BOX	✓	✓	✓	✓	✓
SKID DETECTOR	✓	✓	✓	✓	✓
PILOT METERING VALVE	✓	✓	✓	✓	✓
ANTISKID VALVE	✓	✓	✓	✓	✓
ACCUMULATOR	✓	✓	✓	✓	✓
BRAKE ASSEMBLY	✓	✓	✓	✓	✓
DEBOOST VALVE				✓	
HYDRAULIC FUSE	✓		✓	✓	
RESTRICTOR	✓		✓		
CHECK VALVE			✓		
RELIEF VALVE			✓		
BRAKE SWIVEL ASSEMBLY			✓		
SHUTTLE VALVE	✓				

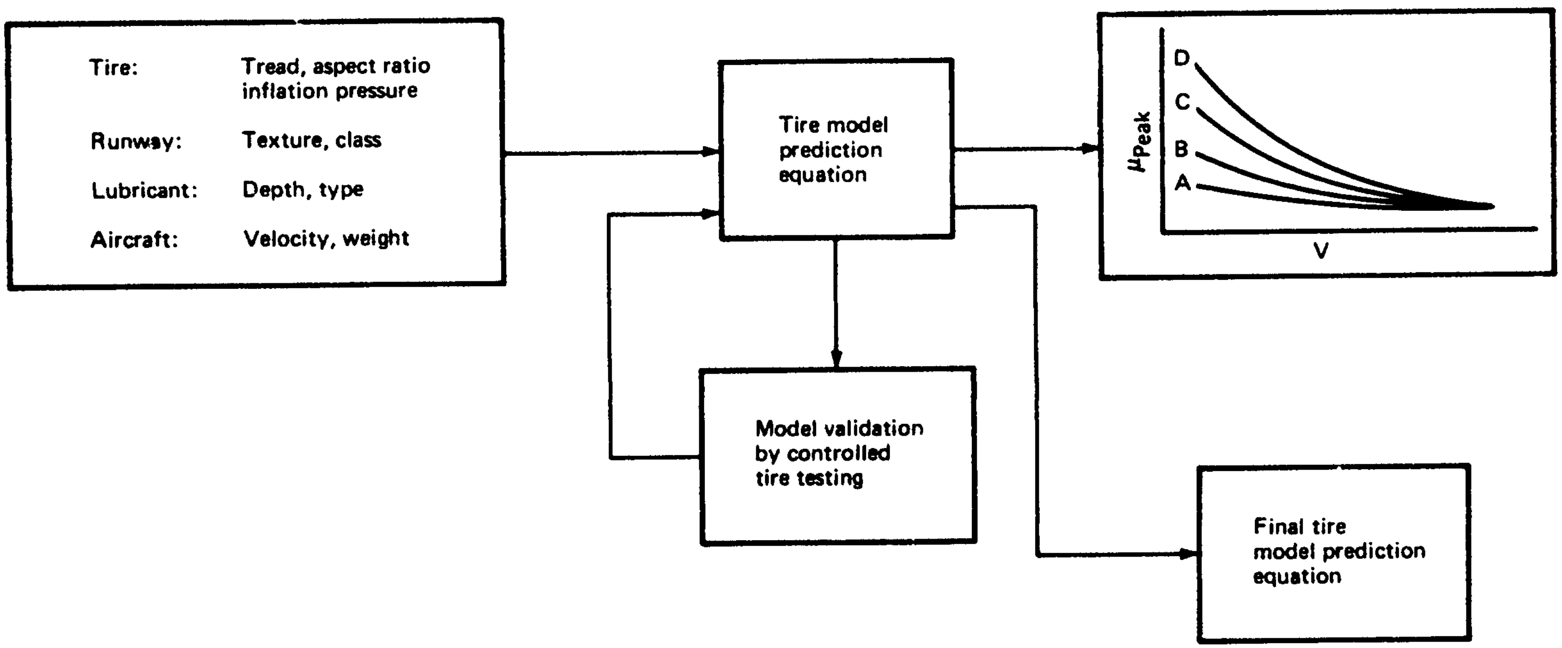

Figure 30.—Tire Correlation Model

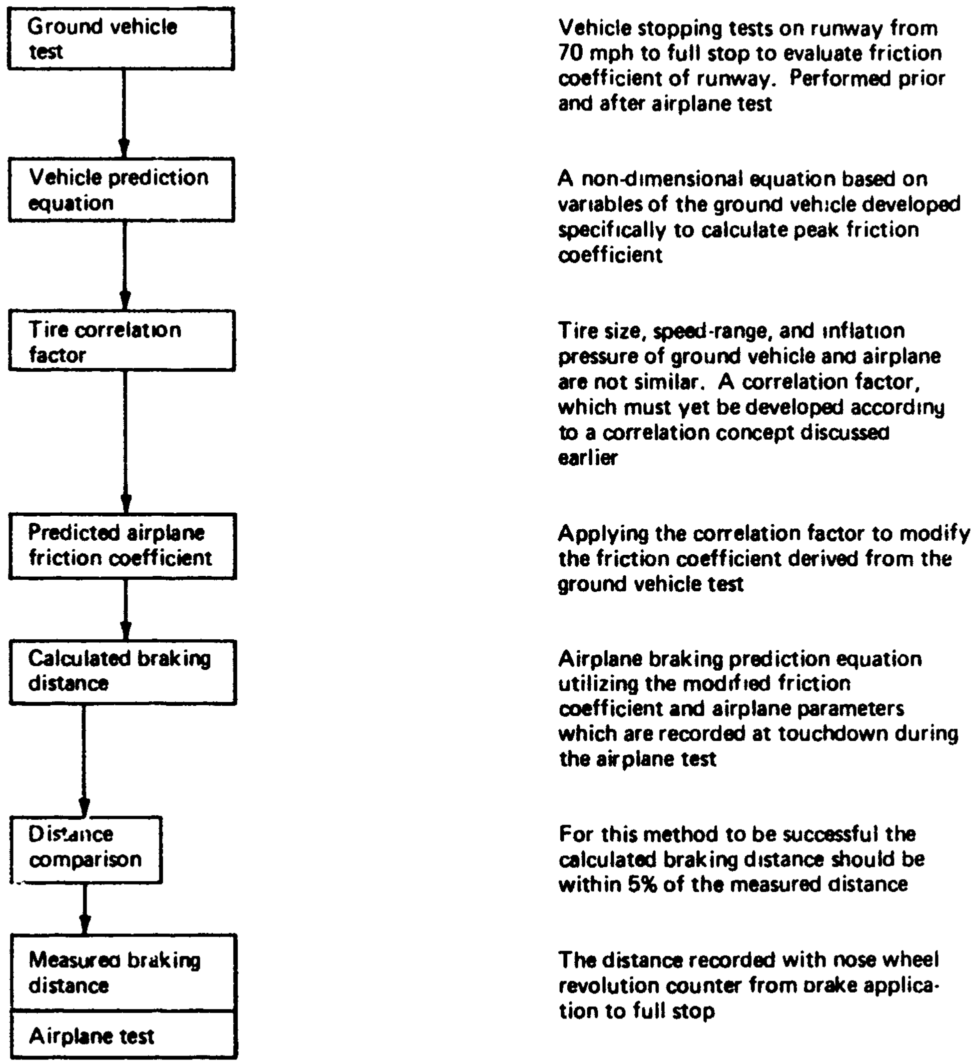

Figure 31.—Block Diagram for Verification Test Program

TEST HARDWARE

The following major items are required for conducting the test program:

a. Friction Prediction Subsystem—(ground vehicle)

A ground vehicle with performance as described in the specification (Task I Report, ASD-TR-77-7) must be available for the measurement of ground friction. The most relevant features of the ground vehicle are that the test tire is an aircraft tire which can be braked with an antiskid system. Performance of the antiskid system must be similar to that of an advanced type aircraft antiskid system. The vehicle is to be used for an assessment of runway friction which will be used for the prediction of aircraft stopping distance. A prediction-equation-Mu is part of the Friction Prediction Subsystem which allows the calculation of Mu based on the brake application speed and the resulting stopping distance. Other variables such as environmental conditions may also be involved.

b. Airplane and Prediction Equation

A suitable aircraft equipped with an antiskid system must be made available and perform braking stops for which the distance will be predicted from FPSS measurements and the Prediction Equation. It is recommended that the Advanced 737 (T-43A) be used for this program for the following reasons:

- Proven short field capability
- Excellent braking performance
- Efficient modern antiskid system
- Economic test airplane due to two engine configuration
- Braking Prediction Equation applicable over a wide range of friction coefficients

The T-43A has proven short field capability and tests could be conducted at a variety of different airfields. Should an extremely long runway be available, the braking tests can be run in an accelerate stop fashion without the aircraft ever becoming airborne. Special brake cooling sources would have to be provided because repeated braking would result in overheating of the brakes.

The T-43A is equipped with a modern, fully modulating antiskid system with efficient operation over all ranges of operating conditions. The operation of the antiskid system is representative of that realized on the latest and most modern jet aircraft.

The T-43A is an economic test bed due to the two engine design. Fuel and maintenance expense will be less than those encountered on three and four engine aircraft.

During the course of the Combat Traction II, Phase II Program, a Braking Prediction Equation has been developed for the T-43A which covers a wide range of friction coefficients. Good correlation to simulator results and flight test data has been demonstrated.

c. **Tire-Correlation Method**

The test tire on the ground vehicle is similar in design and applied antiskid operation to the aircraft tire. However, the size, inflation pressure, and speed range over which the tires are being used are different. It is anticipated, therefore, that the friction coefficient derived from the ground vehicle must be modified before being used in the airplane braking distance prediction equation. Based on a number of isolated data points for different aircraft tires, a correlation concept has been developed. However, a much wider data base must be developed before this correlation concept can be used with any degree of confidence. This tire correlation method must be developed before the Total Braking Prediction System verification test program is initiated.

TEST PLANE

The major portion of the test consists in making performance stops on both wet and dry runways for a variety of initial airplane conditions. These include, but are not limited to, the conditions shown on the matrix of figure 32. The spoiler UP and DOWN configuration will result in the widest possible variation on aerodynamic lift and drag. The overspeed touchdown conditions are very typical of the operational environment airplanes encounter every day.

Ideally, testing should be conducted under calm wind conditions, however, as an upper limit a steady wind of no more than 5 knots from any direction is acceptable. In flying the airplane to touchdown a normal (2.5 degree) glide slope should be maintained, touchdown should be aimed at the 1000 ft marker. During the flare the pilot should cut the engine power to idle. At touchdown the spoilers (speed brakes) should be extended (when required) as the nose gear is lowered to the ground. Then the brakes should be applied smoothly and firmly until maximum metered brake pressure is reached and maintained to a full stop. To limit the transition distance the time elapsed from touchdown to brake application should not exceed four seconds. No reverse thrust should be applied. This technique shall be used for both wet and dry runway tests.

The aircraft shall be instrumented for the recording of at least the following parameters:

a.	Wheel speed transducer signal	(four locations)
b.	Brake pressure and metered pressure	(eight locations)
c.	Antiskid valve voltage	(four locations)
d.	Inboard brake center stator temperatures	(two locations)
e.	Nose gear revolution counter	(one location)
f.	Engine pressure ratio	(two locations)
g.	Spoiler handle position	(two locations)
h.	Braking distance--Theodolite	

ADV. 737, FLAPS 40°, GEAR DOWN						
WT / SPEED AT TOUCH-DOWN	85,000# V_S = 83KN		95,000# V_S = 88 KN		105,000# V_S = 93 KN	
	SPOILERS	BRAKING DISTANCE*	SPOILERS	BRAKING DISTANCE*	SPOILERS	BRAKING DISTANCE*
1.3 V_S	UP	S_D 1170	UP	S_D 1301	UP	S_D = 1426
		S_W 3447		S_W 3833		S_W = 4202
	DN	S_D 1675	DN	S_D 1846	DN	S_D = 2022
		S_W 4937		S_W 5440		S_W = 5960
1.3 V_S + 20 KN	UP	S_D 1565	UP	S_D 1698	UP	S_D = 1837
		S_W 4613		S_W 5007		S_W = 5414
	DN	S_D 2220	DN	S_D 2410	DN	S_D = 2606
		S_W 6542		NOT RECOMMENDED		NOT RECOMMENDED
1.3 V_S + 40 KN	UP	S_D 1991	UP	S_D 2138	UP	S_D = 2289
		S_W 5867		S_W 6300		S_W = 6745
	DN	S_D 2824	DN	S_D 3032	DN	S_D = 3246
		NOT RECOMMENDED		NOT RECOMMENDED		NOT RECOMMENDED

*BRAKING DISTANCE CALCULATED FOR 737 PREDICTION EQUATION (49), ASD-TR-74-41, I, PG. 92,
MU=.575 FOR DRY, MU = .14 FOR WET

Figure 32.-Test Matrix

For the dry runway test no special runway preparation is required as long as there are no excessive rubber or dirt deposits. Considerably more effort is required to prepare the "wet" runway where no rainfall is available. When artificial wetting of the runway is required this is best accomplished with watertrucks, with a capacity of 5,600 gallons per truck. One hour prior to each series of wet runway tests the runway must be prewetted with 14 water trucks. As the truck proceeds down the runway, the water can be dumped on the runway surface through one or two nozzles, on each truck, flooding the runway briefly before it runs off. The actual water discharge rate and truck speed depends to some extent on the runway surface texture and must be adjusted as required. Before each test additional 6 or 7 trucks dump water to either side of the runway centerline. The test conductor must ensure that the proper length of the runway is covered with water. Because the water will gradually run off the runway readings with the ground vehicle shall be taken just before and immediately after the airplane stopping test. The ground vehicle test consists of accelerating to the desired speed and then braking to a full stop with the antiskid braked tire. This test must be repeated for the length of the test runway. Runway friction values can then be derived from the prediction equation and data recorded during the vehicle test. The friction values shall be averaged when they are applied to the prediction equation of the airplane to compensate for the actual time at which the airplane touched down. Close timing of these readings is essential to make the results representative of those that the airplane encounters. Communication by radio between the test coordinator, pilot, ground vehicle driver and the water trucks convoy is essential. Air temperature, wind velocity and direction shall be monitored at two points on the side of the runway, approximately 12 ft above the runway surface. One monitoring point should be located near the touchdown point, the other about 2000 ft down the runway.

TEST CONDITIONS

The recommended test conditions are shown on Figure 32 and include variations in airplane touchdown speeds, weight, aerodynamic configuration with spoiler UP and DOWN, and dry and wet runway. A total of 31 tests are recommended. Due to the resulting long braking distances caused by touchdown with excessive speed and undeployed spoilers on wet runways, some of those conditions are not recommended. If touchdown is accomplished at the 1000 ft marker and 1000 ft is consumed in derotating the airplane and applying brakes, then more than 1000 ft of margin will remain for the longest stop as calculated with the 737 prediction equation when testing is conducted on a 10,000 ft wet runway.

CORRELATION CRITERIA

For this evaluation test the braking distance can only be calculated after the airplane test because the airplane brake application speed can only be determined after the test records are examined. Also for wet runway tests the airplane friction coefficient will be available after the second test which is conducted shortly after the airplane test. The method of correlation is deemed successful if calculated distances are within 5% of those measured with the airplane tests.

In operational use the anticipated brake application speed will be used based on the touchdown weight of the airplane and the friction coefficient will be derived from a calibration chart based on amount of water on the runway. The friction calibration chart must be verified or corrected periodically by comparing it to the results obtained from ground vehicle tests.

TEST EXTENTION

The preceding test plan was formulated specifically for the T-43A (Advanced 737). However, it can be expanded to include other aircraft. Additional testing with satisfactory agreement between measured and calculated braking distance can only help to increase the level of confidence on theTotal Braking Prediction System. Additional aircraft are available for which a Braking Prediction Equation has been developed. These are the 727, 747, KC-135, B-52, C-141, F-111 and F-4. It is anticipated that the best agreement between predicted and measured braking distance will exist for those airplanes equipped with an advanced antiskid system which operates efficiently over a wide range of conditions. In planning tests with the airplanes it must be recognized that the range of variables such as airplane touchdown speed and runway conditions are limited by the runway length. The airplanes listed above land at higher speeds which result in longer braking distances than the T-43A. Hence, the range of variables will be more limited.

SECTION XIII
SUMMARY OF RESULTS

1. B-52

Application of brakes at the same speed regardless of the gross landing weight or touchdown speed (90 Knots for G and H models, 70 Knots for earlier versions) is an operating procedure that is unique to the B-52. Absence of weight as an independent variable in the prediction model/equation required that a correction factor be calculated to convert a given weight change into an equivalent velocity change (see Appendix B) for all mu levels.

A correction factor was also needed to convert a given wind component into an equivalent velocity component to be used in the prediction equation (Appendix A) for all mu levels.

The exponent for the π_4 i.e. $\left(\frac{\rho V^6}{Feg^2}\right)$ term had to be modified to account for air density variation at all mu levels. (Appendix E).

The brake system on the B-52 operates in three distinct regions, a rapid skid cycling region (μ = .05 to .2), a transition regic (μ = .2 to .3) involving a combination of skid cycling and torque limiting and a complete torque limited operation (μ>0.3). The torque limiting is the result of an underdesigned brake and braking distance becomes independent of available mu. Hence, the prediction equation may be simplified to: (also see equation 2b, Section X)

$$\left(\frac{S_g}{V^2}\right) = K \left(C_L/C_D\right)^{\alpha} \left(\frac{\rho V^6}{Feg^2}\right)^{\beta}$$

The numerical methods utilized in calculating the component equations and prediction equations showed that for torque limited cases the exponent of π_2 (mu) approached a value of zero. Hence the prediction equation became independent of mu and this result coincides with the physical nature of torque limiting.

2. KC-135

Lack of repeatability in baseline distances on the simulator was traced back to variations in anti-skid valve characteristics. Extensive testing of the antiskid valve indicated that the allowed tolerance band on the valve performance was not compatible with the target distance scatter of 1 to 2% on the brake control simulator. This in turn prevented the desired ± 5% accuracy in data correlation and cross-correlation, especially at low mu's.

The correction factor for a given wind component was needed only at low mu's (<0.3) conditions.

The modified π_4 exponent for density variation was necessary only at low mu's (<0.3).

Torque limited braking was experienced in only 3 out of 88 test conditions (high wt-high velocity combination) and were excluded from the correlation process.

3. F-111

Due to lack of repeatability in baseline braking distances and/or wheel lockups occurring at 0.1 mu level, 0.15 mu was established as the lower mu limit for the F-111. The data scatter in the skid control valve performance was not as wide as for the KC-135 valve but was enough to substantially exceed the 1 to 2% desired repeatability. As a result, the desired ± 5% cross-correlation of data was not achieved at low mu levels ($<0.3\mu$).

The effect of varying weight alone was inconsistent as it sometimes increased and sometimes decreased the stopping distance. A general trend is however evident (Figure 21).

The correction factor for a given wind component was needed only at low mu's (<0.3).

The modified π_4 exponent for density variation was necessary only at low mu's (<0.3).

Torque limited braking was experienced in only 3 out of 88 test conditions (high-wt, high-velocity combination) and were excluded from the correlation process.

4. GENERAL

One of the requirements of the Task II analysis was to compare the results (prediction model) of the current study with those of the earlier sensitivity analysis, reference (1), and establish compatibility if necessary by modifying the earlier models. The idea was to have one general model applicable to all study airplanes. This exercise showed the need for modifying the π_4 exponent for density variation for F-4 airplane at all mu levels and the wet runway equations for the other four (727, 737, 747, and C-141) airplanes. The general methodology has however remained unchanged in that the number of variables, the number of π terms, the nature of prediction model and the correlation accuracy have remained the same. Validation of the previously developed prediction model has thus been established.

SECTION XIV
CONCLUSIONS AND RECOMMENDATIONS

1. CONCLUSIONS

The following conclusions can be drawn from the analysis of the available data generated during this program as well as the previous contracted effort (reference 1).

- Dimensional analysis technique can successfully express braking distances in the form of an equation.
- The prediction model/equation can predict braking distances within ± 5% for the airplanes studied.
- Simulation and analysis of additional military aircraft has helped validate the previously developed prediction model as well as establish compatibility of the model for various types of airplanes e.g., bombers, transports, fighters, etc.
- Although correction factors may be needed for density, wind velocity and weight alone variation in some airplane prediction equations, the general methodology has been shown to be valid.
- A better understanding of contributions made by unique operating procedures, gear geometry, type of skid control system and operating range has resulted from these sensitivity studies.
- A Total Braking Prediction System (TBPS) concept has been defined and a suitable airplane test program has been outlined to verify the same.

2. RECOMMENDATIONS

Certain conclusions and recommendations were listed in Task I report, ASD-TR-77-7, that must be kept in an overall perspective. The analysis established that:

- Tire test data must be collected under fully controlled conditions in order to validate/modify the tire correlation model established by dimensional analysis.
- A Friction Prediction Subsystem (FPSS) specification criteria could be generated to develop a suitable ground vehicle that gives a meaningful measurement of the tire-runway interface mu.
- None of the existing ground vehicles meets the FPSS specification criteria.

With this background plus the conclusions of Tasks II and III listed earlier the following recommendations should be carried out, preferably in the order listed:

- Tire test data must be collected as outlined under Task I and the tire model validated/modified.
- A suitable ground vehicle must be developed based on the specification criteria established under Task I.
- An extensive test program must be conducted for the verification of the TBPS as outlined in this report.
- In order for the TBPS and its subsystems (FPSS and BPSS) to be operationally meaningful, the following areas of work have to be resolved in addition to the test programs recommended above:
    - Classification of runways
    - Method of measuring/indicating rainfall intensity/water depth
    - Runway monitoring system standardization
    - Enacting and enforcing regulations regarding proper maintenance of runways/friction levels.

APPENDIX A
CALCULATION OF WIND FACTOR

Example for B-52:

$\mu = 0.6$; Baseline brake application velocity, V = 90 Knots

Procedure:

For a 5 knot tail wind component (-ve), at $.6\mu$ the stopping distance is 2021 feet compared to the baseline (no wind) stopping distance of 1779 feet as shown in figure 17, section VIII. At 2021 feet, the equivalent brake application velocity is seen to be 97 knots or an increase in baseline velocity of 7 knots. Similarly a 10 knot headwind component is equivalent of 76.5 knots brake application velocity or a decrease of 13.5 knots. This is illustrated in the first three columns (table) below. The remaining calculations pertain to obtaining an average factor F that reflects change in brake application velocity per knot change in wind component as a function of friction value μ.

Wind component V_W (knots)	Equivalent velocity change $\Delta V_{EQ.}$ (knots)	$(V - \Delta V_{EQ.}) = V_{EQ.}$	$\left[\Delta F = \frac{V_{EQ.}}{V \cdot V_W} - 1\right]$	$(\Delta F / V_W)$	F = Avg. $(\Delta F / V_W)$	μ
-10	-16	106	.0600	.0060	.0051	.6
-5	-7	97	.0210	.0042		
+10	+13.5	76.5	.0457	.0046		
+5	7.5	82.5	.0303	.0060		

Similarly, F was calculated for μ = 0.4, 0.2 and 0.1

μ	F
.6	0.0051
.4	0.0055
.2	0.0130
.1	0.0238

$$\boxed{F = 0.0007 + .002326\,\mu}$$

Steps for implementing a wind velocity change into the prediction equation:

1. Calculate F for a given μ

2. Calculate $V_{EQ} = [(F)(V_W) + 1.0]\ [V - V_W]$

where V_W = wind component

tail wind = -ve

head wind = + ve

V = baseline V

3. $V_{EQ} \approx V$ for using the prediction equation

$$\left(\frac{sg}{V^2}\right) = C(\mu)^{\alpha}\,(C_L/C_D)^{\beta}\left(\frac{\rho V^6}{Fe g^2}\right)^{\delta}$$

APPENDIX B
CALCULATION OF WEIGHT CORRECTION FACTOR

Example: (Variation of weight alone):

B-52, μ = 0.6, Baseline V = 90 Knots, S = 1779', W = 290,000 Lbs.
Weight only variation data (simulator)

W (lbs)	ΔW = W-W (baseline)	S (ft)	ΔV_{EQ}* (knots)	$(\Delta W/\Delta V) = (\Delta W/\Delta V_{EQ.})$	Avg. $(\Delta W/\Delta V)$
450,000	160,000	2822	30.5	5246	
370,000	80,000	2278	15.2	5263	
290,000	0	1779	–	–	5150
245,000	- 45,000	1517	-8.7	5172	
200,000	- 90,000	1246	-18.3	4918	

* The ΔV_{EQ} is the equivalent velocity change from baseline (90 Knots) needed to obtain the distance, S, shown in the previous column, and is obtained from the velocity only variation data shown (table) below.

.6μ	Velocity only variation data (simulator)		
W	V	S	$\Delta V_{EQ.}$
290,000	90Kn	1779	0
	95	1916	5
	100	2116	10
	110	2418	20
	120	2755	30
	85	1633	- 5
	80	1457	-10

Similarly, $(\Delta W/\Delta V)_{(.4\mu)} = 5640$; $(\Delta W/\Delta V)_{(.2\mu)} = 5970$;

$(\Delta W/\Delta V)_{(.1\mu)} = 6088$.

X = μ	Y = $\Delta W/\Delta V$
.6	5150
.4	5640
.2	5970
.1	6088

Y = 6322 - 1877 (X)

or

$$\boxed{\Delta V = \frac{\Delta W}{6322 - 1877\ (\mu)}}$$

Steps for implementing a weight only change into an equivalent velocity only change for use in prediction equation:

Steps:

1) Calculate $(\Delta w / \Delta v)$ for given μ.

2) Divide total Δw by $(\Delta w / \Delta v)$ to obtain Δv

3) Algebraically add Δv of Step 2 to baseline v.

   $v = v + \Delta v$ for higher weights and
   $v = v - \Delta v$ for lower weights.

4) Then use $(v = v_{baseline} \pm \Delta v)$ in the prediction equation:

$$\left(\frac{Sg}{v^2}\right) = c\,(\mu)^{\alpha}\,(C_L/C_D)^{\beta}\left(\frac{\rho v^6}{Feg^2}\right)^{\delta}$$

APPENDIX C

CALCULATION OF PRE-BAKING ROLL DISTANCE FOR B-52 AIRPLANE

A digital computer program was used to compute the distance 'S' expressed by the following integral·

THE GROUND RUN OF AN AIRCRAFT IS GIVEN BY:

$$S = 2.852^* \frac{W}{g} \int_{V_B}^{V_T} \frac{(V - V_W)\, dV}{D + G + Wx - F}$$

S = distance relative to the ground (ft.)

W = weight (lb)
x = runway gradient (positive upwards) (radians)
V = true airspeed (knots)
V_T = touch-down speed (knots)
V_B = brake application speed (knots)

D = total drag (lb) = (aero + drag chute)
G = (rolling) friction force between the wheels and the runway
g = acceleration due to gravity, (32.2 ft/sec^2)
F = thrust (lb)
V_W = Head wind component (knots)

*This is the conversion factor from (knots)^2 to (ft/sec)^2

The program internally computes parameters D, G & F.

Example· W = 450,000 lbs C_L = .305 V_W = 0
$\mu_{rolling}$ = .02   x = 0 V_T = 100 knots
C_D = .152 (Touchdown to Drag Chute deployment speed (135 knots)
C_D = .321 (135 knots to V_B = 90 knots)

Then $[S]_{135}^{160}$ = 3000 feet

and $[S]_{90}^{135}$ = 3375 feet

Total $[S]_{90}^{160}$ = 6375 feet

This is one of the data points shown in figure 23.

APPENDIX D
FORMULATION OF PREDICTION MODEL

1. DETERMINATION OF COMPONENT EQUATIONS

When the experimental data had been arranged as described in reference (2), Appendix C, relationships between π_1, the term containing the dependent variable, and π_2, π_3 and π_4 in turn, the terms with independent variables, were obtained using statistical curve fitting programs. The relationships between π_1 and other individual π terms are called component equations.

Plots were prepared of π_1 versus π_2, π_1 versus π_3, and π_1 versus π_4 for all airplanes using data from ASD-TR-77-6 Volume II, Section XII. An example of these plots is shown (for F-111 data) in Figure D-1. This helped determine the general form of a relationship that could exist between π_1 and π_2, π_1 and π_3, and so on. Figure D-2 is a flow chart depicting the formulation of component equations. The explanation of terms linear regression, polynomial regression, etc. can be found in Appendix D, reference (1).

2. DETERMINATION OF FUNCTIONS

As explained in Appendix E, reference (1), the component equations were combined by the product method. The conditions for the function to be a product and the equivalence of calculated values of C were also developed in the referenced Appendix. The same procedure was repeated in the present study. Tables D-1 through D-4 show detailed calculations for tests of validity.

Having established the type of component equations, a digital computer program was put together to systematically calculate π terms (numerics), formulate component equations, calculate constant "C", and calculate correlation errors.

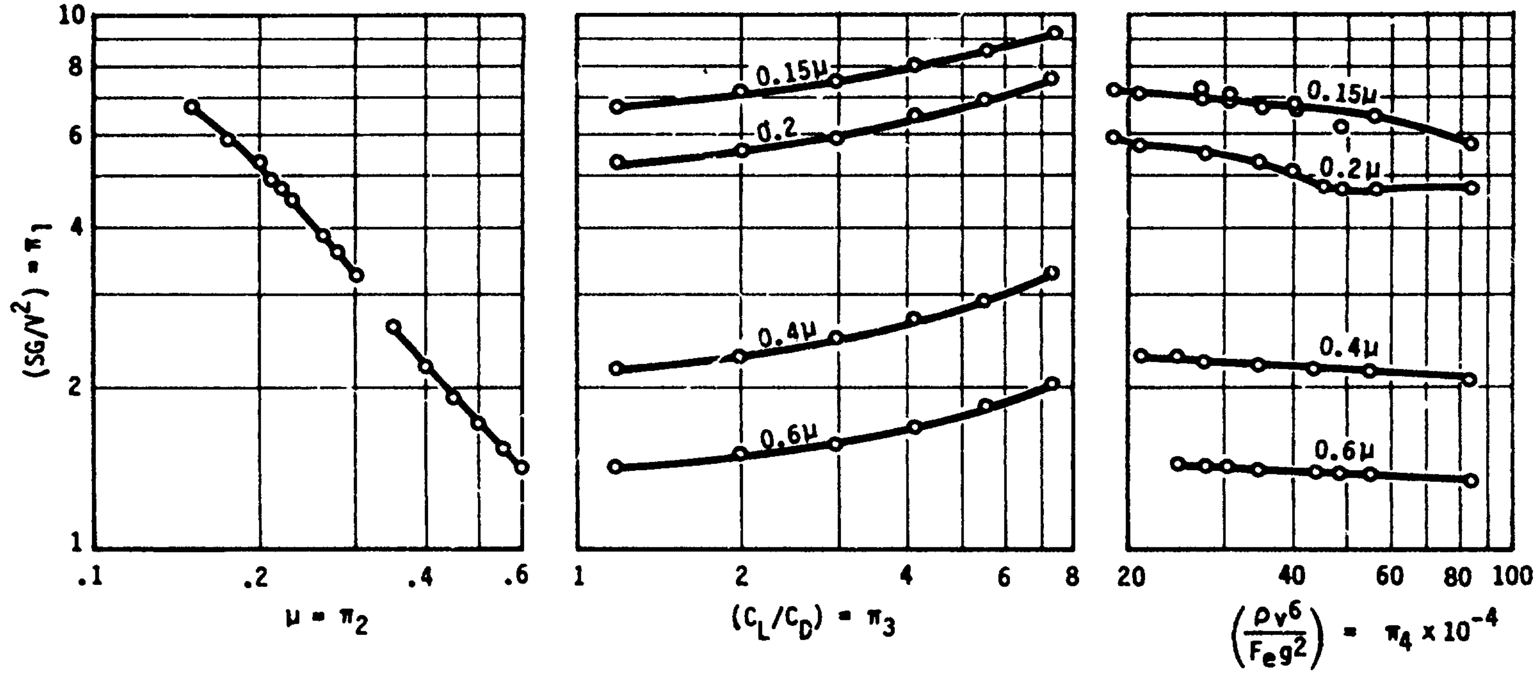

Figure D-1.—Plots of π_1 vs. π_2, π_3, and π_4 (F-111 Data)

$X = \pi_2$ or π_3 or π_4 - the independent variable
$Y = \pi_1$ - the dependent variable

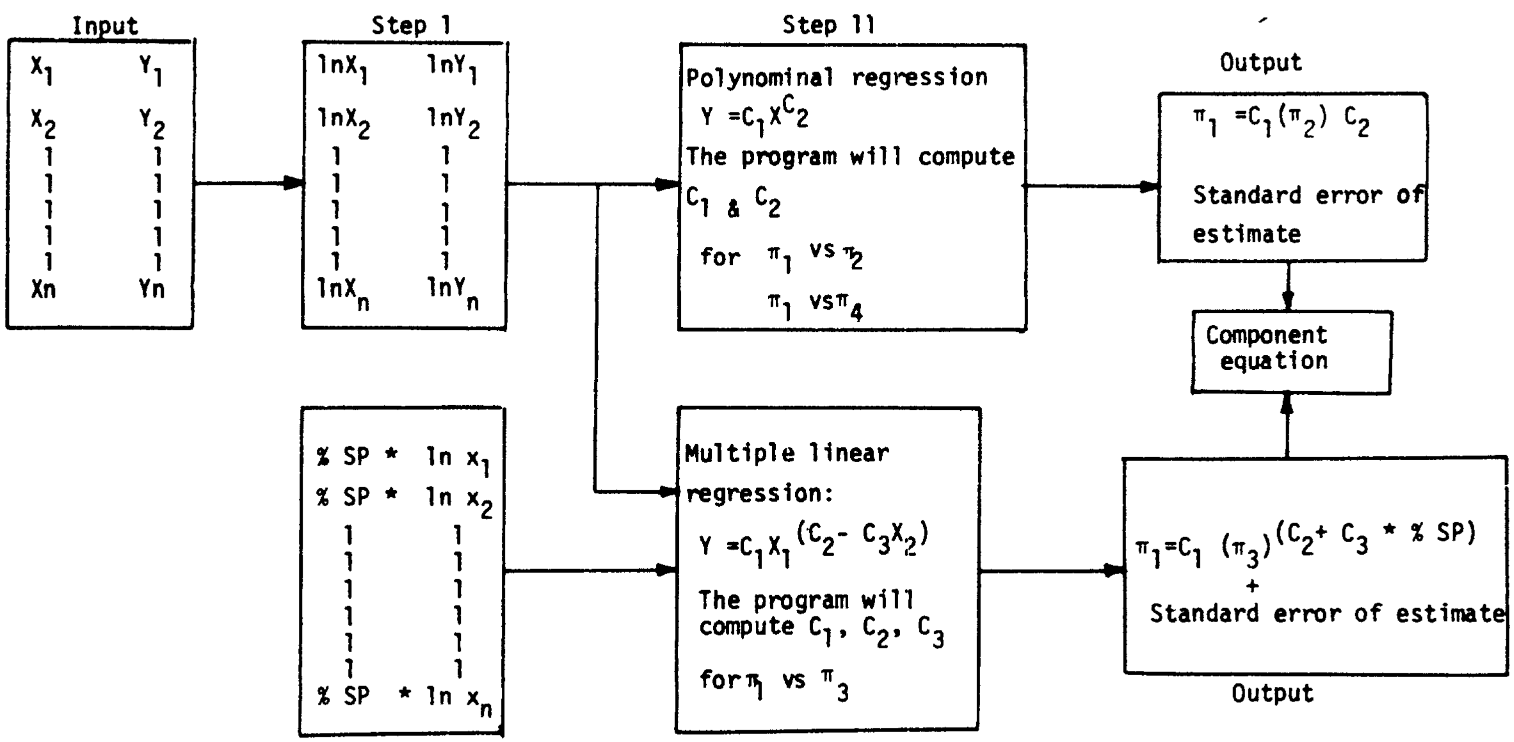

Figure D-2.—Equation Flow Chart

Table D-1.—Calculation of Validity for the Function to be a Product

Airplane	$\bar{\pi}_2$	$(\bar{F})^2$	F_1	F_2	$\frac{F_1 \times F_2}{(\bar{F})^2}$	Error Percentage
B-52	0.6	5.9628	2.4760	2.4540	1.108	1.8
	0.4	6.1652	2.4930	2.4610	0.995	-0.5
	0.2	29.4632	5.4270	5.3000	0.976	-2.4
	0.1	60.3107	7.9260	7.6950	1.011	1.1
KC-135	0.6	1.3340	1.1440	1.1570	1.008	0.8
	0.4	2.8629	1.693	1.694	0.998	-0.2
	0.2	13.6678	3.740	3.796	0.963	-3.7
	0.1	66.4714	8.035	8.025	1.031	3.1
F-111	0.6	1.9321	1.411	1.410	0,971	-2.9
	0.4	4.8753	2.194	2.192	1.014	1.4
	0.2	27.6676	5.122	5.283	1.022	2.2
	0.1	45.1315	6.926	6.701	0.972	-2.8

$$1/C = (\bar{F})^2 = \left[F\,(\bar{\pi}_2, \bar{\pi}_3, \bar{\pi}_4\,)\right]^2$$

$$(F_1) = F\,(\bar{\pi}_2, \pi_3, \bar{\pi}_4\,)$$

$$(F_2) \quad F\,(\bar{\pi}_2, \bar{\pi}_3, \pi_4\,)$$

TEST OF VALIDITY:

$$\frac{(F_1)\ \ (F_2)}{(\bar{F})^2} = 1$$

Table D-2.—Calculation of Validity for Constant Term

Airplane Model	$F(\pi_2, \pi_3, \pi_4) = \pi_1$ (Baseline)				$C = (1/F(\pi_2, \pi_3, \pi_4))^2$				Average Value of Predicted C	Deviation from Ideal Value %	Value of π_2
	Component Equation Used										
	π_1 vs π_2	π_1 vs π_3	π_1 vs π_4	Ideal	π_1 vs π_2	π_1 vs π_3	π_1 vs π_4	Ideal			
B-52	2.443	2.476	2.454	2.477	.1675	.1631	.1660	.1630	.1656	1.59	0.6
	2.483	2.493	2.461	2.472	.1622	.1609	.1551	.1636	.1627	-.53	0.4
	5.428	5.427	5.300	5.436	.03394	.03395	.0356	.0338	.0345	2.07	0.2
	7.766	7.926	7.695	7.929	.01658	.01592	.01689	.01591	.01650	3.70	0.1
KC-135	1.155	1.144	1.157	1.143	.7496	.7641	.7470	.7654	.7536	-1.54	0.6
	1.692	1.693	1.694	1.681	.3493	.3489	.3489	.3485	.3489	-1.40	0.4
	3.697	3.740	3.796	3.762	.0732	.0715	.0694	.0694	.0707	0.99	0.2
	8.153	8.035	8.025	8.017	.01504	.01549	.01553	.01556	.01535	-1.33	0.1
F-111	1.390	1.411	1.410	1.406	.5176	.5023	.5030	.5076	.5076	0.34	0.6
	2.208	2.194	2.192	2.198	.2051	.2077	.2081	.2070	.2070	0.00	0.4
	5.122	5.283	5.260	5.305	.03812	.03583	.03614	.03553	.03670	3.29	0.2
	6.926	6.118	6.701	6.695	.02085	.02216	.02227	.02231	.02176	-2.46	0.15

Table D-3.—Calculation of Validity for the Function to be a Product-Wet Runway

Airplane	$\bar{\pi}_2$	$(\bar{F})^{-2}$	F_1	F_2	$\frac{F_1 \times F_2}{(\bar{F})^2}$	Error Percentage
B-52	.23	22.7529	4.795	4.788	0.9910	-0.89
	.175	33.8491	5.815	5.669	1.0268	2.68
	.127	47.0870	6.866	6.492	1.0563	5.63
KC-135	.166	20.9123	4.564	4.515	1.0148	1.48
	.154	25.0000	5.008	4.911	1.0165	1.65
	.137	32.6269	5.712	5.629	1.0147	1.47
F-111	.231	19.3864	4.447	4.375	0.9964	-0.36
	.218	21.8930	4.694	4.663	1.0002	0.02
	.193	28.2705	5.352	5.358	0.9859	-1.41

$$I/C = (\bar{F})^2 = \left[F\ (\bar{\pi}_2, \bar{\pi}_3, \bar{\pi}_4)\right]^2$$

$$(F_1) = F\ (\bar{\pi}_2, \pi_3, \bar{\pi}_4)$$

$$(F_2) = F\ (\bar{\pi}_2, \bar{\pi}_3, \pi_4)$$

TEST OF VALIDITY:

$$\frac{(F_1)\ (F_2)}{(\bar{F})^2} = 1$$

Table D-4.—Calculations of Validity for Constant Term-Wet Runways

Airplane Model	$F(\pi_2, \pi_3, \pi_4) = 1$ (Baseline)				$C = (1/_F(\pi_2, \pi_3, \pi_4))^2$				Average Value of Predicted C	Deviation from Ideal Value %	Value of π_2
	Component Equation Used										
	π_1 vs π_2	π_1 vs π_3	π_1 vs π_4	Ideal	π_1 vs π_2	π_1 vs π_3	π_1 vs π_4	Ideal			
B-52	4.770	4.795	4.788	4.782	.04395	.04349	.04362	.04373	.04369	.10	.230
	5.818	5.815	5.669	5.818	.02954	.02957	.03112	.02954	.03008	1.83	.175
	6.862	6.866	6.492	6.854	.0212	.02121	.02373	.02129	.02206	3.62	.127
KC-135	4.573	4.564	4.515	4.570	.04782	.04801	.04906	.04788	.04830	0.88	.166
	5.000	5.008	4.911	5.000	.04000	.03987	.04146	.04000	.04044	1.10	.154
	5.712	5.712	5.629	5.712	.03065	.03065	.03156	.03065	.03095	0.99	.137
F-111	4.403	4.447	4.375	4.430	.05158	.05057	.0522[illegible]	.05096	.05146	0.99	.231
	4.679	4.694	4.663	4.694	.04368	.04538	.04599	.04538	.04589	0.67	.218
	5.317	5.352	5.358	5.341	.03537	.03491	.03491	.03483	.03506	-0.06	.193

APPENDIX E

CALCULATION OF DENSITY CORRECTION FACTOR:

Definitions.

Standard day = 59°F, sea level, ρ = .00238 lb-sec^2/ft^4

Non-standard day = Hot day or cold day as follows:

Hot day = 83°F/28°C, ρ = .00189 lb-sec^2/ft^4

Cold day = -60°F/-51°C, ρ = .00309 lb-sec^2/ft^4

Example: KC-135; 0.1 μ

Component Equation 25 (unmodified) had the form:

$$(\pi_1) = 82.268669\,(\pi_4)^{-.200863}$$

When this equation was used to predict stopping distances for hot and cold day cases the correlation error exceeded the desired ± 5% (see the following tabular data).

Condition	(π_4)	Actual (π_1)	Predicted (π_1)	% Error
Hot day	85517	9.131	8.453	7.420
Cold day	139813	6.976	7.658	-9.776

A modified exponent was calculated for the term (π_4) such that the correlation error would be minimal.

Let modified exponent = B

Then for no error; $B = \log\left(\dfrac{\text{Actual }(\pi_1)}{82.2687}\right)\Big/\log(\pi_4)$

i.e., for a hot day;

$B_{HOT} = \log(9.131/82.2687)/\log(85517) = -.193574$

Δ exponent = .200863 -.193574 = .007289

Similarly $B_{COLD} = -.208263$

and $\Delta_{expo} = .007400$

This Δ_{expo} cannot be directly added to the π_4 exponent since the π_4 term is also used to predict affects of varying V and Fe, i.e. an explicit form of Δ_{expo} for density change $\Delta\rho$ should be calculated. This is illustrated below:

Condition	ρ (density)	$\Delta\rho$	$\Delta_{exponent}$	$\Delta_{ex}/\Delta\rho$	$\Delta_{ex}/\Delta\rho$ (avg.)
Std day	.00238	–	–	–	–
Hot day	.00189	.00049	.007289	14.875	12.65
Cold day	.00309	.00071	.007400	10.423	

The modified component equation is:

$$(\pi_1) = 82.268669\,(\pi_4)^{\left[12.65\Delta\rho - .200863\right]} \tag{25}$$

$$\boxed{\text{where } \Delta\rho = \rho_{std} - \rho_{non\text{-}std}}$$

REFERENCES

1. Warren, S.M., Wahi, M.K., Amberg, R.L., Straub, H.H., and Attri, N.S., (The Boeing Company), "Combat Traction II, Phase II. Technical Report Number ASD-TR-74-41, Volume I, October 1974.

2. Ibid. Volume II,–October, 1974.

B-52 TECHNICAL REFERENCES

3. Aircraft Antiskid Performance and System Compatibility Analysis; Technical Report AFFDL-TR-70-128; B.H. Anderson, W.C. Kreger; February, 1971.

4. Boeing Technical Report D-10-967, Subject: B-52 Metering Valve; Last Revision Date March 16, 1959.

5. Boeing Technical Report D3-1633, Subject: Aerodynamic Data

6. B-52 Flight Manual, T.O. 1B-52H-1

7. B-52 Landing Gear Manual, T.O. 1B-52B-2-10

8. B-52H Flight Manual. Appendix 1, Performance Data T.O. 1B-52H-1-1

KC-135 Technical References

9. Bendix Absorption Engineering Laboratory Report; Report No. EAL-64-75 January, 1965.

10. Boeing Technical Report; D6-5599, Section IV, Aerodynamic Data, January, 1965.

11. Boeing Technical Report; D6-9317

12. KC-135 Flight Manual; T.O. 1C-135 (K) A-1

13. KC-135 Flight Manual; T.O. 1C-135 (K) A-1-1 Appendix 1, Performance Data.

14. KC-135 Landing Gear Manual; T.O. 1C-135 (K) A-2-7.

15. Peterson, D.C. and Cross, C.S., "Evaluation of a Five-Rotor Brake and Modulated Antiskid System Installed on a KC-135", Technical Report No. FTC-TR-64-63, March, 1965.

F-111 TECHNICAL REFERENCES

16. Anderson, B.H. and Kreger, W.C., "Aircraft Antiskid Performance and System Compatibility Analysis", Technical Report No. AFFDL TR-70-128, February, 1971.

17. B.F. Goodrich Brake Qualification Report, Report No. Q-6069.

18. F-111 Flight Manual, T.O. LF-111A-1.

19. F-111 Flight Manual, Performance Data, T.O. 1F-111A-1-1.

20. F-111 Landing Gear Systems, T.O. 1F-111A-2-9-1.

21. Pierson, J.H., and Parsons, R.K., "Initial Category II Landing Performance Evaluation, F-111A", Technical Report No. FTC-TR-66-37, January, 1967.

22. Skid Control Generator, T.O. 4BA8-23-3, Part No. 9542613.

23. Skid Control Solenoid Valve, T.O. 4BA4-90-3, Part No. 9550255.

OTHER REFERENCE

24. Palmer, R.W., et al, "Effect of Skid Control, Tires, and Steering on Aircraft Ground Performance (Rain tire)" Final Report, MDC A2683, February, 1974.